



UNIVERSITÀ DELLA CALABRIA

Dipartimento di Biologia, Ecologia e Scienze della Terra

Scuola di Dottorato

ARCHIMEDE

Indirizzo

Scienze della Terra

CICLO

XXVII

TITOLO TESI

Petrographic and geochemical study of the Jarosite-bearing layers of
Aeolian Islands

Settore Scientifico Disciplinare GEO/07

Direttore:

Ch.mo Prof. Pietro Salvatore Pantano

Firma Pietro Pantano

Supervisore:

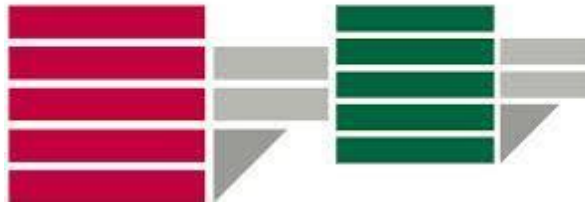
Dott.ssa Donatella Barca

Firma Donatella Barca

Dottoranda: Dott./ssa Fahimeh Ryazi Khyabani

Firma Fahimeh Khyabani

UNIVERSITÀ DELLA CALABRIA



**Archimedes PhD School in Science, Communication and Technologies
Cycle XXVII - Earth Sciences Curriculum**

**The dissertation submitted to fulfill the requirements for the degree of
Doctor of Philosophy in Earth Sciences**

Title:

**Petrographic and geochemical study of the
Jarosite bearing layers of Aeolian Islands**

Tutor:

Dr. Donatella Barca

Co-Tutor:

Prof. Gino Mirocle Crisci

Researcher:

Fahimeh Ryazi Khyabani

November 2014

Abstract

A thin reddish-brown Surface Coating (SC) layer has diffusely covered many outcrops of Vulcano Island (one of the Aeolian Islands), located in the Tyrrhenian Sea, south Italy. Vulcano, in the last 120ka has been subjected to volcanic activities including both eruptions (pyroclastic and lava types in shoshonitic and leucite-tephritic series) and fumarolic degassing. The SC that has been formed on almost all these lithologies appears as a reddish (sometimes pinkish) brown glass-like rind with a greasy luster which adheres to substratum and fills and completely seals its surface irregularities. The precise formation process of the SC is what we have tried to model in the present work. The SC in Vulcano, like other active volcanic precincts, includes amorphous silica associated with a sulfate phase as jarosite mineral. Jarosite as a basic hydrous sulfate of potassium and iron is the head member of jarosite subgroup. Under the microscope, SC is consisted of a micro laminated layer (less than 1 μ m to 7 μ m in thickness) which is composed of alternative dark and light laminae. The light laminae are composed of jarosite, while the darker ones are made of almost pure silica. In many cases of the SC, the laminae encompass lenticular areas containing coarser mineral crystals and noticeable number of glass shards, very fresh to altered in different grades, within an inexplicit background. The relations between all these components (laminated portion and the trapped area between different subsets of laminae) creates some particular textures such as lentic/eye texture; convoluted texture (flow of laminae); branching, rejoining, and tee-shaped perpendicular junctions of the laminae. These particular textures are quite comparable to the patterns of Liesegang Bands in the microscopic scale. Permeability of the rock; the presence of reactants such as oxygen, iron, and sulfur; and a potential fluid to be supersaturated are required factors for developing the Liesegang bands. The porous surface of the pyroclastic deposits of Vulcano can be exposed to the acidic fluids (produced by the interaction between water and fumarolic gases) and the availability of the iron and sulfur can provide the suitable condition to form the Liesegang patterns.

Key words: Surface coatings; Jarosite; Micro lamination; Vulcano; Fumarolic activities; Convoluted texture; Lenticular texture.

Learning
is finding out
what you already know.

Doing is demonstrating that
you know it.

Teaching is reminding others
that they know just as well as
you.

You are all learners, doers, teachers.

“Richard Bach”

Acknowledgements

I have fulfilled my triennial PhD work in the University of Calabria in Italy and within this period I have spent a six-month period of sabbatical in the University of Bristol in UK. So, at this juncture, I take the opportunity to express my profound gratitude and deep regards to everyone who has helped me throughout this scientific endeavor, whom without them the present assignment wouldn't be possible. Of course, in completing this task, the people to whom I feel an intense appreciation are not limited to only those who I have mentioned in the following.

I sincerely appreciate my PhD supervision team members, Dr. Donatella Barca, for her guidance; Prof. Gino Mirocle Crisci, for his official and financial support during my first year; Prof. Stephen Sparks for his exemplary and so precious advising, constant help and encouragement; and Dr. Alison Rust for her constructive criticism and suggestions.

I'd like to thank all the academic and technical staff of Department of Biology, Ecology, and Earth Sciences in the University of Calabria and Earth Sciences School of the University of Bristol for their provided information and cooperation in their respective fields. I am especially grateful to Dr. Mariano Davoli (the responsible of SEM Lab in UNICAL) for his availability and ever friendly behavior, Dr. Stuart Kearns and Dr. Ben Buse (the responsible ones of the SEM and Microprobe Labs in the UOB) for their patient instructions on how to use the SEM, and Dr. Heather Buss (researcher at UOB) for sacrificing many hours to discuss the micro-organismic aspects of the subject. I should also thank Dr. Jens Najorka from the Natural History Museum of London who very hospitably assisted me in carrying out some of the Micro-XRD analyses.

A special thank you goes to Dr. Paola Donato (researcher at UNICAL) for her valuable help and for having an ear to listen to me whenever I needed it. Also, she and Dr. Giancarlo Niceforo generously allowed me to use all the rock samples and related data from Stromboli Island which they had previously collected.

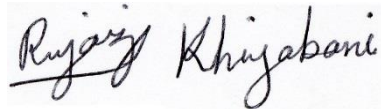
I'm extremely grateful to every single one of all my lovely friends. Their great inspiration and genuine friendship makes me able to feel their intimacy, no matter how distant I am. Here, I should also particularly mention to my ex-officemates in Room G3, in the University of Bristol, who have always lent a helping hand.

Finally, I place a deep sense of gratitude to my wonderful family. I wouldn't be where I am now without their unwavering love, support, and encouragement. It is priceless that they allowed me to dream and to know I can be whatever I want to.

Author's declaration

I declare that the work in this dissertation was carried out in accordance with the requirements of the University's Regulations and Code of Practice for Research Degree Programs and that it has not been submitted for any other academic award. Except where indicated by specific reference in the text, the work is the candidate's own work. Any views expressed in the dissertation are those of the author.

SIGNED:

A handwritten signature in black ink, reading "Rujainy Khujabani". The signature is written in a cursive style with a horizontal line under the first name.

DATE: 28/11/2014

TABLE OF CONTENTS

Chapter 1. Introduction	1
1.1. Introduction	2
1.2. The general aims of this research	4
1.3. The structure of the dissertation	5
Chapter 2. Principal concepts and literature review	7
2.1. Aeolian Islands	8
2.2. Vulcano Island	9
2.2.1. Geology of Vulcano	10
2.3. Surface Coatings	14
2.3.1. Jarosite mineral	15
2.4. Jarosite bearing surface coatings	18
2.4.1. Suggested models for the formation of Jarosite-bearing surface coatings	21
Chapter 3. Methods and materials	26
3.1. Introduction	27
3.2. Sampling	28
3.3. Petrographical Approach	29
3.4. Analytical Methods	30
3.4.1. SEM - EDS	30
3.4.2. Microprobe	31
3.4.3. ICP-MS	32
3.4.3.1. Laser Ablation (LA-ICP-MS)	32
3.4.3.2. Solution nebulization	33
3.4.4. XRD	34
3.4.5. Micro-XRD	34
Chapter 4. Findings and discussion	37
4.1. General	38

TABLE OF CONTENTS

4.2. The results of the field investigations	38
4.3. Petrographical findings	42
4.4. Results of the XRD	52
4.5. Geochemical findings	53
4.5.1. SEM-EDX findings	54
4.5.2. ICP-MS results	55
4.6. Discussion	58
4.6.1. Liesegang bands	66
4.6.2. Liesegang bands in SC samples	68
Chapter 5. Conclusion and recommendations	71
5.1. Summary	72
5.2. The process of the formation of surface coatings	74
5.3. Not answered questions	75
5.4. Suggestions	75
References	76
Appendices	86
Appendix A	87
Appendix B	88
Appendix C	102
Appendix D	123
Appendix E	135

TABLE OF CONTENTS

List of tables and illustrations

Fig. 2.1. The location of the Aeolian Archipelago	8
Fig. 2.2. Tectonic map of the south Tyrrhenian Sector (modified after Billi, et al .2006)	9
Fig. 2.3. Local names of different parts of Vulcano	10
Fig. 2.4. A photo history of morphology of Vulcano (modified after Forni, et al. 2008)	11
Fig. 2.5. Jarosite sample from the Coromandel Peninsula in New Zealand (Kotler, 2008)	16
Fig. 4.1. A typical view of SC in the macroscopic scale (sample F019 ¹ taken from Monte Lentia in Vulcano)	39
Fig. 4.2. The rock wall of Monte Lentia, covered by SC	
Fig. 4.3. Following the direction of runoff waters, the SC has formed downward (yellow arrows); the SC on both sides of the fractures (red arrows)	41
Fig. 4.4. A) the SC on the surface of loose sands; B) easily differentiated layers of unconsolidated materials (Part A of this figure, while trying to make sampling); C) totally strewed grains of the A and B parts of this figure, after a storm	41
Fig. 4.6 A) A micro depression of SC (CPL); (B) Lamination of SC filling a micro-cavity/micro-depression (CPL)	46
Fig. 4.7. Lenticular form of SC with some crystals inside (PPL)	46
Figure 4.8. a) branching and rejoining of subsets of SC (CPL); b) compacted laminae on a microlithic fragment which have been divided and flowed into a hole (CPL); c) Reference point of laminae branching from the boundary between two rock types (CPL); d)	48

¹ Coordination of the sample by GPS is N 38 24. 329 - E014 56. 787 - Alt. 400 ft.

TABLE OF CONTENTS

Tee-shape junctions, convoluted texture (PPL); e) different subsets have surrounded eye-like and elongated concave lentic areas (PPL)	
Fig. 4.9. Different shapes of the glass shards (CPL)	50
Fig. 4.10. Clear view of the typical lamination of SC (photo by SEM)	51
Fig. 4.11. Needle shaped crystals of secondary minerals (photo by SEM)	52
Fig. 4.12. SiO ₂ versus SO ₃ plot of finely laminated portion of SC (weight percentages are determined by SEM-EDS)	56
Fig. 4.13. Sr versus Y plot of finely laminated portion of SC. The contents of Sr and Y (in ppm) were determined by LA-ICP-MS	57
Fig. 4.14. – FeO _(tot) versus Ni plot of finely laminae of SC. Weight percentages of FeO _(tot) were determined by SEM-EDS, Ni contents (in ppm) were determined by LA-ICP-MS	57
Fig. 4.15. The location of analysed cross section of the laminae	61
Fig. 4.16. The weight percentages of the four oxides of the laminae	62
Fig. 4.17. Binary scatterplot of the SO ₃ versus SiO ₂ content of the laminae. The black dotted line is the trendline of all the plot points. The red line connects the analogue points of the silica and the normative SO ₃ content of the jarosite	64
Fig. 4.18. Binary scatterplot of the Fe ₂ O ₃ versus SiO ₂ content of the laminae. The black dotted line is the trendline of all the plot points. The red line connects the analogue points of the silica and the normative Fe ₂ O ₃ content of the jarosite	65
Fig. 4.19. Binary scatterplot of the K ₂ O versus SiO ₂ content of the laminae. The black dotted line is the trendline of all the plot points. The red line connects the analogue points of the pure silica and the normative K ₂ O content of the jarosite	65

TABLE OF CONTENTS

Fig. 4.20. (A) The Liesegang bands in the nature. (taken in Southern Illinois, 2014). (B) The curved laminae set in the SC sample (taken in PPL)	69
Fig. 4.21. (A) The Liesegang bands in the nature. (by Zoltan Sylvester,). (B) The similar texture in laminae of the SC (taken in CPL)	70
Table 2.1. The evolutional stages of Vulcano, subdivided by De Astis, et al. (1997)	12
Table 2.2. Secondary minerals identified in distal RC (rock coatings) through optical microscope, XRD, and SEM-EDS investigation (from Fulignati, et al. 2002)	20
Table 4.1. Selected samples to be analyzed by different technics	53
Table 4.2. Weight percentage of the major element oxides of a cross section of the laminae. Since the first and the last points of the line S2 had obvious differences with the results of the other points, were discarded. The results of the points having a total amounts of less than 80% were discarded as well, because these points were partially included the emptiness of the porosity	60

TABLE OF CONTENTS

List of abbreviations

BSE	Black Scattered Electron
EDAX	Energy Dispersive X-Ray Analysis
EDS	Energy Dispersive X-Ray Spectroscopy
ICP-MS	Inductively Coupled Plasma Mass Spectrometer
LA	Laser Ablation
NHM	Natural History Museum
RC	Rock Coatings
SC	Surface Coatings
SE	Secondary Electron
SEM	Scanning Electron Microprobe
SES	School of Earth Sciences
SUTW	Super Ultra Thin Window
UNICAL	University of Calabria
UOB	University of Bristol
XRD	X Ray Diffraction

Chapter 1

Introduction

1.1. Introduction

From deserts to the islands in the middle of the oceans, rock coatings have been found and reported from all over the world. In a specific case, a superficial crust of coatings on the surfaces of two given volcanic islands could attract our interest enough to be taken as the subject of the study of the present dissertation.

A thin layer has coated the surface of different outcrops of Vulcano and Stromboli Islands which, as a part of Aeolian Archipelago, are located in the Tyrrhenian Sea, above the Italy's Sicily Region. Both Vulcano and Stromboli Islands were born due to the formation of Aeolian Volcanic Island Arc. Although these two islands still show volcanic activities, the form of their activities are not alike. Vulcano has fumarolic activities around its degassing crater, La Fossa Cone, while Stromboli shows persistent magmatic eruptions and effusions. Vulcano and Stromboli are geographically close enough to experience equal weather conditions such as temperature, humidity, wind (strength and direction), and duration of the day.

The aforementioned layer can be seen on various lithologies of the islands. It is very thin and has a thickness range of a few micrometers to more than 1 centimeter. The distinct reddish-brown / pinkish-brown color of the coating makes it very easy to be distinguished in the field, even when it has its minimum thickness. In a macroscopic view, this surface coating appears in a homogenous color and a smooth surface, which usually have a greasy luster, too. The appearance characteristics of this surface coating is independent of its substratum. However, the thicker it is, its color goes slightly darker.

CHAPTER 1. INTRODUCTION

While the surface coating doesn't significantly vary in macroscopic view, it has many different features under the microscope. Its first and most typical specification is its lamination. The laminated parts of the coatings are consisted of micrometer scaled alternative dark and light laminae. The laminae run evenly on the brim of the rock and every now and then they curve in the bottom and become thicker to fill the little depressions, and again get their previous thickness and proceed. This kind of lamination is not the only characteristic of the surface coating, but without any exception it is present in all the samples. In many studied species, the laminated part is not limited to just one layer on the brim of the rock. In this case, the laminae get divided into different branches which penetrate into the rock.

The subdivided laminae, as the linear or curved subsets, trend in different directions and may meet each other again. Thus, some spaces are left between these subsets, which gives a particular appearance to the rock. The compartments that are restricted and trapped between the subsets of laminae are usually lentic or eye-shaped. Also, it is common for the lenses to be elongated. Symmetric or asymmetric, they are all wider in the middle part and thinner in their tails of both sides. These compartments contain some clastic material which includes the crystals of minerals (common phenocrysts of a basic rock), quite a lot of glass shards, and a porous background.

On the other hand, when two subsets meet each other, they can join together again or simply cross and end in the cross point.

All these particular textures (steady lamination, micro depressions, lentic areas of clastic materials, and various forms of the relative positioning of the laminae) plus the presence of the glass shards within the

CHAPTER 1. INTRODUCTION

surface coatings inspired us to try to find the responsible processes of their formation.

There were many questions to be answered: Have all the components of the surface coatings been formed simultaneously or the formation of one has caused the other to be created? How have the laminae been deposited one on another? What are the chemical composition and the mineralogical phases of the light and dark laminae? How long has it taken for the laminae to be formed? What has made the laminae to curve in the bottom and make the depressions? How the severing and rejoining of the laminae have happened? What is the relation between the laminated part and the clastic one? Whether the clastic materials (glass shards and minerals) are in-situ or they have been transported? If the clastic materials are transported, what has carried them and how? Why are there so many fresh and non-altered glass shards in thick and probably old surface coatings? In sum, what is the geological scenario of the formation of these surface coatings?

1.2. The general aims of this research

In the scientific literature, the works on surface coatings in the volcanic areas are not many, and the researches about the textures of these coatings are even less. Although, some of the abovementioned questions have already been discussed, not all of them have been expressed yet. So, along with questioning the nature of the observed particular textures for the first time, we have made an effort to answer the stated questions, too. Our approach to deal with this was firstly to get deep detailed information of the samples and later, combining all the results of findings from the field studies, mineralogy, and geochemistry to find out an appropriate process for the genuine formation way of this kind of surface coatings. To reveal the most accurate answer for the conundrum the biggest challenge was the

CHAPTER 1. INTRODUCTION

very small scale of the laminated material, so that with the technology of the day, there is no way to do some analyses for each single lamina. The fact that we were not able to separate the material of each lamina to determine their age or mineralogical phase, we tried to seek for some similar textures to use as a clue for modelling our own material. However, it was not the only difficulty that we faced. Although there were certain cases having some similar textures of our samples, none of them possessed all those textures. Thus, we had to find a way to pick out all the possible ways of the formation of the present textures and then to hypothesize a single possible way to have all of them together.

The desire to discover a little part of the nature was motivating us and leading us all the time, since we believe that understanding the precise mechanism by which these amazing textures have developed can help us find out a logical relation between sedimentary and volcanological processes as well as between the chemical and physical processes, which as a key information may be used for the future investigations.

1.3. The structure of the dissertation

Before describing the structure, it should be mentioned that although we collected and studied the samples from two islands (Vulcano and Stromboli), almost all of the discussion in this dissertation is based on the samples from the Vulcano Island. Since all the main characteristics of the samples of both islands were similar and they were different only in the sense of their thicknesses and probably their ages (the surface coatings on Vulcano are thicker and probably older), and also because of the time shortage to investigate all the details from two islands, the samples from Vulcano are given more weight and importance.

CHAPTER 1. INTRODUCTION

In order to introduce the issue and to find an approach to achieve the aims of the present research, this dissertation has been prepared in 5 chapters. After stating the matter and the importance of the subject of the research in chapter 1, some general information about the Vulcano Island as well as a summarized review of the previous research on surface coatings have been described in chapter 2. All the theoretical and analytical methods which have been used in the related experiments are explained through the third chapter. Chapter 4, which can be assumed as the most important chapter of the present thesis, has been represented in two main parts, consisting of petrography and geochemistry. Within chapter 4 all the gathered information of empirical part of the research have been demonstrated. These information feed the discussion part of the chapter. Finally, the main conclusions and the suggestions for the future works have been referred in chapter 5, which is the last one.

Chapter 2

Principal Concepts

and

Literature Review

2.1. Aeolian Islands

Aeolian Arc is a volcanic archipelago formed of eight islands (Vulcano, Lipari, Salina, Filicudi, Alicudi, Panarea, Basiluzzo and Stromboli) and numerous seamounts, located at the north of Sicily, in the southern Tyrrhenian Sea (Figure 2.1). Aeolian Islands are sometimes known as the Lipari Islands; Lipari is the largest island of the group.



Fig. 2.1. The location of the Aeolian Archipelago.

Vulcano, together with Lipari, and Salina represent an emerged portion of the NNW–SSE-elongated volcanic belt in the central part of the Aeolian Arc. This morpho-structural setting is related to the occurrence of a main NNW–SSE regional fault system (Ventura, 2013). See figure 2.2 for more information.

Romagnoli, et al. (2013) subdivide a different structural settings of the archipelago into western, central and eastern sectors.

The presence of a NW dipping Benioff Zone under the complex has been taken by Anderson & Jackson (1987) as the strongest evidence of subduction of the African plate under the southern Italian peninsula.

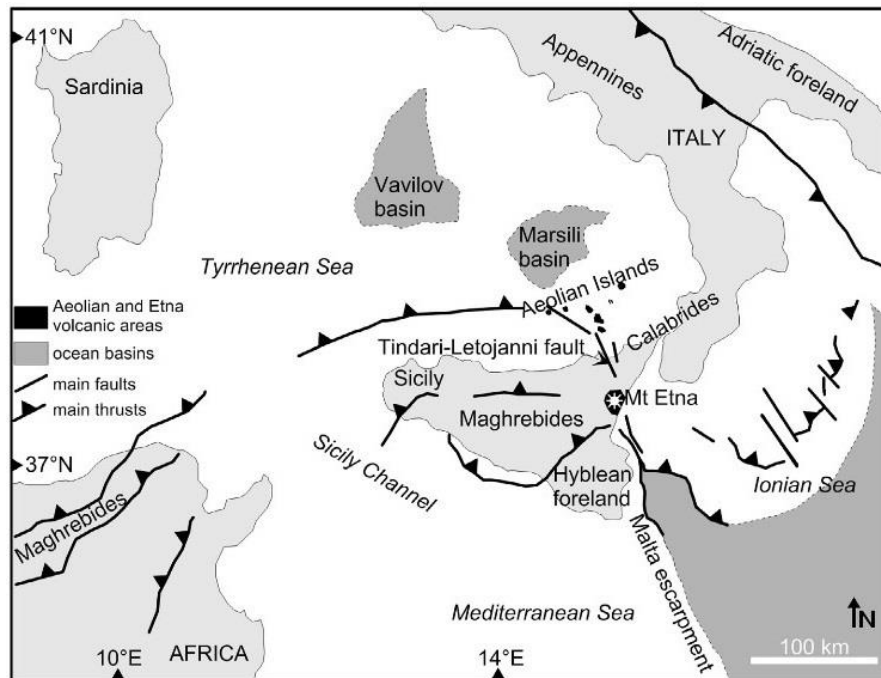


Fig. 2.2. Tectonic map of the south Tyrrhenian Sector (modified after Billi, et al. 2006).

Among all the islands of the arc, Vulcano and Stromboli are still active. The former is characterized by intense fumarolic activity while the latter by persistent explosion and effusion.

2.2. Vulcano Island

Vulcano that has lent its name to an entire branch of geology is one of Italy's active volcanoes with fumarolic activities around its crater, La Fossa. Vulcano is located at the central southernmost part of the Quaternary Aeolian Island Arc (Barberi, et al. 1994). Geographically, the island with a NW-SE trend is weakly elongated and has a small appendix at its northernmost part (Figure 2.3). With a 21.2 Km² area, Vulcano has risen from the bottom of the Tyrrhenian Sea circa 1000m below mean sea level up to the highest point of Monte Aria, 499m above mean sea level

(De Astis, et al, 2013). The underwater structure reaches up to 15 km in diameter (De Astis, et al, 2006) and the submarine flanks of the island have slopes ranging between 10° - 30° (Romagnoli, et al. 2013). Figure 2.3 illustrates the local names of different parts of Vulcano. Later, some of those local names will be used to refer to the sampling areas.

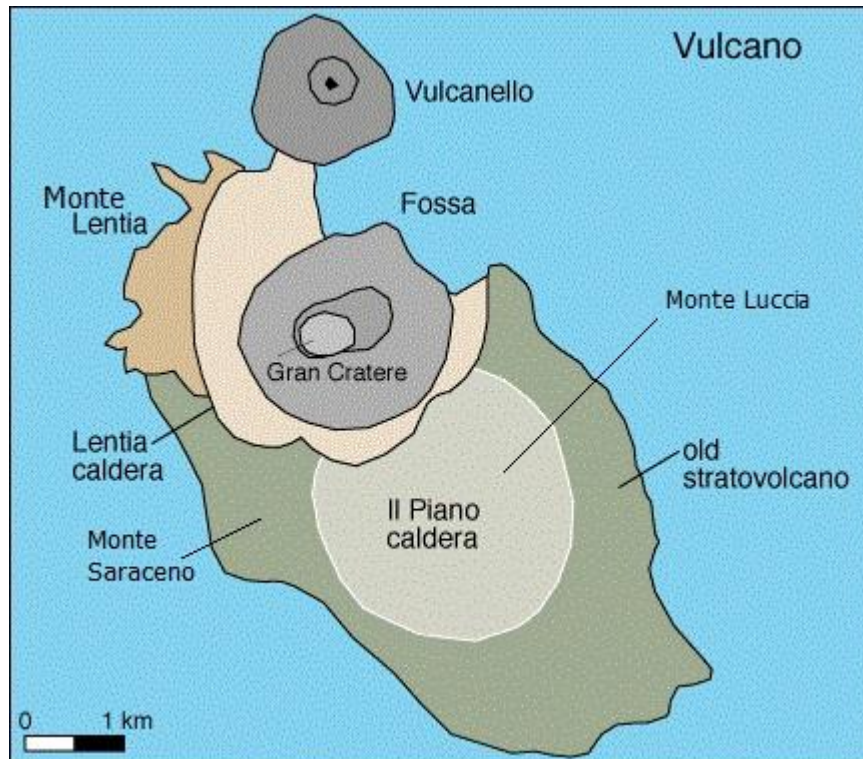


Fig. 2.3. Local names of different parts of Vulcano.

2.2.1. Geology of Vulcano

The island of Vulcano is a volcanic complex which as a part of a volcanic belt and together with the Lipari and Salina Islands cross-cut the archipelago from its central part along the Tindari–Letojanni strike-slip fault (De Astis, et al. 2003)

Vulcano is quite a young volcano that has volcanic activities from 130ka to the present. These volcanic activities are characterized by recurrent medium to high energy explosive eruptions at times associated with sector collapses (Pasquarè, et al. 1993). The present morphology of the island is mainly affected by two main collapses: 1) the first collapse of

the central part of Primordial-Vulcano which has caused the development of a caldera that is successively filled by the erupted products in three different periods and 2) the second collapse which occurred after 20 ka leading to the formation of a new depression called “Caldera della Fossa” which later is occupied by the Fossa cone in the northern sector (Frazzetta, et al. 1983). The rims of these two collapses are shown in Figure 2.4.

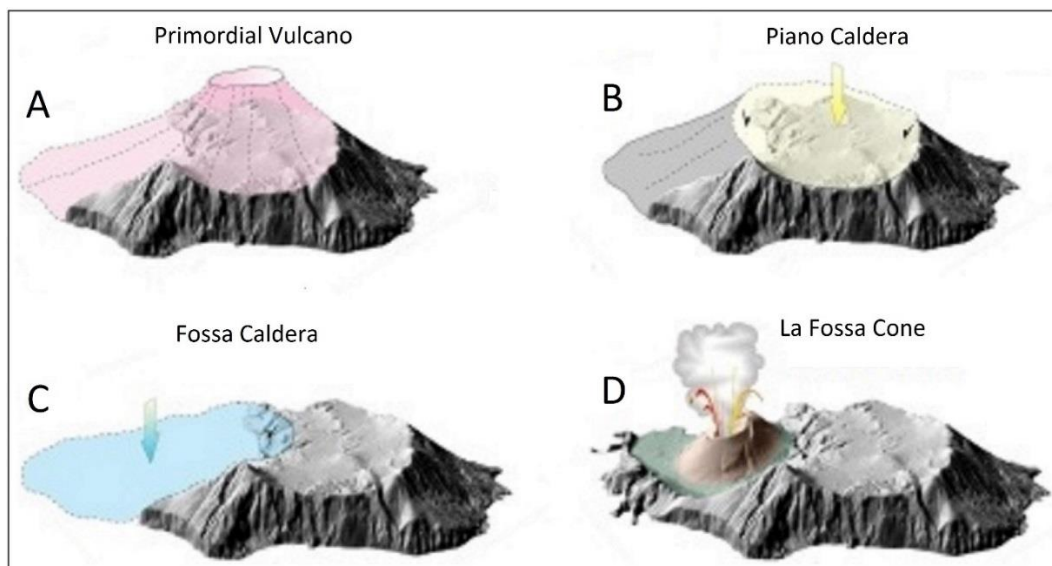


Fig. 2.4. A photo history of morphology of Vulcano (modified after Forni, et al. 2008).

The last eruption of Vulcano has been occurred in 1888–1890 AD (Mercalli & Silvestri, 1891). Presently there is intense fumarolic activity centred along the northern border of the Fossa Cone.

Since the last eruption to the present, Vulcano has been characterized by fumarolic activities which vary in the sense of their intensity and temperature. The maximum temperature of the fumaroles (690 °C) has been reported by Chiodini, et al. (1995).

After considering all the Stratigraphical, volcanological, and petrological aspects, six stages of evolution of Vulcano were determined by De Astis, et al. (1997). Table 2.1 summarizes these stages of the

CHAPTER 2. PRINCIPAL CONCEPTS AND LITERATURE REVIEW

evolution of Vulcano. Based on the tectonic setting, composition, the chronology of the erupted materials Peccerilo, et al. (2006) added more details to this classification and subdivided this evolution into seven main Synthems².

	Name of Stage	Age (ka)	Description
1	Primordial Vulcano	120 - 100	Lava flows; Scoriae deposits; minor pyroclastic units
2	Piano Caldera in-fill	> 20	A thick lava flow followed by tuff and/or products
3	Lentia Complex	24 - 15	Rhyolitic lava flows and extrusive domes overlying on explosive and effusive latitic products which contain subordinate trachytic juvenile clasts
4	Fossa Caldera deposits	15 - 8	Several pyroclastic and effusive volcanic units
5	La Fossa Cone	6	pyroclastic products and minor lava flow
6	Vulcanello	183 B.C.	Composite lava platform

Table 2.1. The evolutionary stages of Vulcano, subdivided by De Astis, et al. (1997).

Later, De Astis, et al. (2006) produced a new geological map of the island. According this map, and on the basis of the main unconformities, eight different formations have been distinguished in the deposits of La Fossa. In the time order, these formations are: (1) Punte Nere Formation, (2) Grotta dei Palizzi 1 Formation, (3) Grotta dei Palizzi 2 Formation, (4)

² Synthem: A chrono-stratigraphic unit that defines an unconformity-bounded regional body of deposits and represents a cycle of deposition in response to changes in relative sea level or tectonics.

CHAPTER 2. PRINCIPAL CONCEPTS AND LITERATURE REVIEW

Grotta dei Palizzi 3 Formation, (5) Caruggi Formation, (6) Forgia Vecchia Formation, (7) Pietre Cotte Formation, and (8) Gran Cratere Formation.

The majority of the La Fossa Cone is comprised of the oldest formation (Punte Nere) which is consisted of shoshonitic to trachytic phreatomagmatic pyroclastic density current (PDC) and fall deposits, and ends with trachytic lava. This formation has been dated by Soligo, et al. (2000), as $3800 \pm 900/800$ years old.

The erupted lava flows and bombs of Vulcano's recent eruption range in silica content from 58% to 72%, whereas the silica content of the of the glassy matrix of the rhyolitic lavas (shoshonitic group with high k_2O content) reach up to 75%. Also, the glassy particles of the pyroclastic deposits have almost the same range of compositions (Villari, 1986). The modes of the silica content of these pyroclastic deposits match the SiO_2 of the lava flows (De Fino & La Volpe, 1988).

The second formation is consisted of PDC and fall deposits; the third one of a PDC and fall deposits unit and a lava unit; the fourth one of a PDC deposits unit and a lava unit.

The Caruggi Formation (the fifth one) contains the products of the Breccia di Commenda (BC) explosive eruption of Vulcano and mainly consists of PDC and minor fall deposits (Gurioli, et al. 2012). Thick deposits of very thinly bedded, varicolored tuffs (De Astis, et al. 2006) lie above the BC. The BC eruption has been contemporaneous with the Mt. Pilato's activity of Lipari which is known by laminae of rhyolitic ash correlated with the Upper Pilato Pumice (Keller 1980; Frazzetta et al. 1983) interbedded with the BC. The age of the BC eruption has been assigned to 6th century, because the ash of Upper Pilato Pumice has laid on

the Roman ruins of 4th and 5th centuries (Keller, 1970). Also, the dating conducted by Bigazzi & Bonadonna (1973) confirmed the age of 6th century for the BC eruption.

The Forgia Vecchia Formation is made of lahar deposits which underlies the Pietree Cotte Formation, consisted of two stratigraphic units: fall and PDC deposits, and lava.

Eventually, there is the Gran Cratere Foemation which is the youngest formation of Vulcano. This formation consists of fall and PDC deposits, covered by fall deposits.

The magmatic evolution of Vulcano during the time created a wide variety of volcanic rocks with different K-alkalinity and a full range of acidity from basalt to rhyolite (Ellam, et al. 1988). The composition of recent materials from the Fossa is variable, ranging from trachytes to rhyolites (bread crust bombs from the 1888 eruption and obsidian from Pietre Cotte lava; Keller, 1980).

There have been many mineralogical and geochemical researches indicating that in the Vulcano there has been an active hydrothermal system of high sulfidation type (e.g. Fulignati, et al. 1999; Boyce, et al. 2007) that has affected both surficial and subsurface altered rocks of the island. The responsible acidic gases for this system mainly include SO₂, HCl, and HF which are released from a shallow magma (e.g. Clocchiatti, et al. 1994; Gioncada, et al. 1998) and ascended to the main crater.

2.3. Surface Coatings

Although considerable number of scholars have investigated it, the presence of thin, hard, and finely laminated surface coatings in many active volcanic areas on at least two planets of our solar system (Earth and Mars),

still is a challenging issue to research about. The genuine formation way of surface coating, the physical and chemical features of involved solid surfaces and fluids, determining possible supply source(s) of materials and their transportation procedure(s), and the modality of development of different microscopic textures are the most critical questions to be answered.

Almost all the reported surface coatings in the acid active volcanic precincts include amorphous silica associated with a sulfate phase as jarosite mineral. Hence, different theories about the affiliated subject or rather the mineralogical characteristics of jarosite will be discussed.

2.3.1. Jarosite mineral

In 1852, the jarosite mineral was discovered by Johann Friedrich August Breithaupt (a German mineralogist) in Barranco del Jaroso along the southeastern coast of Spain. He named this mineral “jarosite” after the name of its originally observed place (Anthony, et al.1990).

Jarosite (Jrs³) as a basic hydrous sulfate of potassium and iron is the head member of the jarosite subgroup within the alunite super-group with the general formula of $[AB_3(XO_4)_2(OH)_6]$, where A = Na⁺, K⁺, Ag⁺, Rb⁺, H₃O⁺, NH₄⁺, Pb⁺²; B = Fe⁺³, Al⁺³ (Fe⁺³ > Al⁺³), Cr⁺³; and X = S, As, (S > As), P (Dutrizac & Jambor, 2000). Empirically, most natural jarosites are solid solutions of jarosite (potassium end member), natrojarosite (sodium end member) and hydronium-jarosite (hydrogen end member) (Brophy & Sheridan 1965).

The chemical formula of jarosite (KFe³⁺₃(SO₄)₂(OH)₆) reflects the portion of its composition as: sulphur trioxide= 31.9 wt%; iron

³ All abbreviations for minerals are from Whitney & Evans (2010).

sesquioxide= 47.9 wt%; potash = 9.4 wt%; and water = 10.8 wt% (Dana, 1932).

The color of jarosite mineral is ocher-yellow, yellowish brown, and clove-brown. Figure 2.5 illustrates the common view of jarosite as seen in the field. It is brittle with a distinct cleavage in $c\{0001\}$, a hardness of 2.5-3.5, and a specific gravity of 3.15-3.26. Jarosite is translucent to opaque with a vitreous to sub-adamantine of brilliant to dull luster. Sometimes it can be confused with limonite or goethite which commonly occur in the gossans (oxidized cap over an ore body). The crystal of jarosite is uniaxial negative, it appears golden yellow in thin section and is strongly pleochroic in yellow and brown $O^4 > E^5$ [O = deep golden brown, or red brown; E = pale yellow, pale yellow-green, or colorless].



Fig. 2.5. Jarosite sample from the Coromandel Peninsula in New Zealand (Kotler, 2008).

The crystal system of jarosite is trigonal or hexagonal (Desborough, et al. 2010). The tiny crystals of jarosite are usually tabular plates on $\{0001\}$ or rhombohedral (Dana, 1932), rounded forms that appear as an encrusted

⁴ Ordinary ray

⁵ Extra-ordinary ray

CHAPTER 2. PRINCIPAL CONCEPTS AND LITERATURE REVIEW

coating on other minerals. It may be seen as granular, fibrous, or scaly with common small colloform structures (Philips, et al. 1981).

Besides the terrestrial occurrence, jarosite has been also found on Mars (e.g. Kraft, et al. 2003; Wray, et al. 2008; Farrand, et al. 2009), where the large shield volcanoes resemble Hawaiian shield volcanoes.

In addition to the different natural ways for the genesis of the jarosite, it can also be produced synthetically (e.g. Drouet & Navrotsky, 2003; Swayze, et al. 2008). Rothstein (2006) and references therein, mentioned the following 4 occurrences for the jarosite mineral on the Earth:

a) The first one is in the oxidized zone of ore deposits or pyrite-rich rocks such as coal, in which jarosite forms as a secondary coating phase on the other iron-sulfide minerals. Jarosite minerals also can be produced as a by-product of the metal processing industry, or associate with acid mine drainage and acid sulfate soil environments (Desborough, et al. 2006).

b) The second occurrence is in clays where jarosite exists either as nodules, small and hard lumps, or diffused in other clay minerals. It is thought that the oxidation of the pyrite in the clays provides the iron and sulfate, while the acid is drawn out of the clay and provides the alkalis (Rothstein, 2006).

c) The third is in acid soils. If the acidic substances of the soil are sufficient to make its pH around 3 – 4, and it happens in the marine sediments which usually contain pyrite, the jarosite will form and create yellow soil (Warshaw, 1956).

d) Finally, the fourth occurrence is as a hypogene mineral in the alteration zone, whereas jarosite is formed under the Earth's surface (Rothstein, 2006).

In general, the temperature, composition of the volcanic gases, duration of hydrothermal exposure, and oxidation following hydrothermal alteration are the most potential factors contributing to jarosite formation (Drouet & Navrotsky, 2003).

2.4. Jarosite bearing surface coatings

Thin and laminated Jrs-bearing rock coatings have been reported in many terrestrially active and passive volcanic areas such as Mauna Kea and the Ka'u Desert in Hawaii (Curtiss, et al. 1984); Mauna Loa in Hawaii (Farr & Adams, 1984); Kilauea in Hawaii (Naughton, et al. 1976; Malin, et al. 1983); Vulcano Island in Italy (Capaccioni & Coniglio, 1995; Fuglignati, et al. 2002); Aso Volcano in Japan (Matsukura, et al. 1994); Nicaragua, including Cerro Negro, Momotombo, and Telica Acidic Volcanos (Hynek, et al. 2013); and on the soils and even occasionally on the surfaces of remnant dead roots from previous vegetation, of four active volcanoes (the Arenal, the Turrialba, the Poas, and the Rincon de la Vieja) in Costa Rica (Jongmann, et al. 1996). These kind of coatings have been found on the Martian surface as well (e.g. Bishop, et al. 1999; and McLennan, 1999).

Generally, the appearance and the physical characteristics of these defined coatings are significantly alike, and only vary in minor details. Typically, the coatings are consisted of alternative amorphous, hydrous lamellae which are a few to hundreds micrometers thick. They are bright and colorless on younger and reddish-brown on older rocks. Yet, Fuglignati, et al. (1998) defined some coatings with irregular color gradation from white to red that have seamlessly coated the surfaces. This kind of coatings may or may not be interbedded with fine-grained clastic material.

CHAPTER 2. PRINCIPAL CONCEPTS AND LITERATURE REVIEW

The above mentioned textures are very similar to textures of desert varnish surfaces, reported by Perry & Adams (1978), Borns, et al. (1980), and Dorn & Oberlander (1982). Desert varnish is alternatively dark and light layered and different in contents of some of their elements; normally, it is enriched in oxides, silicon and detritus (Perry, et al. 2005).

Also, in some cases, surface coating can be as a knobby and finger shape thin coating as reported on the pahoehoe of Mauna Iki by Farr & Adams (1984), or as knobs coalescing into ridges more than 100 μm wide, in pyroclastic deposits surrounding the La Fossa Crater by Fulignati, et al. (2002). They have demonstrated a very comprehensive definition of characteristics of rock coating which are called “patina” or simply “RC” as abbreviation for “rock coatings”.

Depending on how far the rock coatings (RC) is from the La Fossa Crater, they have classified it into proximal and distal types which differ in mineralogy, texture, and chemical composition. A summarized definition of proximal and distal RC is demonstrated in table 2.2.

Furthermore, Farr & Adams (1984) described a thin glassy layer of silica under the scraped surface of the rock coatings of Hawaii. They determined the compositions of these coatings, via EDAX analyses, as the wholly silica and minor amounts of alumina and iron. The reported coating has a sharp contact with substrate.

Rock Coatings	Optical Microscopy	XRD	SEM-EDS
Distal RC	Silica Goethite Jarosite	Amorphous Silica Jarosite	Amorphous Silica Barite Jarosite: $\text{KFe}_3(\text{SO}_4)_2(\text{OH})_6$ Fe oxide-hydroxide containing: Cr, V, Zn, Sn, Ni and Cu Chloride bearing phases with : Ca-K, Ca-Fe, Fe-Ni, Na-Zn, Pb-Sb, (Fe), Cu-Zn and Ni Fe-REE phosphate-.sulphate Fe phosphate Native elements: Au, Ag, Hg and traces of Se and As

Table 2.2. Secondary minerals identified in distal RC (rock coatings) through optical microscope, XRD, and SEM-EDS investigation (from Fulignati, et al. 2002).

2.4.1. Suggested models for the formation of Jarosite-bearing surface coatings

According to many carried out studies, the formation rate of surface coatings is very fast. For instance, Curtiss, et al. (1984) calculated the average rate of coatings formation as 2.5 to 7.5 micrometers per 100 year.

Jarosite and fine grained magnetite-bearing soils, collected from a cinder cone in the Haleakala Crater Basin in Hawaii contain both jarosite and iron oxides/oxy-hydroxides which are expected by Bishop, et al. (1999) to form via hydrothermal alteration of glassy tephra in the presence of sulfur-bearing volcanic gases. In other words, volcanic steam vents are responsible for the production of hematite, maghemite/magnetite, and jarosite/alunite which usually in comparison with palagonitic alteration products are less common in volcanic areas (Calvin et al. 1994).

Barca et al. (1991) referred to the coatings on Italy's Vulcano Island as a particular magmatic event related to an interaction between a magma batch and a geothermal brine.

Fulignati et al. (2002) demonstrated that the RC on exposed surfaces to the volcanic acid plum is generally provided by passive degassing of the La Fossa active cone. In order to support this, they referred to the texture and secondary paragenesis of RC which show that the RC is a result of fluid-rock interaction processes. Additionally, the distribution of the RC matches to that of the fumarolic plume which is under control of the local winds. This idea is supported by the presence of chloride and/or sulfide components enriched in metals and volatiles, which are usually carried out by the volcanic aerosols.

CHAPTER 2. PRINCIPAL CONCEPTS AND LITERATURE REVIEW

Corresponding to the classification of RC into proximal and distal, the general formation way is considered differently. The RC forming processes in the proximal RC have affected the coarse grain pyroclastic materials and have welded them in a hard amorphous cement phase. As it has been implied in the definition of proximal RC, it is composed of almost only silica. This can be easily explained by the high sulfuric nature of Vulcano hydrothermal system (Fulignati and Sbrana, 1998). Therefore, its alteration facies represents strong acid condition and is mainly found in the high temperature fumarolic fields which characterized by the complete leaching of the protolith, $\text{SiO}_2 > 90\text{-}95\%$.

Meanwhile, distal RC has been formed due to direct interaction of fumarolic aerosol - rock and interaction of rains/dews acidified by the absorption of acidic gasses (SO_2 , HCl, and HF) from the fumarole plume with the volcanites. Albeit acid fluids incorporated in the RC formation are mainly yield of the interactions of acid fumarole plume with surficial waters and rock outcrops, but in the case of Vulcano Island, the rains are not as important as dew. Dew is present daily, but rains are sporadic little showers. In subsequence, the acidity of the fumaroles is strongly diluted by the high volume of water (heavy shower) and not able to react perfectly. As a result, RC forms in the surfaces exposed to more dew, instead of rain or washing away mechanisms.

Despite the thoroughness of this model which explains many physical and chemical features of the coatings, it includes a conflict. Since it claims that rock coatings form on the surfaces with low slope as they are less affected by erosional processes. This is while on the Vulcano Island, the thickest and most representative coatings are developed on the vertical surface of the big rock wall on the west side of the island.

CHAPTER 2. PRINCIPAL CONCEPTS AND LITERATURE REVIEW

Most of the proposed models by different researchers are affiliated with volcanic activities; at least one of these models supposes a completely volcanic-independent process (creation and development of rock coatings due to weathering in Hawaii, suggested by Farr and Adams, 1984).

The compositions of these coatings, via EDAX analyses are described as entirely silica and minor amounts of alumina and iron. The reported coating has a sharp contact with substrate. These scientists have considered a more physical approach than a chemical for the development of the coatings. Namely, the weathering processes exfoliate the surface of the rocks to the spalls and then these spalls remove from their original position and then carried out by the wind and alike the dust grains, adhere to the exterior part of the coating and afterwards they join to the coating or dissolve to form the coating. In this model, the formation of coatings has been related to the relatively wetter and dryer areas, stating that in wet areas, owing the hydration, oxidation and decationation reactions, rock surface breaks down to clay and typical oxide minerals of laterites (this means dominance of chemical weathering processes), while in dryer areas, instead, weathering includes the spalling process of rock surface (dominance of physical weathering processes).

On the other hand, Curtiss et al. (1984) have supposed a “dissolution-precipitation” method. In their model, as the beginning process, wind blows the fine-grained materials (locally derived components of future coating) to the rock surface. Availability of fine grained material is the most effecting parameter in this stage. Then, these materials dissolve in the atmospheric water such as fog or dew, where the wetting time of rock surface is very impressive. Finally, the solution evaporates and deposits the poorly ordered minerals which forms the surface coatings. Since in this

CHAPTER 2. PRINCIPAL CONCEPTS AND LITERATURE REVIEW

stage, the heavy showers can be wrecking and wash all the formed lamella away, the stability of the rock surface is a very important factor.

In this model, two points should be considered: the first is that coatings of amorphous silica are not stable in the wetter climates and have been restricted to the low-precipitation areas, as the more dynamic events such as heavy rainfalls can wash them away. The second one is the reason for the poor ordering of the clasts. During the evaporation the composition of the solutions change rapidly. Therefore, colloidal or gels develop instead of well-ordered crystalline minerals.

Yet, Curtiss Team has not depicted that how the all potentially present minerals in the coating can be dissolved in a very low quantities of water (fog or dew) within the pretty short time (in the most perfect case, less than 24 hours as no fog or dew in the arid or semi-arid areas lasts for a full day) they have.

Also, formation of alteration rinds (Jrs-bearing coatings) on the Martian Surfaces is premised by Bishop, et al. (1999) due to the interactions between the atmospheric dust particles and physical and chemical processes. They hypothesized that when the reactive particles of suspended dust such as sulfate or ferric-bearing phases are let to rest on the surface, long enough to reaction with the primary rock minerals, then resistant alteration rinds would be formed while the needed minimal water for this can be obtained from atmospheric ice particles.

Topography and precipitation rate are two influencing factors (in the case of weathering related models) and having the all potential requirements, eruptive flows of more than 100 years ago provide a good opportunity for early weathering.

CHAPTER 2. PRINCIPAL CONCEPTS AND LITERATURE REVIEW

Besides, the age of the underlying (the older it is, the more time it provides for the coating formation), the rate of material supply and mechanical stability of flow surface are the efficient parameters on the thickness of the coatings.

In sum, although the presented models, reflecting the process of rock coatings formation, are different in some aspects, they all have an identical point: acidic condition of environment during the coatings development, which corresponds to the precipitation of Jarosite minerals from sulfate-rich waters in the pH range of 1–3 (Alpers et al., 1989).

Chapter 3

Methods and Materials

3.1. Introduction

The present study involves the investigation of the nature of rock coatings at two volcanic islands and tries to find accurate answers for all those affiliated questions which have already been propounded in chapter 1 of this dissertation.

The general procedure to answer these questions started by bibliographical studies. In this way, tens of articles and geological maps and online sources, related to our topic, were obtained and studied. It should be mentioned that the library work was done not only at the first step, but also during the whole procedure of the research. Then, there was a period of field work followed by a period of analyzing and interpreting the collected data so that, it proceeded by the practical steps that included: getting the samples (the ready samples from previous works done by other researchers, as well as those collected from the field for just the purpose of this work); making thin sections and bulk samples, and preparing the samples for the special use in different analytical instruments; investigation of thin sections by binocular optical microscopes, and acquiring microscopic pictures; analyzing the prepared samples by different lab methods. The analytical methods used for the present work were: SEM-EDX⁶, ICP-MS⁷ (as both LA⁸ and liquid solution sample), Microprobe, XRD⁹, and Micro-XRD), which all will be described at the following.

⁶ Scanning Electron Microprobe - Energy Dispersive X-Ray Spectroscopy

⁷ Inductively Coupled Plasma Mass Spectrometer

⁸ Laser Ablation

⁹ X-Ray Diffraction

The benefitted facilities for the lab work were consisted of petrography labs of DiBEST¹⁰ in UNICAL¹¹ and School of Earth Sciences in UOB¹², SEM Labs of both universities, ICP-MS Lab of UNICAL, microprobe lab of UOB, XRD Lab of UNICAL and Micro-XRD Lab of NHM¹³.

After all these, it was turn to office work to gather all the data, recalculate the needed ones, plot them on some given graphs, and use them to get a sense making conclusion.

3.2. Sampling

The field work was essential in order to form a mental picture of the processes that are taking place at the volcanic island. This was done during the late November and early December in 2012 which included taking some demonstrative photos from the locations of the coatings, and taking some representative samples. The easiest way to access to the study area is taking boats/ferries from the board of Milazzo (a town in the northeast coast of Sicily Island). Also, hydrofoils are available during the summer.

To sample the study area, like many geological works, purposive sampling method was chosen. The samples have been taken from some parts of island which show more thickness of RC. Some samples with thinner RC, visible by naked eyes in thickness, have been taken too. For saving more time and energy and finance, the majority of samples used for examining were selected from those were already collected by some researchers of the University of Calabria. The samples are mainly from four areas of island (figure 2.3), having RC with rather more thickness:

¹⁰ Dipartimento di Biologia, Ecologia, e Scienze della Terra (Department of Biology, Ecology, and Earth Sciences)

¹¹ Università della Calabria (University of Calabria)

¹² University of Bristol

¹³ Natural History Museum

- a) Vulcanello (the northernmost and youngest part of island formed of lava flows)
- b) Monte Lentia (domes and lava flows located as a wall in the west of island, faced to the main crater)
- c) Monte luccia (southeast of island)
- d) Monte Saraceno (pyroclastic deposits, middle west of island in the south of Fossa Caldera)

Yet, during the latest field investigation in the 2012 winter, a few more samples, as the most representative coated rocks, were taken from the Monte Lentia (see figure 2.3).

Plus all the described taken samples from Vulcano, 23 samples of coated rocks from Stromboli Island, which have been previously collected by other researchers, were obtained (Appendix A presents the detail information of collecting these samples).

3.3. Petrographical Approach

After performing the field investigation and sampling, in order to do a wide petrographical study, about 150 thin sections were prepared. Before being observed under the binocular polarized optical microscopes, they manually were polished/re-polished by being rubbed in a paste, made of the 6 and 1 micron-diameter diamond powder and a lubricant, to let them reach to 30 μm thickness, and finally washed off by isopropane.

The optical microscope used for petrographical studies in UNICAL was a ZEISS Axioskop 40 with the magnification of 10x/20 in eyepiece and 1x/0,025, 5x/0,12, 10x/0,30, 20x/0,40 polarized objective lenses, equipped with an AxioCam MRc, all connected to a PC.

CHAPTER 3. METHODS AND MATERIALS

Further, the petrography fulfilled in the microscope lab of UOB with a PRIOR PX022pol Binocular with 1x, 5x, 10x, 40x objectives.

For acquiring some micrographs, a Nikon LV100-UDM-POL stereomicroscope with 2.5x, 5x, 10x, 20x, 50x, 100x objectives was used. The objectives were dry (not oil immersion), working fine for covered section up to 20x and uncovered ones up to 100x. The camera was a color one, with resolution from 640x480 pixel to 2560x1920 pixels. There was the possibility to use different tools, such as measurements (distances, angles, areas ...) and object counting. This microscope could be adapted to every specific needs, as it was very easy to remove or add pieces (heating-cooling stage, point counter). It had transmitted and reflected light, a polarizer and a rotating stage.

3.4. Analytical Methods

3.4.1. SEM - EDS

Pursuing the research, the mineralogical and micro-morphological probes, chemical analyzes of major elements, and linear analyzes of samples carried out in both the SEM Lab of the department of the Biology, Ecology, and Earth Sciences of UNICAL and the modern equipped SEM-lab of SES¹⁴ of UOB. Those for the former one conducted using the Cambridge Instruments Stereoscan360S equipped with a SUTW (Super Ultra-Thin Window) X-ray microanalysis detector, a crystal Si/Li PHOENIX model of EDX. For the both thin sections and bulk samples, selected for studying by SEM, became carbon coated. the sample preparation system was a Sputter Coater with a Carbon Coater model Q150T ES - QUORUM TECHNOLOGIES which within a turbo molecular

¹⁴ School of Earth Sciences

pump (TMP), the pure carbon from 5nm thick rods by pulse-lengths of 3 seconds lied on the samples in an ultimate vacuum (5×10^{-5} mbar). For the SEM itself, an accelerating voltage of 5/40 KV and the signal types of SE (Secondary Electron image) and BSE (Back Scattered Electron) were applied.

In proceed, some of thin sections as well as some bulk samples were chosen for re-examining in UOB. Using an EDWARDS AUTO306 Carbon Coater, the thin sections were coated by pure graphite. Then some random spots of each sample were analyzed. Here, The SEM was run in conjunction with two electron microprobes, which enabled us to provide a full range of electron and x-ray imaging, together with in-situ chemical analysis of both major and minor elements heavier than carbon. The scanning electron microscope facility was operating a Hitachi S-3500N variable pressure microscope equipped with Thermo Noran Ultra-dry energy dispersive spectrometer (EDS x-ray detector). The microscope was fitted with a tungsten filament which was producing a stable and high beam current, making it ideal for x-ray analysis. Ultimate resolution is better than 10 nm at 25 kV, using the secondary electron (SE) detector, so we chose that mode. The instrument also was equipped with a backscatter electron (BSE) detector which was allowing imaging of specimens that had a mean atomic mass change of $\sim >0.1$. Detection limits were in the order of 0.5 wt% (depending upon element and operating conditions).

3.4.2. Microprobe

Later, in order to go from the whole to the part, using the microprobe, some linear analyzes accomplished on the samples. The linear analyses, with the consecutive spots of 1 μ m diameter were performed by uses of a JEOL JXA-8530F FIELD EMISSION Electron Probe Micro-analyzer,

equipped with five JEOL Wave Dispersive Spectroscopy (WDS) and one JEOL Energy Dispersive Spectroscopy (EDS). The analyses were achieved by an accelerating voltage of 15kV and the beam current of about 9.8 nA. Before each set of analyzing, the necessary calibrations were carried out using international standard samples for the Na, Mg, K, Ti, S, Ca, P, Cl, Cr, Fe and Mn elements.

The software, used for transforming the result data to an user-friendly format and also for re-demonstrating the images and the graphs was NSS Thermo-Pc, version 1.0.

3.4.3. ICP-MS

3.4.3.1. Laser Ablation (LA-ICP-MS)

The inductively coupled plasma mass spectrometry (ICP-MS) analyzes carried out by using an Elan DRCE instrument (Perkin Elmer/SCIEX), connected to a New Wave UP213 solid state Nd-YAG laser probe (213 nm). In a chamber with a moderate flow of pure He gas, samples were ablated by laser beam and the ablated material was flushed in a continuous flow of a helium and argon mixture to the ICP system, where it was atomized and ionized for quantification in the mass spectrometer. The initial alignment of the instrument was performed through solution nebulization, whereas a second optimization of LA-ICP-MS was obtained using NIST612-50 $\mu\text{g g}^{-1}$ glass reference material. Ablation was fulfilled with spots of 50, 80 μm , with a constant laser repetition rate of 10 Hz and fluency of $\sim 20 \text{ J cm}^{-2}$. Data were transmitted to a PC and processed by the Glitter program. Calibration was carried out using NIST612-50 $\mu\text{g g}^{-1}$. Internal standardization to correct instrumental instability and drift was achieved with SiO_2 concentrations from SEM-EDS analyses. The monitored isotopes were: ^{107}Ag , ^{75}As , ^{137}Ba , ^{114}Cd , ^{53}Cr , ^{59}Co , ^{63}Cu , ^{57}Fe ,

^{177}Hf , ^{55}Mn , ^{98}Mo , ^{93}Nb , ^{60}Ni , ^{208}Pb , ^{85}Rb , ^{121}Sb , ^{45}Sc , ^{120}Sn , ^{88}Sr , ^{181}Ta , ^{232}Th , ^{49}Ti , ^{238}U , ^{51}V , ^{89}Y , ^{66}Zn and ^{90}Zr ; and for REEs were: ^{139}La , ^{140}Ce , ^{141}Pr , ^{146}Nd , ^{149}Sm , ^{151}Eu , ^{157}Gd , ^{159}Tb , ^{163}Dy , ^{165}Ho , ^{167}Er , ^{169}Tm , ^{173}Yb and ^{175}Lu ; but only the elements: Co, Ni, Sr, Y, La, Ce, Eu, Yb showed significant concentrations that can be used for our purpose¹⁵.

3.4.3.2. Solution nebulization

Along with benefitting the LA analysis, the trace elements composition of whole rock was determined using an ICP-MS system by solution nebulization. First, two samples were selected for making the solutions to be analyzed. Then, about 100mg of the powder of each sample was dissolved in a mixture of hydrofluoric acid (2ml HF), nitric acid (8ml HNO_3), and perchloric acid (2ml HClO_4). All acids were from Merck “suprapur” quality, into teflon (TFM) digestion vessels. The powder were dissolved by microwave digestion using Mars5 microwave apparatus (CEM technologies).

Before the completion of acid evaporation, 2ml of perchloric acid was added to the solution to ensure the complete removal of hydrofluoric acid. Then, in order to obtain the mother solutions, the liquid samples were left to cool down gently and later they were diluted to 100ml with Millipore Water.

For each sample, two diluted daughter solutions (1/4 and 1/5) were prepared. Internal standard indium, germanium, and rhenium were used, whereas the external calibration curves were prepared using Merck and Perkin Elmer standard solutions. Three external calibration curves were prepared: the first was prepared with Merck “ICP multi-element standard

¹⁵ The method is comprehensively defined by Barca, et al. (2011)

solution VI” to analyze As, Ba, Be, Cd, Co, Cr, Cu, Mn, Ni, Pb, Sb, Sc, Se, Tl, V, Zn; the second was prepared using Perkin Elmer “multi-element Calibration Standard 2 solution” to analyze REE (La, Ce, Pr, Nd, Sm, Eu, Gd, Tb, Dy, Ho, Er, Tm, Yb, Lu) and Sc, Y and Th.

Standard reference materials (BCR2 Columbia Basalt River by USGS) were prepared in the same way and were used as the unknown samples. Eventually, to evaluate the accuracy and the precision of the analytical data, the concentrations of the elements were compared with the certified values.

3.4.4. XRD

A Bruker AXS Diffraction Solution (model D8 ADVANCE) Machine was benefitted to determine the crystalline phases of two of our samples. To match the crystalline phases to the measured reflections in the diffractogram a DIFFRACplus SEARCH was used, which compared the entire diffractogram with tens of thousands of entries in the latest ICDD¹⁶ data base.

There was neither a restriction to only the most intense reflections nor where reflection asymmetries or shoulders disregarded. This scientifically recognized method ensured that we were also be able to reliably analyze rigorous and complicate phase mixtures with complex peak overlaps.

3.4.5. Micro-XRD

The last and the only series of analyzes which were conducted by the facilities out of the universities were Micro-XRD analyzes which were accomplished in the modern equipped X-ray lab of Natural History

¹⁶ International Centre of Diffraction Data

CHAPTER 3. METHODS AND MATERIALS

Museum of London. These included two series of the analysis, done on polished samples or thin section, and on the powdered rocks.

For the first mentioned ones, a GeniX Cu high flux X-ray source, (Cu source had a wavelength of K alpha = 1.5402 Å (this was K alpha 1 and 2)) was used. A FOX 2D 10_30P mirror was focusing the X-ray beam to 230 micron and an INEL 120° position sensitive detector (PSD) enabled rapid data collection simultaneously over 120° 2Theta. The operation ran under the conditions of X-ray source 50KV and 1mA, Collimator with a pinhole of 100 micron. The samples were measured in flat-plate asymmetric reflection geometry (no angular movement of tube, sample and detector position).

Incidence angle of the X-ray beam between sample and X-ray source was about 10° 2Theta and the beam footprint on the sample was about 0.1 x 1 mm.

Angular linearity of the PSD was calibrated with silver behenate and Y2O3 as external standards. 2-Theta linearization of the PSD was performed with a least-squares cubic spline function. These were measured directly on the thin sections.

Yet, the second series, on powdered samples, were carried out by an Enraf-Nonius PDS 120 X-ray diffractometer. By using Ge monochromator (in primary beam path), Cu K alpha 1 radiation was done. With an operating conditions of 40 kV and 40 mA X-ray source, rapid data acquisition by using an INEL 120° curved position sensitive detector (PSD), and simultaneous data collection over 120° 2Theta were conducted. Constant tilting angle was between incident beam and sample surface about 5° 2Theta. Horizontal and vertical slits with the dimensions of 0.14 x 5 mm were made to confine the beam dimension. Silicon powder (NIST SRM

CHAPTER 3. METHODS AND MATERIALS

640) and silver behenate were used as calibration standards. The 2-theta linearization of the PSD was performed using a least-squares cubic spline function. Sample powders (a few tens of milligrams) were placed on sapphire substrates with a drop of acetone, sapphire substrates are zero-background holders cut in a way to produce very low background. The samples were rotated during the measurements.

Finally, the powder diffraction file PDF-2 from the International Centre of Diffraction Data (ICDD) was used as a source for phase identification.

Chapter 4

Findings and Discussion

4.1. General

In this chapter, the results of the carried out investigations will be showed. Then, there will be tried to interpret the findings and achieve a reasonable relation between all the found out results.

Beside the interesting nature of the subject itself, this thesis offered the possibility to get acquainted with various optical techniques. Yet, the petrographical examinations became more and more fascinating and we would have liked to study it for some more time. Then, in the next step and after the optical observations, the chemical analysis were accomplished. The combination of these optical techniques with chemical analyses was a fascinating one.

It is already mentioned that the main aim of the present work was to understand the scenario of the birth of surface coatings (SC). Still, we were interested to find out an appropriate model for the formation of the different textures in SC. To do this, first, all the findings from the field investigations, petrographical, and geochemical studies will be expressed. Later, our suggestions and possible hypothesis will be discussed.

4.2. The results of the field investigations

Although, surface coatings have lied on various lithology of the Vulcano Island, their role appear more significant in the case of basic volcanites and pyroclastic rocks. Sometimes, in our study area, on the surface of a macroscopically homogenous basalt, two kinds of coatings may be seen at the same time: a) black and shiny varnish, made of bivalence metallic elements oxides, which is ordinary product of chemical weathering of basaltic flows; and b) the brownish red coat which is mainly

CHAPTER 4. FINDINGS AND DISCUSSION

contained of sulfur bearing minerals (the mineralogical and chemical composition will be discussed soon).

Generally, in this research, the first mentioned group won't be discussed so that from now on, wherever it's referred to surface coatings (SC), the second group (group b) should be taken in account.

In the Vulcano, the thickest SC can be found on the pyroclastic rocks of the west part of the island which is vertically exposed to the fumarolic gasses released from the La Fossa Crater (chapter 2).

Our SC usually appears as a very hard and shiny reddish (sometimes pinkish) brown rind with a greasy luster and it adheres to its substratum and follows the major irregularities of the surface, but completely seals the micro-cavities (Figure 4.1).



Fig. 4.1. A typical view of SC in the macroscopic scale (sample F019¹⁷ taken from Monte Lentia in Vulcano).

¹⁷ Coordination of the sample by GPS is N 38 24. 329 - E014 56. 787 - Alt. 400 ft.

CHAPTER 4. FINDINGS AND DISCUSSION

Depending of the substratum, its thickness varies and ranges between a few micrometers to about 2 centimeters (usually thicker on the pyroclastic rocks and thinner on the lavas).

In the field, the SC can be found on all horizontal, diagonal, and vertical surfaces. The SC on the big rock wall of Monte Lentia is the most eye catching example of SC on vertical surfaces (Figure 4.2). This wall is located in the northwest of the Vulcano and with an N-S trend faces to the degassing crater of La Fossa Cone.



Fig. 4.2. The rock wall of Monte Lentia, covered by SC.

Usually, the SC has coated the solid surfaces of the rocks (Fig. 4.1), but it also can be seen on the two sides of some fractures (Fig. 4.3). Compared to the narrower ones, the wider fractures have more developed SC on their sidewalls.

In some cases, SC has formed and distributed from the ground surface downward, depending on the direction of surface water and runoff flow (Figure 4.3).

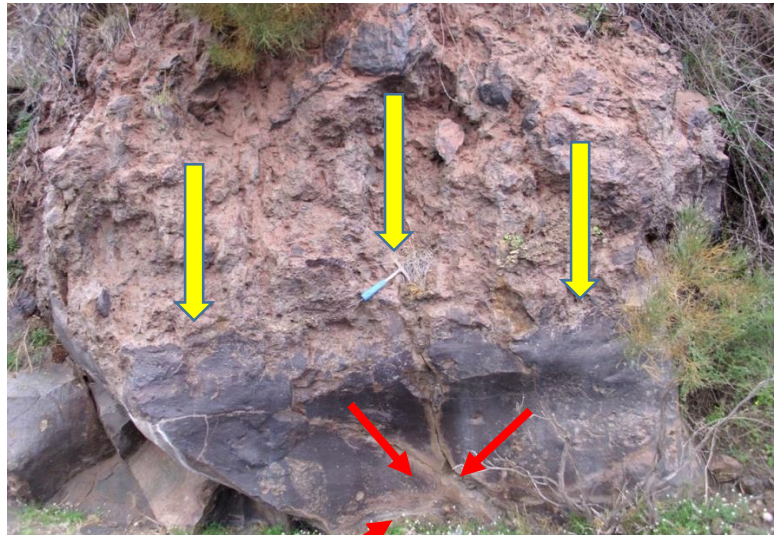


Fig. 4.3. Following the direction of runoff waters, the SC has formed downward (yellow arrows); the SC on both sides of the fractures (red arrows).

Also, in one single case, a thin layer of purplish-colored SC was found on the surface of some weakly layered unconsolidated sands (Figure 4.4).

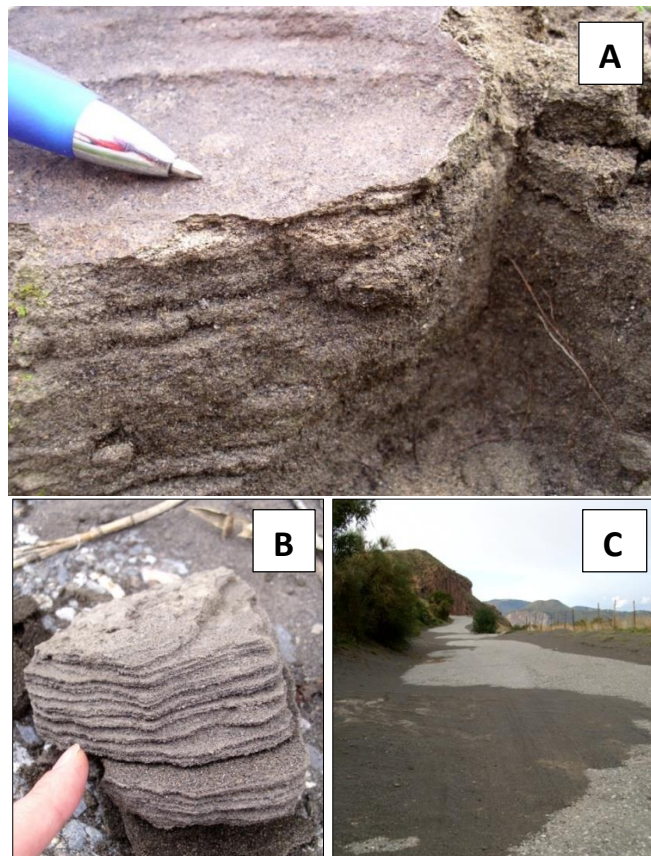


Fig. 4.4. A) the SC on the surface of loose sands; B) easily differentiated layers of unconsolidated materials (Part A of this figure, while trying to make sampling); C) totally strewn grains of the A and B parts of this figure, after a storm.

4.3. Petrographical findings

To conduct the petrographical studies, firstly, every single one of all the 150 thin sections was studied under the optical microscope. Then, the thin sections with trivial SC, and the ones which were vague and incapable to show a clear view of the SC were eliminated. These thin sections might or might not include some ordinary altered (weathered) mineral crystals/glasses.

Still, there were about 100 thin sections left for a deeper investigation. To be able to handle the results better, the thin sections with alike characteristics of the SC were classified into two main classes:

Class I- (Steady and thin lamination on the surface of the rock, with or without micro-pits or curved micro-depressions):

In this type, the SC appears as a few parallel dark and light laminae (usually not more than 10) laid on the whole or part of the outer rim of the rock or on the boundary between two rocks with different textures and/or mineralogy. A set of laminae has an even thickness unless it becomes a few times thicker to fill the micro-cavities or micro-depressions.

This class of SC is developed on the outer margin of the basic rocks that have porphyry textures and show no porosity in their entire body.

Class II- (Laminations + Lentic districts of clastic material ± Intersections of laminae ± Convoluted texture of laminae):

Within this type which is more complicated than type I, the positions of different subsets of laminae of SC create diverse textures. The subsets commonly are branched and joined again so

CHAPTER 4. FINDINGS AND DISCUSSION

that many lentic (symmetric or asymmetric; often elongated) districts have been formed in the trapped spaces between these laminae. These districts, showing a clastic texture, include mineral crystals (mostly phenocrysts of pyroxene group, feldspar group, opaque minerals, and sometimes other minerals like iddingsite, zeolite group) glass shards (usually fresh and not-altered with absolute sharp edges) within a glassy or spongy background.

This class is formed on the surfaces of the pyroclastic substrates, which are mineralogically composed of pyroxenes, feldspars, opaque minerals, and quite a lot of glass shards within a permeable background (the geological units containing the pyroclastic deposits are described in chapter 2).

On the whole, as the common specification in both above mentioned classes, the typical SC demonstrates a very fine lamination with the successive light and dark laminae (e.g. fig. 4.5 and fig. 4.8). Depending on their composition and thickness, the light laminae can be seen as colorless, white, light gray, golden yellow, light brown, light orange, and creamy, while the colors of the dark laminae are ranging from reddish brown to dark brown and crimson.

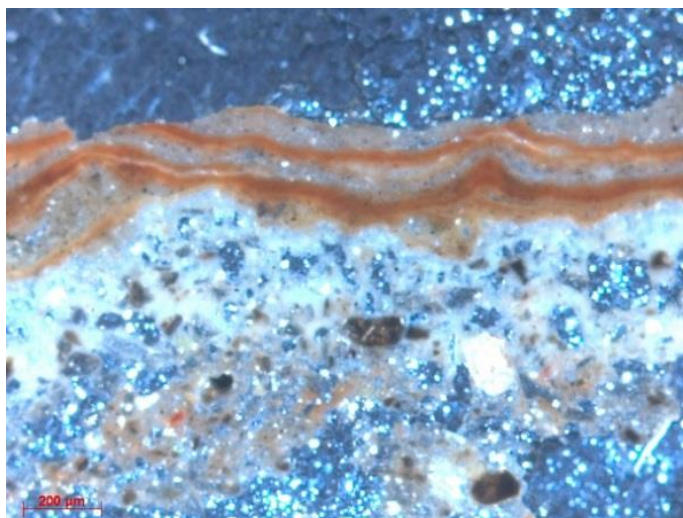


Fig. 4.5. Light and dark parallel lamination of the SC on the border of the rock (taken in CPL¹⁸).

All these laminae are formed in parallel sets and have laid down on the outermost brim of the rock. The parallel laminae of SC are evenly and smoothly sealed the margin of the rock and usually follow the irregularities of the surface, but it is also common seen that every now and then they have become ticker in the form of some micro-depressions (Fig. 4.6).

As mentioned before, under the microscope, the SC can be seen in two main forms: a) one main set of laminae on the surface of the rock; b) many subsets of the laminae, branching and being deviated in different directions. These subsets display very spectacular textures. They usually encompass lens shaped portions of the rock which have composed of different clastic components such as mineral crystals, glass shards and crypto crystalline matrix. This kind of texture absolutely resembles an eye-texture in the metamorphic rocks whereas our study cases are certainly not metamorphed volcanic rocks (fig. 4.7). The forms of the encompassed areas vary from a symmetrical lentic shape to elongated concave form.

¹⁸ Crossed Polarized Light

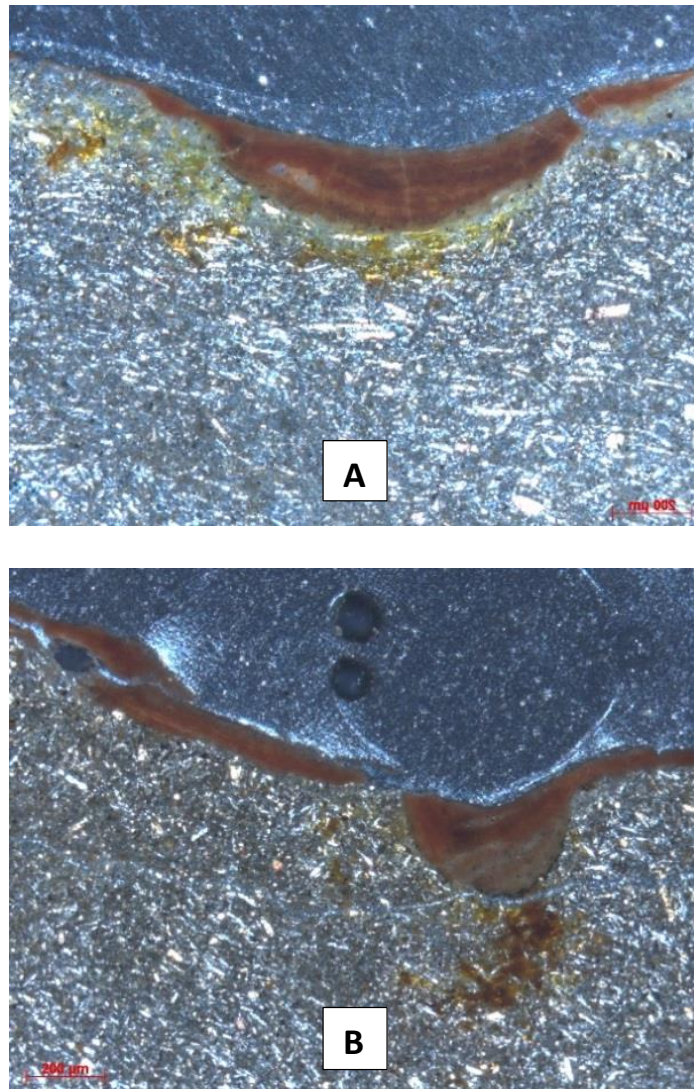


Fig. 4.6 A) A micro depression of SC (CPL);
(B) Lamination of SC filling a micro-cavity/micro-depression (CPL).

While, branching and forming eye-like/lentic templates is very frequent in SC, still the trend of each subset in continue can create many interesting forms. The subsets of laminae have various spatial forms which in their relative positions to each other and to the clastic portions, create different textures.

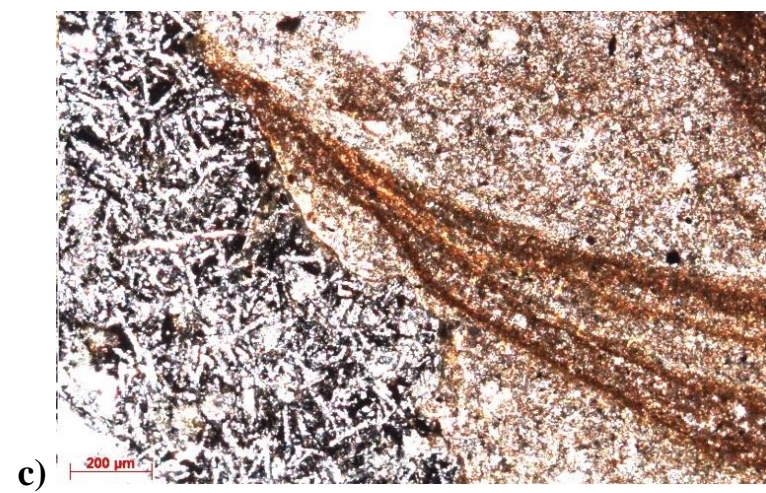
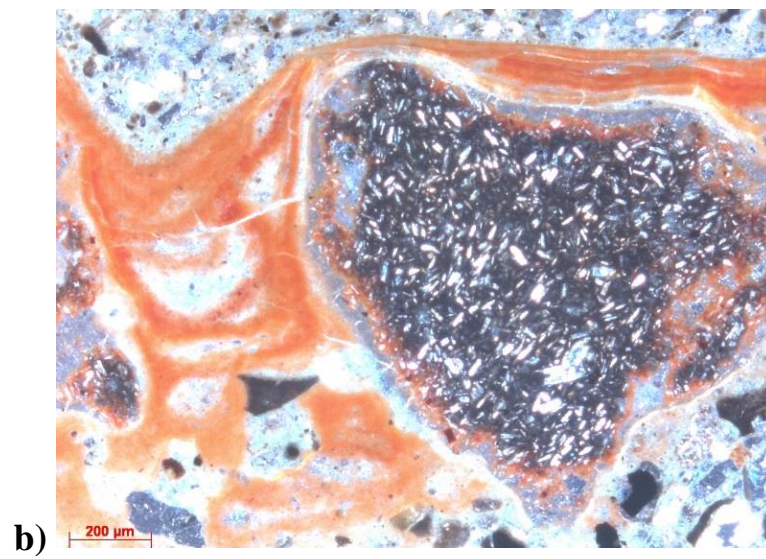
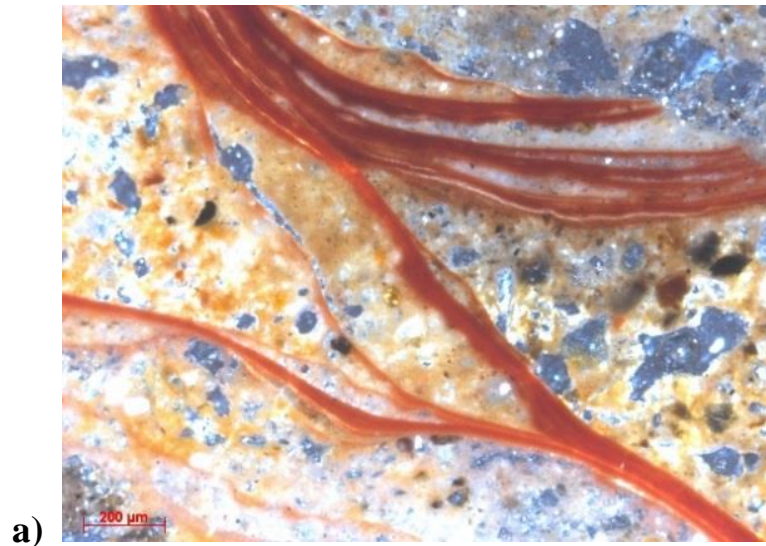


Fig. 4.7. Lenticular form of SC with some crystals inside (PPL¹⁹).

The subsets that are severed branches of the major set of the laminae may be continued and join other subsets; cross and pass each other; meet the other subset and end in the cross point with an acute angular or perpendicular junction (in the later form, the junction creates Tee texture which is a T-shaped cross point); curve like a flow and make convoluted templates; form a micro-cross bedding texture; or even lie down on the internal circumstances of the holes. Some of these holes have a polygonal shape which represent the location of idiomorphic ex-phenocrysts which are now removed, and some seem to be just asymmetrical bubbles, or the location of ex-microlithic fragments without having any geometrical form. Also, the holes are different in contents. Most of them include some clastic materials inside whereas there still are some completely empty ones (fig. 4.8).

¹⁹ Plain Polarized Light

CHAPTER 4. FINDINGS AND DISCUSSION



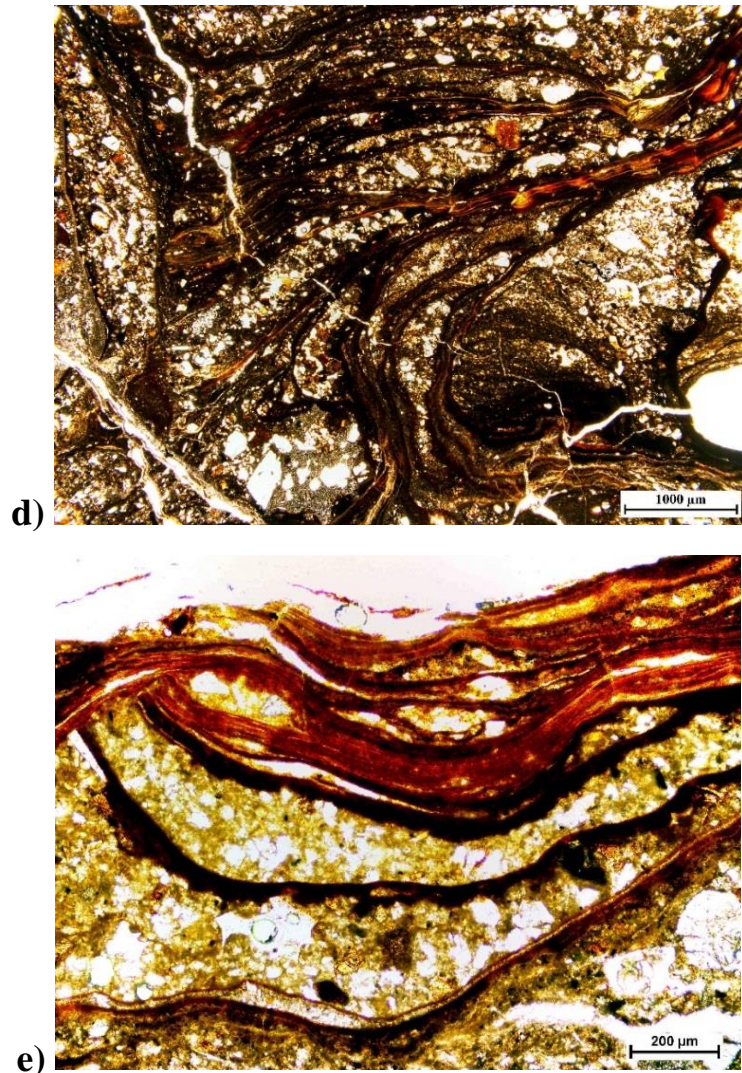


Figure 4.8. a) branching and rejoining of subsets of SC (CPL); b) compacted laminae on a microlithic fragment which have been divided and flowed into a hole (CPL); c) Reference point of laminae branching from the boundary between two rock types (CPL); d) Tee-shape junctions, convoluted texture (PPL); e) different subsets have surrounded eye-like and elongated concave lentic areas (PPL).

In all samples, the SC includes at least one type of the aforementioned groups of laminae, but this doesn't mean that the SC is always made of merely these laminae. Whenever the SC is not only one simple set of alternative laminae, and the laminae are multiply divided and curved, they are accompanied with massive portions of rock. In other words, the laminae have encompassed some non-laminated parts of the rock which these

CHAPTER 4. FINDINGS AND DISCUSSION

districts have their own special physical and chemical characteristics. The massive portion of SC consists of particles which can be classified into three main groups:

- 1) Colourless to dark brown glass shards of variable dimension (from a few microns to 0.1 mm). They show different colours as well as different shapes. The glassy particles appear in two main forms: the first group are elongated, bubble-walled splinters with very acute edges. They are colourless or very light coloured and have clear and crackless surfaces; the other group are glass shards with more or less equal dimensions (not elongated), dark orange to brown, still with sharp corners (less sharp than the first group). Contrariwise the first group, these glass shards contain many tiny micro cracks on their surfaces. Figure 4.9 shows a lentic district containing many glass shards.
- 2) Idiomorphic micro phenocrysts of plagioclase, k-feldspar, clinopyroxene, and opaque minerals. Sometimes, curved edged lithic components can be seen too (e.g. figure 4.8.b). These lithic rounded particles seem to be micro-lithic fragments within their related erupted materials.
- 3) Other materials which include the microcrystalline to cryptocrystalline background or spongy-looking micro-refractive aggregates of colloidal silica.

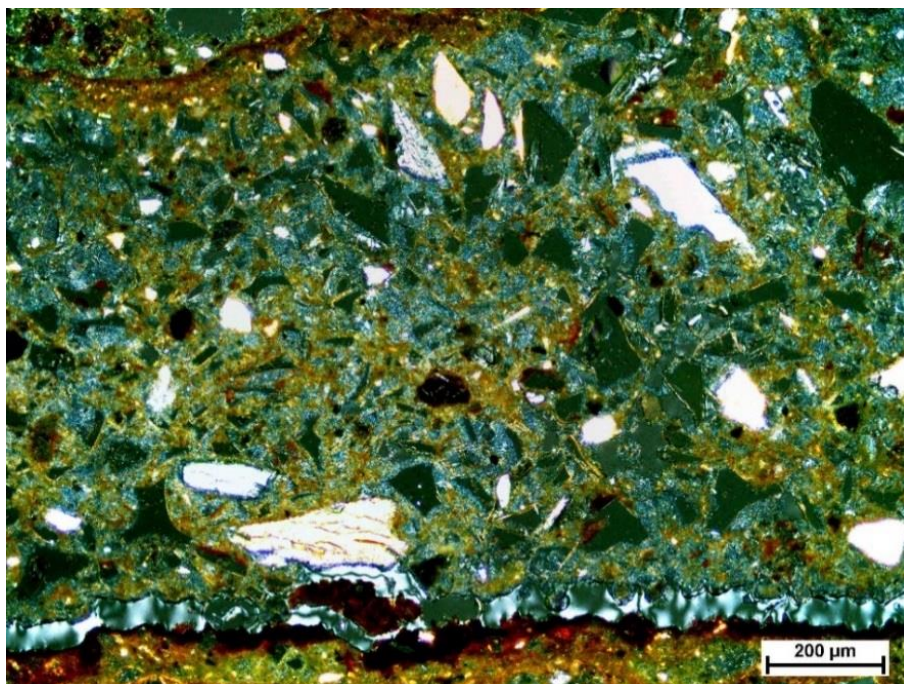


Fig. 4.9. Different shapes of the glass shards (CPL).

Beside the optical microscopes, also SEM was utilized for a deeper investigation of the micro morphology of SC in thin sections. It should be mentioned that only the thin sections and polished bulk samples were used, so it could provide just two dimensional morphological data. Anyhow, from a single sample we had prepared many thin sections in different angles. Accordingly, we could have a simple rough imagination of the three dimensional shapes and sizes of the components.

Using the SEM the shapes of the crystals in the lentic areas as well as the structure of the laminations were more obvious (fig. 4.10). Also, the thickness of the very fine laminae was precisely measured. The thickness of each lamina ranges from about $0.3\mu\text{m}$ to $7\mu\text{m}$.

The SEM studies revealed another form of mineral crystals which couldn't be seen and recognized by optical microscope. Plus all the materials which previously are defined in above, some tiny needles of

CHAPTER 4. FINDINGS AND DISCUSSION

minerals were observed. These needle shaped crystals, as secondary minerals, are formed in empty spaces between the other common materials and often are radially grown outward from a virtual centre, or simply are overlapped each other without fitting in any special format (fig.4.11). Due to the complicated chemical composition of them (e.g. the data rows from F186(20)-P1 to F186(20)-P5 in Appendix B), it was not possible to determine their exact mineral phases, but they can be assumed as zeolites, because zeolite in its crystalline structure can consist all the same elements with more or less the same proportions which are determined in these needles.

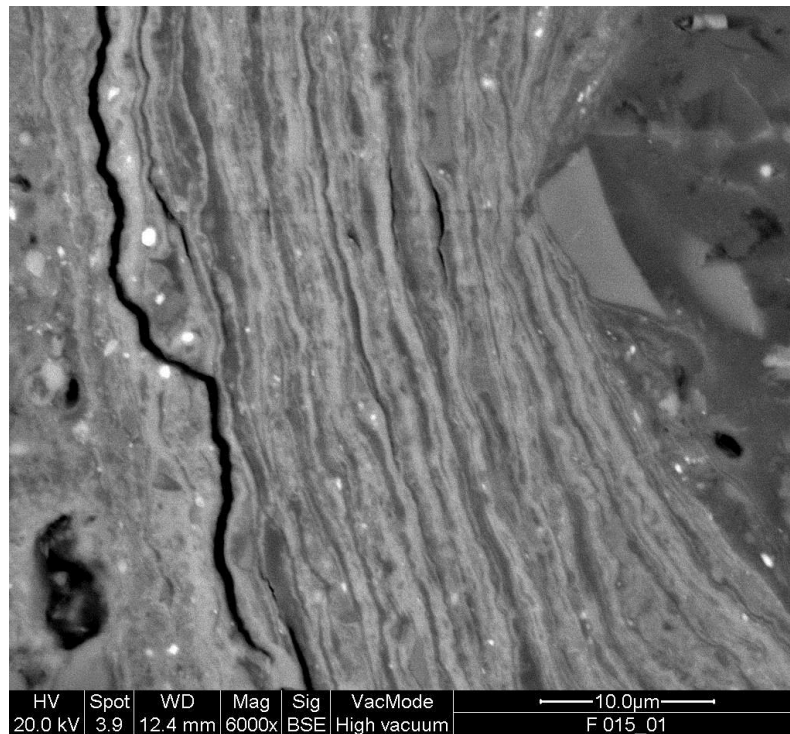


Fig. 4.10. Clear view of the typical lamination of SC (photo by SEM).

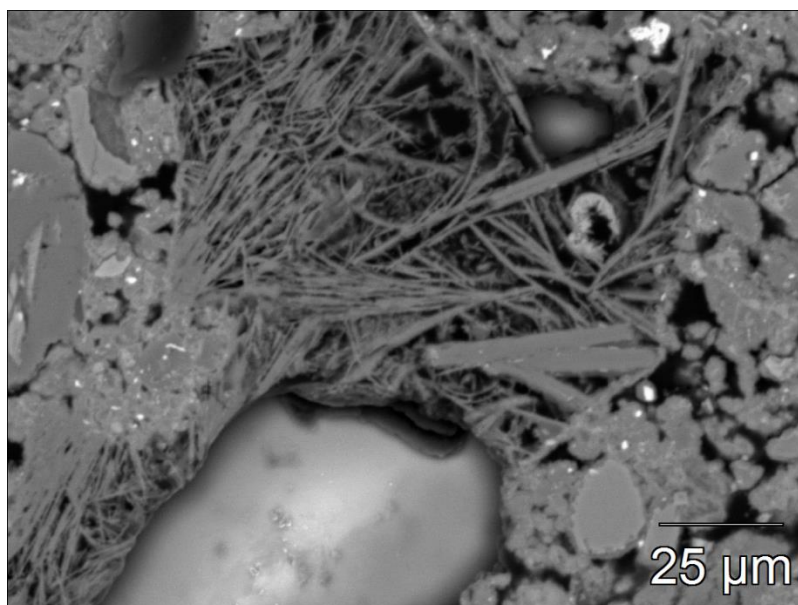


Fig. 4.11. Needle shaped crystals of secondary minerals (photo by SEM).

4.4. Results of the XRD

In the primary evaluation by XRD, two samples (F019 and F030) were analyzed. The mineral phases of these two samples were determined as jarosite, diopside, augite, another anorthosite, sanidine, and calcite. The presence of calcite made a doubt about the accuracy of the XRD analyzes, since we were sure about not having calcite in our samples. Therefore, those samples beside other representative samples were selected to be examined by the modern Micro-XRD method. The common minerals in the all investigated samples were jarosite, pyroxene (diopside or augite), feldspar (sanidin, anorthite). In some samples, trolleite mineral was distinguished as well, but considering its occurrence (in the amphibolite-grade metamorphic rocks) it assumed to be mistaken by the machine which is a quite possible and common case during the investigation of very low content of the analyzed materials (Appendix D).

CHAPTER 4. FINDINGS AND DISCUSSION

4.5. Geochemical findings

After accomplishing the petrography of all the thin sections, geochemistry seemed to be the best way to get some probable clues of the geological history of the SC. Geochemical evidences could be strong enough to support or refuse the preliminary hypothesis about the story of the SC's formation. Obviously, considering the limitations of the time and the facilities, it was not possible to analyze all the in-hand samples. Thus, the most representative and well prepared samples were selected to be analyzed. Since, some specific areas in the Vulcano, possess tigger SC than the other parts, also the sampling points are been considered to select the representative samples for geochemical analysis. Table 4.1 demonstrates the name of the selected samples for different kinds of analysis.

Location	SEM-EDX	Microprobe	ICP-MS		XRD	Micro-XRD
			Sol ²⁰ .	LA		
EGS-18C	F010					
EGS-48	F014					F014
EGS-14C	F015					
Lentia Wall	F019		F019	F019	F019	F019
EGS-48A	F030		F030	F030	F030	F030
8B	F032			F032		
Vulcanello	F040					
Monte Lentia	F041					
Monte Saraceno	F042					
Monte Luccia	F043					
Monte Lentia	F185					F185
Monte Lentia	F186	F186				F186
Stromboli Island						F203

Table 4.1. Selected samples to be analyzed by different technics.

²⁰ Solution

4.5.1. SEM-EDX findings

The SEM-EDX analysis functioned as the most data producing analysis. Since this kind of analyses can be performed within a relatively short time and provides a trustable data we used it as the first and principal analyzing method to find the chemical composition of the SC's materials.

In order to determine the amounts of 10 major element oxides²¹, some random spots and rectangular areas (15 – 20 μm^2) from the both laminae and clastic materials were analyzed. In particular, specific analyzes were conducted on both finely laminated part and on glass fragments and mineral crystals (feldspar, pyroxene, and opaque minerals) which were present in the massive portions between the laminar levels.

Then, the preliminary result data were reviewed to calculate the normative mineral compositions of the materials. Afterward, referring the typical oxide contents of the minerals provided by Deer, et al. (1982) and Deer, et al. (1992), the main present mineral phases were obtained. Having these phases, helped to speed up the next analyzes, because the appearance (color intense and the pattern) of the same phases were very similar so that the other equal crystals (from the same mineral phases) could be easily recognized.

In this manner, about 1000 of spots and rectangular areas were analyzed (results in appendix B). In the procedure of the SEM analyzes, the mineral crystals or glass shards were mostly analyzed in the spot-analyzing mode, whereas for the laminated parts some rectangular shaped areas were analyzed. Still, some spot analyzes have been carried out on the laminated portions and particularly on the single lamina.

²¹ Na₂O, K₂O, MgO, Al₂O₃, SiO₂, P₂O₅, SO₃, CaO, TiO₂, and FeO(total)

CHAPTER 4. FINDINGS AND DISCUSSION

Geochemical studies were conducted on a total of 13 samples distributed as following: four samples collected at *Monte Lentia* (F010, F014, F015, F019, F030, F032, F041, F184, F185, and F186), one sample from *Vulcanello* (F040), another one from *Monte Saraceno* (F042), and the last one from *Monte Luccia* (F043). The geographical locations of these samples are shown in figure 2.3. Besides, table 4.1 indicates the number of analyzed samples by each different method.

4.5.2. ICP-MS results

Since analyzes done by the SEM/Microprobe provide only the contents of major elements oxides, we benefited from the innovative technique of the LA-ICP-MS to detect the quantities of trace element (quantitative point analyzes) in the SC which might provide more information to support or reject the proposed hypothesis (see chapter 5).

In this process, 85 analyzes were carried out on the SC taken from three representative samples (F019, F030, F032) of *Monte Lentia*, the area that possesses the thickest laminated SC. Since the diameter of each beam spot 50 or 80 μm , the outcome could comprise the chemical composition of complete or partial part of mineral crystal(s), glass shard(s) and laminae. Some of analyzing results had to be discarded because they were a mixed data of amounts of aforementioned portions. The results of these analyzes are shown in the Appendix E.

In the next step, the obtained results from chemical analyzes by both SEM and LA-ICP-MS were applied to plot of some detective elements on different binary diagrams in order to disclose the relationship between their amounts and the origin of SC (Figures 4.12 to 4.14).

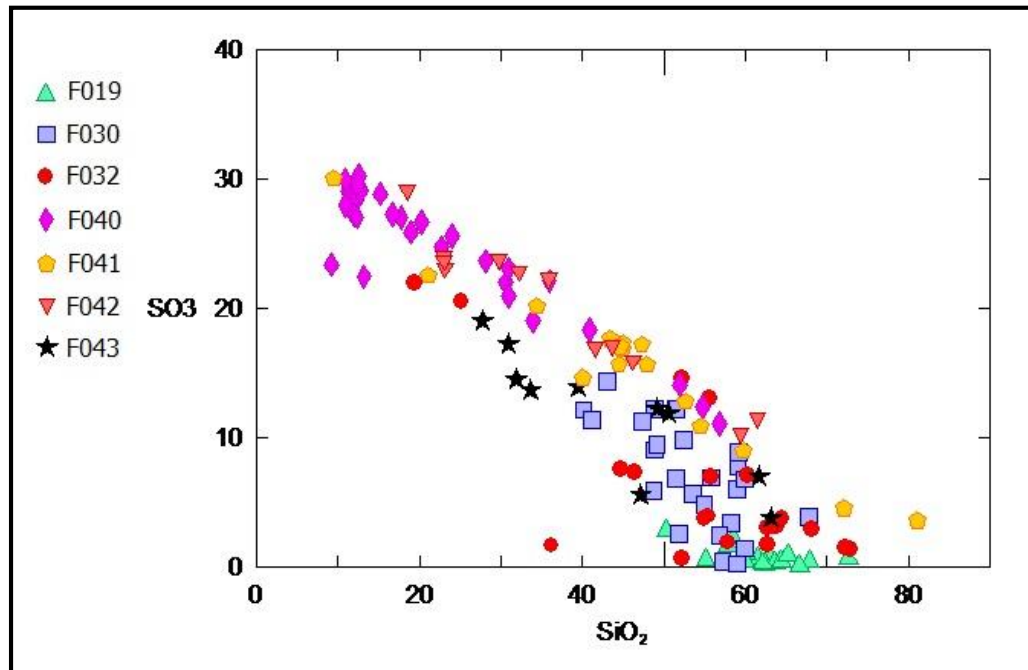


Fig. 4.12. SiO_2 versus SO_3 plot of finely laminated portion of SC (weight percentages are determined by SEM-EDS).

The diagram SiO_2 vs SO_3 (Fig. 4.12) allows to geochemically distinguish between the F019 sample and the other samples. The analyses of F019 show very low concentration of SO_3 and higher content of SiO_2 (in general higher than 54 wt%). On the contrary the other samples show similar trend with a negative correlation between SiO_2 and SO_3 .

Also, as it comes from the figure 4.12, the maximum amount of the SO_3 content of the samples reaches 31% and coincides to the normative SO_3 of the jarosite mineral (31.7%).

The diagram Sr vs Y (figure 4.13) confirms the difference, already observed in Fig.4.12, between the F019 sample and the other two M.te Lentia samples ((F030 and F032). The sample F019 in fact is characterized by higher contents of Y than the other two samples F030 and F032.

CHAPTER 4. FINDINGS AND DISCUSSION

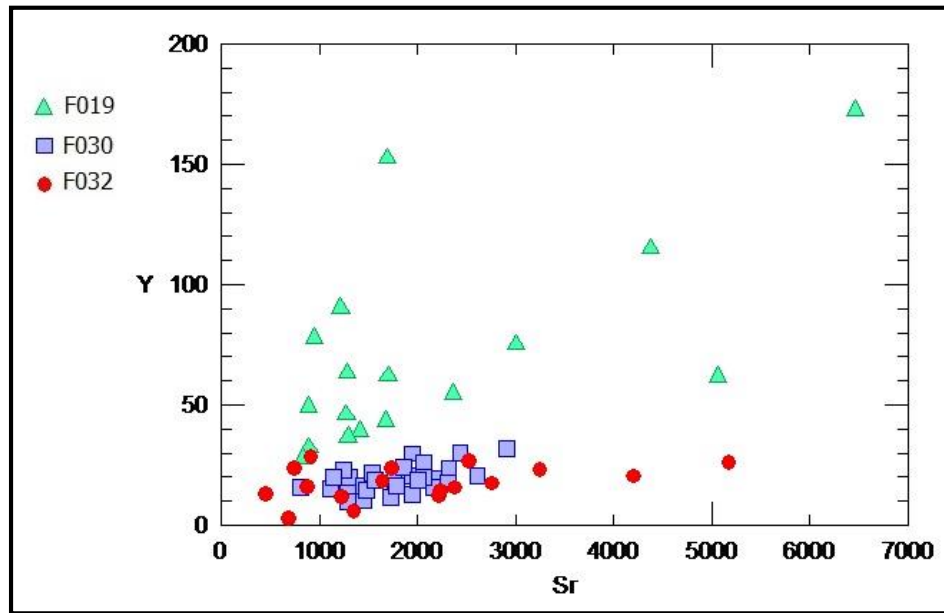


Fig. 4.13. Sr versus Y plot of finely laminated portion of SC.

The contents of Sr and Y (in ppm) were determined by LA-ICP-MS.

The diagram $\text{FeO}_{(\text{tot})}$ vs Ni highlights (Fig. 4.14) the similarity of the concentrations of these elements among the three samples collected on M.te Lentia.

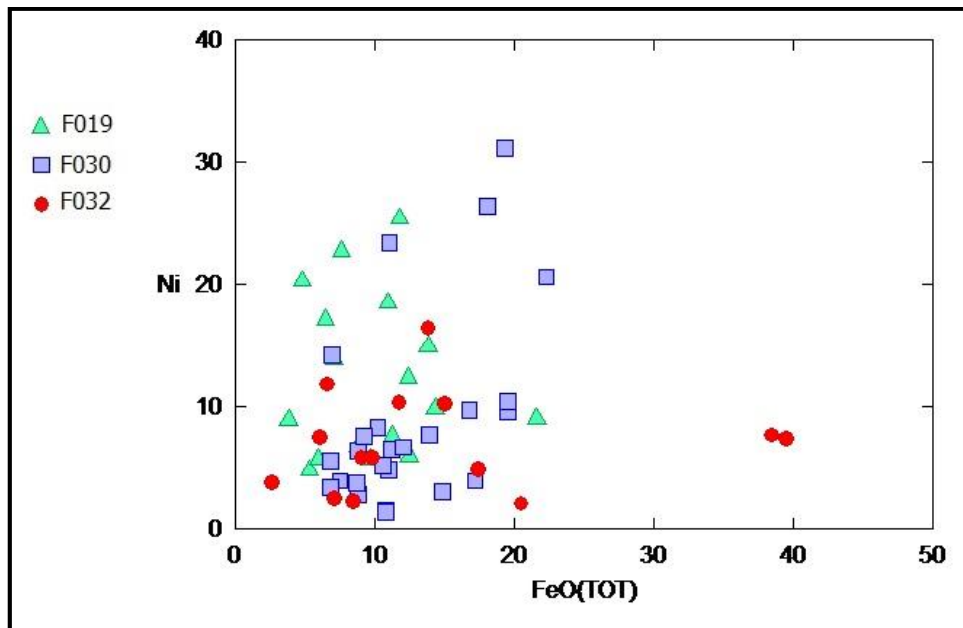


Fig. 4.14. – $\text{FeO}_{(\text{tot})}$ versus Ni plot of finely laminae of SC. Weight percentages of $\text{FeO}_{(\text{tot})}$ were determined by SEM-EDS, Ni contents (in ppm) were determined by LA-ICP-MS.

CHAPTER 4. FINDINGS AND DISCUSSION

The differences between the oxide amounts and the REE amounts between the sample F019 and the other samples are considerable. It may return to the location of the sample F019 (Fig. 4.3). The sample has been collected from the surface of a rock which has been under the runoff water.

4.6. Discussion

Microprobe analysis seemed the only solution to get the purest chemical compositions of just the laminated portions of the sample. Considering the fact that the data resulted from the very fine-scaled analysis may have been affected by the chemical composition of their circumstances, and in order to decrease this error to the least possible amount, the linear analysing method was chosen. The most accurate linear analysis were done on the most typical thin section of the samples. First, a diagonal cross section of whole thin section was analysed, but since this lines crossed all the components (including the mineral crystals, glass shards, and the lithic fragments within the lenticular portions), the produced data were very scattered so that coming from the general to the more detailed, the shorter lines were selected to be analysed. These lines were passing from only the laminated portions of the sample so that it could assure to produce only the pure data of the chemical compositions of the laminae, without any clastic materials. Table 4.2 demonstrates the result data of the most representative linear analysis on the laminated part while figure 4.15 illustrates the photo location of this line in the thin section.

	Na2O	MgO	Al2O3	SiO2	P2O5	SO3	K2O	CaO	TiO2	FeO(tot)	MnO	Cl2O	Cr2O3	TOT
S2-2	0.55	0.37	5.25	24.74	2.59	20.55	7.38	0.47	0.26	30.24	0.04	0.32	0.02	92.76
S2-3	0.38	0.34	4.56	20.91	2.38	22.09	7.22	0.31	0.23	30.28	0.01	0.32	0.01	89.04
S2-4	0.21	0.48	4.44	37.92	1.93	17.73	5.31	0.27	0.32	21.61	0.04	0.23	0.00	90.49
S2-5	0.33	0.69	5.22	39.58	1.85	17.59	5.10	0.30	0.58	23.98	0.05	0.24	0.00	95.52
S2-6	0.26	0.97	4.91	37.98	1.74	18.54	5.50	0.67	0.43	25.41	0.11	0.23	0.01	96.75
S2-7	0.25	1.10	4.50	29.39	1.67	21.81	6.42	0.70	0.40	29.22	0.10	0.31	0.03	95.90
S2-8	0.16	0.77	3.26	40.01	1.08	18.06	5.03	0.41	0.34	22.16	0.12	0.27	0.00	91.67
S2-9	0.12	0.74	2.34	63.32	0.70	10.02	2.96	0.31	0.28	10.17	0.02	0.14	0.04	91.15
S2-10	0.28	0.96	2.67	54.66	1.01	10.93	3.30	0.93	0.31	15.27	0.07	0.17	0.02	90.56
S2-11	0.30	0.74	3.48	38.44	1.52	19.17	5.48	0.29	0.73	28.73	0.12	0.25	0.01	99.26
S2-12	0.40	0.55	3.84	23.50	1.85	24.66	7.13	0.31	0.31	32.27	0.10	0.34	0.00	95.25
S2-13	0.26	0.46	3.76	23.98	1.92	22.89	7.11	0.35	0.22	28.90	0.10	0.32	0.01	90.28
S2-14	0.29	0.39	3.45	25.06	1.92	22.75	6.75	0.27	0.27	28.53	0.03	0.36	0.04	90.10
S2-15	0.32	0.35	3.00	17.56	1.67	26.09	7.27	0.33	0.36	31.51	0.04	0.45	0.03	88.97
S2-16	0.25	0.45	4.36	18.99	1.94	24.98	6.60	0.35	0.44	28.09	0.08	0.56	0.01	87.11
S2-17	0.23	0.43	4.63	17.85	2.57	24.71	5.82	0.28	0.48	30.23	0.06	0.49	0.00	87.78
S2-18	0.20	0.61	4.27	11.84	3.03	26.71	6.18	0.27	0.35	34.62	0.04	0.33	0.01	88.47
S2-19	0.14	0.81	4.07	8.71	3.23	26.37	6.17	0.27	0.34	35.75	0.07	0.29	0.02	86.24
S2-20	0.21	0.49	3.97	11.23	2.87	26.75	6.64	0.32	0.27	32.20	0.05	0.29	0.03	85.32
S2-21	0.18	0.51	3.36	21.35	2.10	24.23	5.82	0.27	0.21	27.50	0.06	0.29	0.00	85.88
S2-22	0.16	0.50	3.32	29.09	1.43	23.27	5.68	0.19	0.15	24.91	0.06	0.32	0.02	89.10
S2-23	0.08	0.46	2.53	52.96	0.70	13.83	3.59	0.12	0.07	13.41	0.01	0.19	0.00	87.96
S2-24	0.51	0.54	4.22	39.51	1.19	18.96	5.27	0.30	0.15	22.93	0.06	0.28	0.00	93.91

	Na2O	MgO	Al2O3	SiO2	P2O5	SO3	K2O	CaO	TiO2	FeO(tot)	MnO	Cl2O	Cr2O3	TOT
S2-25	0.38	0.48	4.19	33.21	1.28	22.15	5.86	0.32	0.18	25.97	0.07	0.30	0.02	94.40
S2-26	0.24	0.36	3.64	27.34	1.55	23.31	6.10	0.21	0.12	27.70	0.09	0.30	0.00	90.98
S2-27	0.23	0.37	4.12	36.98	1.52	19.94	5.76	0.26	0.25	23.86	0.06	0.25	0.00	93.59
S2-28	0.29	0.67	6.25	44.19	1.21	13.98	5.41	0.90	0.32	19.54	0.02	0.26	0.04	93.07
S2-29	0.24	0.40	5.01	28.09	1.11	18.84	6.01	0.29	0.25	30.57	0.04	0.32	0.02	91.21
S2-30	0.39	0.57	3.66	24.93	0.98	24.08	6.83	0.24	0.28	30.65	0.06	0.42	0.06	93.14
S2-31	0.30	0.56	3.58	37.59	0.96	20.06	5.99	0.25	0.40	23.40	0.04	0.40	0.04	93.58
S2-32	0.30	0.45	4.20	34.04	1.21	20.31	5.94	0.38	0.80	24.63	0.05	0.32	0.02	92.66
S2-33	0.34	0.42	4.36	33.16	1.32	21.23	5.93	0.30	0.54	26.59	0.05	0.31	0.02	94.56
S2-34	0.12	0.50	4.22	44.59	1.10	15.89	4.53	0.26	0.37	18.36	0.06	0.25	0.01	90.27
S2-35	0.11	0.74	4.22	51.99	0.90	10.42	3.16	0.41	0.30	12.72	0.05	0.25	0.01	85.29
S2-38	0.23	0.53	5.24	38.61	1.12	12.31	4.24	0.53	0.31	18.63	0.04	0.33	0.03	82.15
S2-39	0.48	0.49	6.09	41.87	1.28	15.24	5.22	0.64	0.39	21.18	0.00	0.26	0.00	93.13
Min.	0.08	0.34	2.34	8.71	0.70	10.02	2.96	0.12	0.07	10.17	0.00	0.14	0.00	82.15
Max.	0.55	1.10	6.25	63.32	3.23	26.75	7.38	0.93	0.80	35.75	0.12	0.56	0.06	99.26

Table 4.2. Weight percentage of the major element oxides of a cross section of the laminae. Since the first and the last points of the line S2 had obvious differences with the results of the other points, were discarded. The results of the points having a total amounts of less than 80% were discarded as well, because these points were partially included the emptiness of the porosity²².

²² All the original data are presented in the Appendix C.

CHAPTER 4. FINDINGS AND DISCUSSION



Fig. 4.15. The location of analysed cross section of the laminae.

Using the data of the table 4.2., it is illustrated in the scatterplot of figure 4.16 that the amounts of the three plotted oxides fluctuate in a zigzag manner with alternative apexes and nadirs. Considering the diversity of the chemical composition of the dark and light laminae, this pattern is expected. Again, because of the natural chemical characteristics of the Fe, S, and Si elements, which brings out a negative correlation between their abundances (whenever the amount of iron or sulfur goes up, the amount of the silicon content goes down and vice versa) the opposition and negative correlation between the blue, and the other two lines in the figure 4.16 is expected too. The only point that should be noticed in this graph is that the apexes and nadirs don't fall on the two consequent points. This can be for the sake of the sizes of the laminae that don't allow a perfect coincidence between the location of the analyzed spot and the center of the lamina. Scilicet, the distance between the consequent analyzed points is selected to be constant, whereas the thickness of the consequent laminae is not necessarily constant. So, during the analyze performance there might be

CHAPTER 4. FINDINGS AND DISCUSSION

more than one spots on one lamina analyzed or even simply a lamina might have been skipped from the beam target.

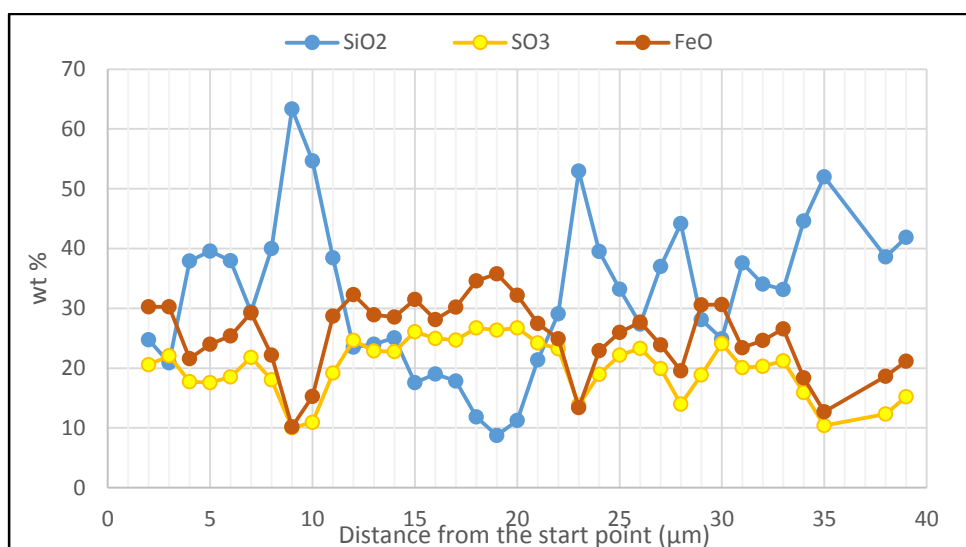


Fig. 4.16. The weight percentages of the four oxides of the laminae.

Examining the samples by XRD and Micro-XRD revealed that jarosite is the only sulfur-bearing phase of the SC (see Appendix D). This is also supported by several spot analysis run on the laminae (the lighter ones) which their compositions coincide to their analogous in the normative jarosite (table 4.2). The spot analyzes are done by both SEM-EDX and Microprobe.

As mentioned in chapter 2, the chemical formula of the jarosite is $KFe^{3+}_3(SO_4)_2(OH)_6$ which within that the weight percentages of the SO_3 , Fe_2O_3 , K_2O , and H_2O are 31.9%, 47.9%, 9.4%, and 10.8% in order. All these amounts are more than the even maximum amounts of the data of the analysis showed in table 4.2.

The difference between the normative amount and the maximum amounts of oxides comprised in jarosite mineral can be attributed to the substitution of some elements in the lattice of jarosite, regarding its family group's general formula $[AB_3(XO_4)_2(OH)_6]$. According to this formula, the

CHAPTER 4. FINDINGS AND DISCUSSION

Fe^{3+} can be substituted by Al^{3+} and in like manner the S can be substituted by P. In fact, the presented results in table 4.2 show more amounts of Al_2O_3 and P_2O_5 than the expected ones that can support the idea of the substitution.

To find a way to geochemically evaluate the XRD results and explore the normative phases of the laminae it seemed logical to dedicate all the SO_3 content of the samples to the jarosite mineral to see what will be left after excluding all the SO_3 and the other analogue components within the jarosite mineral (Al_2O_3 , Fe_2O_3 , and K_2O) from the total amount of oxides. Doing this calculations, we confronted a mathematical vicious cycle, because there was not any absolute amount of the oxides and all were in the relative amounts, so that it became impossible to extract the proportions of the oxides included the jarosite mineral normative proportions from the total weight percentages of the all major element oxides. Neither, calculating the proportions of FeO and Fe_2O_3 was possible.

In addition to the composition of the light laminae, we also need the composition of the dark ones which is also determined by spot analyzes. The dark laminae of the SC are composed of a high silica amorphous gel with SiO_2 content reaching 96.56 wt% (Appendix B).

Therefore, all the while knowing the two phases (the presence of jarosite and silica) in the laminae, the silica and sulfur trioxide contents of the both light and dark laminae were plotted in a scatterplot (fig. 4.17).

CHAPTER 4. FINDINGS AND DISCUSSION

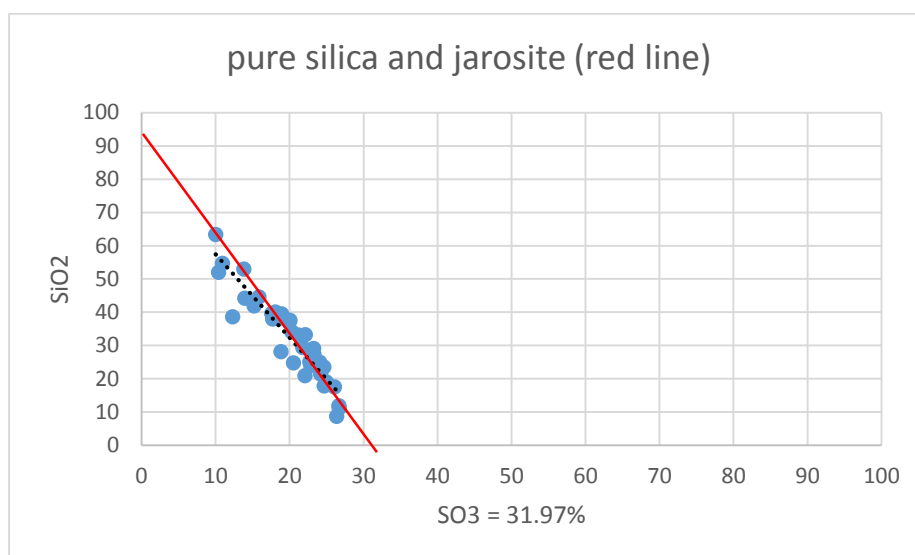


Fig. 4.17. Binary scatterplot of the SO_3 versus SiO_2 content of the laminae. The black dotted line is the trendline of all the plot points. The red line connects the analogue points of the silica and the normative SO_3 content of the jarosite.

In the graph exhibited in figure 4.7, there is a good coincidence between the trendline of all the spots and the red line (the red line is an imaginary line that connects the compositions of the both ends of the compositional spectrum of the laminae). This good overlapping of these two lines can confirm again the exact composition of the laminated part of the SC that is determined before by the different other analytical methods (by SEM-EDX and by Micro-XRD).

In a like manner with figure 4.17, also the total iron oxide and the potash percentages were plotted versus silica (figures 4.18 and 4.19).

In the both of the below graphs (fig. 4.18 and 4.19) despite of the parallelism of the trendline and the red line, there is a little shift between them. This can be most probably as the result of the mobility of the iron and potassium which can be easily depleted or enriched due to the alteration processes. However, it also can be interpreted by either the

CHAPTER 4. FINDINGS AND DISCUSSION

presence of another phase/s additional to the silica and jarosite, which is/are enriched in Fe_2O_3 and K_2O ; or the impurity of the silica which brings the silica content of the dark laminae under the given percentage (96%).

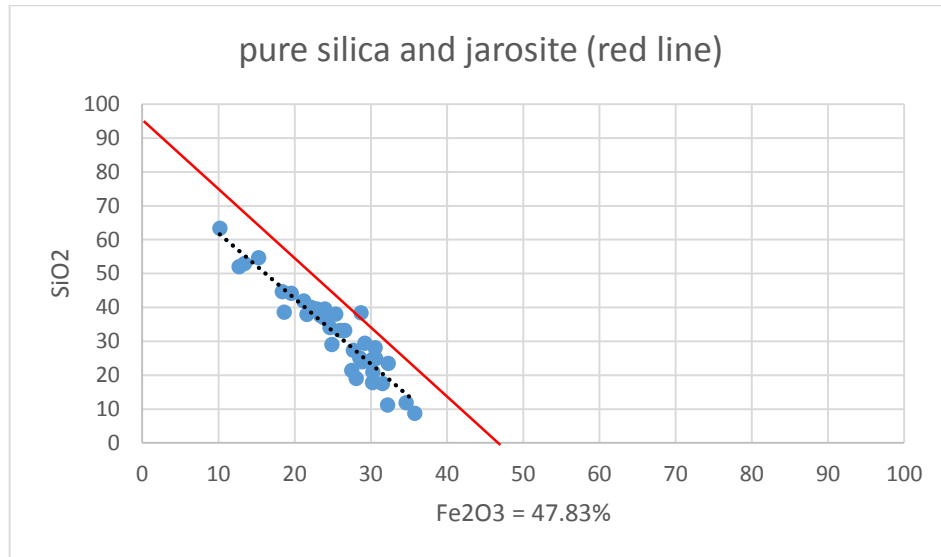


Fig. 4.18. Binary scatterplot of the Fe_2O_3 versus SiO_2 content of the laminae. The black dotted line is the trendline of all the plot points. The red line connects the analogue points of the silica and the normative Fe_2O_3 content of the jarosite.

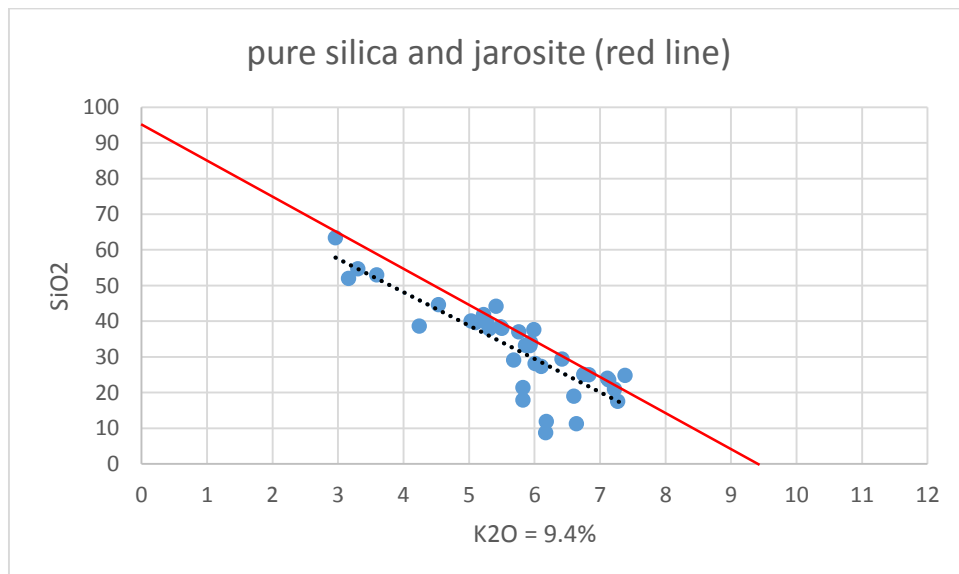


Fig. 4.19. Binary scatterplot of the K_2O versus SiO_2 content of the laminae. The black dotted line is the trendline of all the plot points. The red line connects the analogue points of the pure silica and the normative K_2O content of the jarosite.

In the following, a phenomenon, related to our study subject, will be discussed which can be used as a key information to find out the formation way of the amazing textures of the SC.

4.6.1. Liesegang bands

Liesegang bands are first noticed and named by German chemist, Raphael E. Liesegang, who was doing his experiment on the reaction of a silver nitrate solution drop placed onto the surface of potassium dichromate gel (Liesegang, 1896 and 1913; Liesegang & Watanabe, 1923).

Since, Liesegang bands form in a concentric pattern of rings, they are also called as Liesegang rings.

Liesegang bands occur in various types of rocks but more common in sedimentary rocks. They are known as secondary (diagenetic) structures which exhibit bands of (authigenic²³) minerals that are set in a regular repetitive pattern (Middleton, et al. 2003). Also, since they show an unbroken pattern, they can easily be misinterpreted as pseudo-faults (McBride, 2003). They appear as colored bands of cement that typically cut-across bedding in the sedimentary rocks (Jackson, 1997; Stow, 2009).

Although, Liesegang bands are frequently reported in sedimentary rocks (Merino, 1984), they can develop in some igneous and metamorphic rocks, too. The igneous and metamorphic rocks which are reported to show Liesegang bands are permeable and chemically weathered (McBride, 2003).

The exact process of the formation of Liesegang bands is not entirely known and is still under research (Krug, et al. 1996). However, a probable

²³ Of constituents that came into existence with or after the formation of the rock of which they constitute a part.

CHAPTER 4. FINDINGS AND DISCUSSION

model is known by the geologic community as the responsible mechanism to form them (Decelles & Gutschick, 1983) which is a precipitation process that is thought to be the catalyst for Liesegang bands formation. This process is known as the Ostwald-Liesegang Supersaturation - Nucleation-Depletion Cycle.

Wilhelm Ostwald was the first one who tried to explain the formation of Liesegang bands. He just one year after that Liesegang introduced the phenomenon, proposed a theory based on the idea that a precipitate is not formed immediately upon the concentration of the ions exceeding a solubility product, but a region of supersaturation occurs first. When the limit of stability of the supersaturation is reached, the precipitate forms, and a clear region forms ahead of the diffusion front because the precipitate that is below the solubility limit diffuses onto the precipitate (Ostwald, 1897 and Ostwald, 1925). In simpler words, Ostwald suggests that when the fluid reaches the right level of supersaturation, crystal seeds initiate to form (nucleation) and grow. Then, the growth of crystals cause to lower the level of the fluid saturation in the porosity of around the growing crystals. Therefore, the mineralization in the crystals surrounding areas develops in the form of separate bands (Steefel, 2008).

Decelles & Gutschick (1983) described that in this model, the diffusion of particular reactants leads to supersaturation and nucleation in given zones and meanwhile depletion of reactants in adjacent zones.

Yet, geochemists have suggested a popular mechanism which indicates that Liesegang rings develop when there is a lack of convection so that some reacting species such as oxygen and iron precipitate via inter-

diffusion in separate bands (laminae) which become spaced apart in a geometric pattern. (Steefel, 2008).

Accordingly, the chemical segregation of iron oxides and other minerals during the weathering is suggested to develop the Liesegang rings (Stow, 2009).

4.6.2. Liesegang bands in SC samples

Though there is a high occurrence of Liesegang rings in sedimentary rocks, relatively few scientists have studied their mineralogy and texture in enough detail to write more about them (Fu, et al. 1994). Particularly, they are much less investigated on the microscopic scale.

Still, considering the high similarity between the Liesegang bands and the laminae of the SC lead us to assume the same origin for developing the laminae. Figures 4.20 and 4.21 depict the resembling appearances of the Liesegang bands in the field and the laminae of the SC under the microscope.

In Vulcano, the textures of the laminae developed in the different rock types (from pyroclastic deposits to basaltic flows). This could be confusing at first, but again it can be explained referring to the formation of Liesegang bands.

In general and as it is mentioned by Chen, et al. (1990) Liesegang rings are geochemically self-organized and they have been distributed independent from the features that were established prior to their formation just like our samples which show the constant features on the different surfaces.

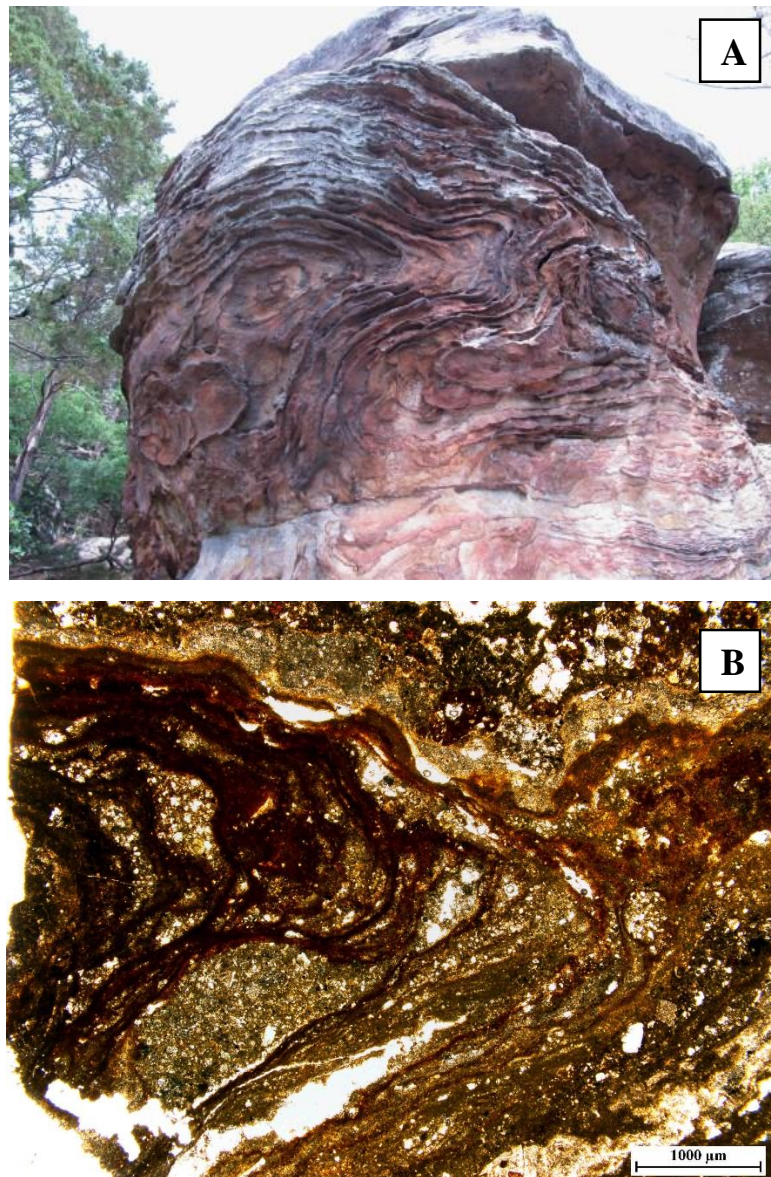


Fig. 4.20. (A) The Liesegang bands in the nature. (taken in Southern Illinois, 2014²⁴).
(B) The curved laminae set in the SC sample (taken in PPL).

²⁴ Referenced as Naturesnippets (2014).

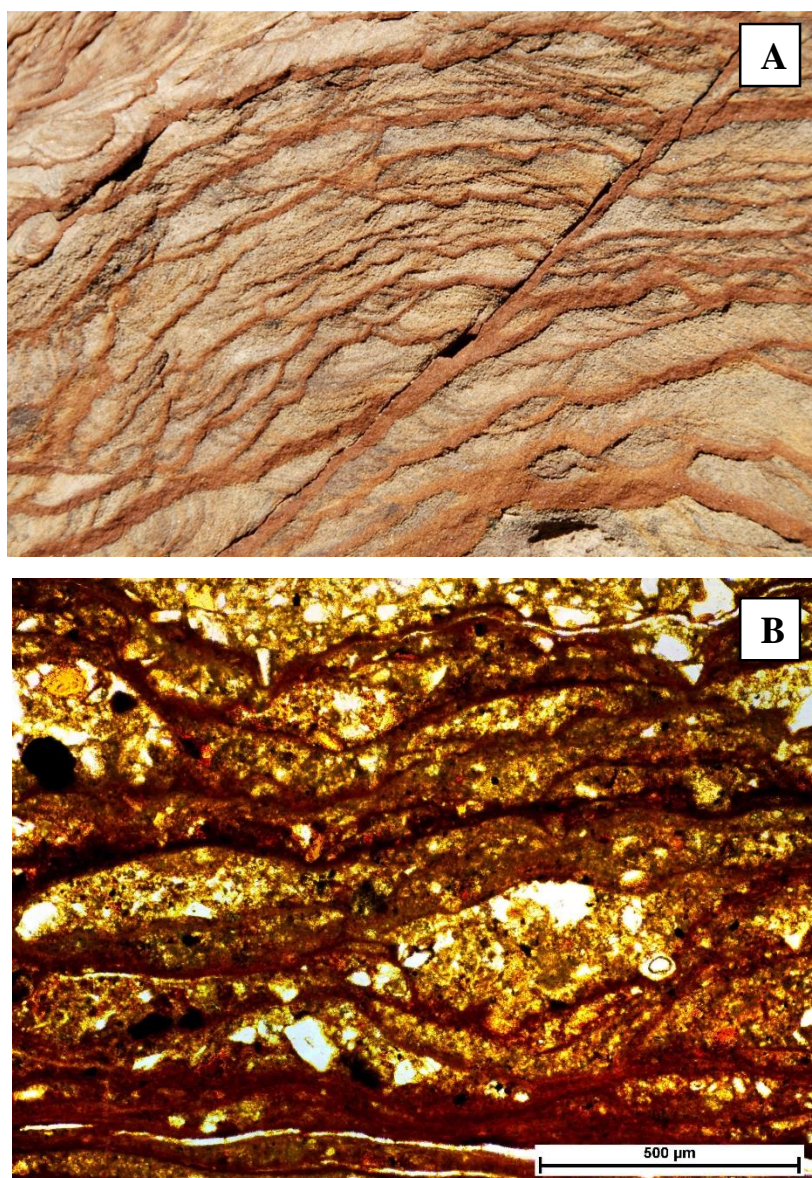


Fig. 4.21. (A) The Liesegang bands in the nature. (by Zoltan Sylvester,).
 (B) The similar texture in laminae of the SC (taken in CPL).

In the formation of Liesegang bands it is also referred to the water - rock interactions in the pore space (Steefel, 2008) which can be used as another common feature between the Liesegang bands structures and our textures. This is in absolute accordance with the SC on the pyroclastic deposits of Vulcano which make a porous space to the interaction of the rock and environment water (runoff, rain, or dew).

Chapter 5

Conclusion

and

Recommendations

5.1. Summary

Vulcano Island as an active volcano has some fumarolic activities. The interaction between the released acidic gases and the wet surface of the different rock types has caused to develop a superficial thin layer of coatings on the surface of the outcrops.

Macroscopically, this coating resembles the desert varnish and in microscopic scale, it shows a succession of alternative dark and light laminae. Through calculating the normative phase of the laminae and re-examining by micro-XRD analysis, the mineral phase of these laminae have been determined as the jarosite for the light laminae and a high silicic phase (non-mineral phase of almost pure silica) for the darker laminae.

Depending the substratum, the laminae may be observed in two general forms: a) with a thin and even trend and consisted of a few laminae which sometimes get curved toward the bottom and fill micro-depressions; b) in the form of subsets which the shape of their curviness and spatial positions create different textures such as convoluted texture, eye texture, branching and rejoining laminae, and etc..

The coating in the case of later form (b) is not consisted of solely laminae, but of the lentic areas filled with mineral crystals, glass shards, and a spongy matrix. The minerals are mainly consisted of pyroxene, feldspar, and magnetite. Most of the glass shards are bubble-walled and have very sharp edges that means they are very fresh and non-altered and have not experienced physical transportations.

The presence of the fresh glass shards and other magma-origin minerals show the magmatic origin of these clastic materials which have been preserved in-situ. On the contrary, through some reasons the entire

CHAPTER 5. CONCLUSION AND RECOMMENDATIONS

surface coatings and particularly laminae can be considered to have a non-magmatic origin:

- So far, there is no magmatic origin reported for the jarosite and it is usually known as a secondary mineral.
- The surface coatings are post-eruptional and have developed on the outermost surface of the many rocks, even the youngest of them that belongs to the last eruption of the Vulcano.
- The coatings are present on the surface of an entirely vertical wall (not tectonically re-angled), which makes it impossible to be covered by the pyroclastic deposits.
- In the field, the coatings have developed on the surfaces that are faced windward. If the rock surface has been protected by an obstacle, it has remained not coated.
- The thin crust has not merely coated the rocky hard surface, but also during the first initializing to coat, it has covered the surface of the loose sands of recently wind-transported sediments.
- The surface coatings are found in different levels of stratigraphic sequence of the Vulcano, which means they have been formed repetitively between the eruption intervals.

The microscopic textures of the surface coatings are quite similar to the structure of the Liesegang bands. The presence of potential factors (reactants like oxygen and iron; porous host, a supersaturated fluid) provides the suitable condition to develop the Liesegang bands in surface coatings of the Vulcano.

According to all the observations and by interpreting the result data of the geochemical analysis, the scenario of the genesis of the surface coatings in the Vulcano Island may be expressed as following:

5.2. The process of the formation of surface coatings

1. The released gases from the degassing crater (SO_2 , HCl, and HF) in the reaction with the surficial water (including rain and dew) produce an acidic fluid.
2. As a chemical alteration, the acidic fluid interacts with the surface of the outcrops in the island.
3. In the cases that the substrate rock is completely seamless and without any porosity, the fluid deposits on the surface of the rock as a very thin and smooth set of laminae.
4. If the host rock of the acidic fluid be a pyroclastic deposit, the fluid penetrates into the pore space of the rock.
5. Due to the capillary action, the fluid runs into the intergranular space of the clastic materials and creates curved or convoluted patterns inside the rock.
6. By being trapped in the limited space and by lack of the convection, the fluid within the pyroclastic rock, gets supersaturated in some reactants (probably oxygen, iron, and sulfur).
7. Then, the nucleation occurs and the fluid starts to differentiate into different bands.
8. This process proceeds and the bands become more developed and distinguishable.

9. By the time, other fluid(s) may intrude into the same rock and make another set of laminae, or simply been added to the previous ones.

Although, the above mentioned hypothesized scenario can fulfill most the requirements of the formation of the surface coatings, as a rough scientific theory, it is not able to cover all the aspects of the surface coatings and still there are some non-answered question left.

5.3. Not answered questions

- Why some glass shards in the lentic areas are remained completely fresh and non-altered, while their surrounding have the sets of laminae which are formed due to the chemical alteration?
- If jarosite and silica are the only phases making the laminae?
- What has been the primary composition of the parent fluid of the laminae?

Accepting the fact that research is something that proceeds non-stop, we are aware that many possible works can be done on this subject. Here, as the last state of the dissertation, there are some suggestions to do which may help to better understand the formation process of the surface coatings.

5.4. Suggestions

- Simulation of the penetration of a resembled gel in a porous host to experiment the creation of similar textures.
- Investigating the possible role of micro-organisms in developing the SC.
- Doing some experiments to model the precipitation (differentiation to different bands) from a jellylike fluid with a similar composition to the studied surface coatings.

References

REFERENCES

- Alpers, C.N., & Brimhall, G.H. (1989). Paleohydrologic evolution and geochemical dynamics of cumulative supergene metal enrichment at La Escondida, Atacama Desert, northern Chile. *Econ. Geol.* 84, 229–255.
- Anderson, H. J., & Jackson J. A. (1987). The deep seismicity of the Tyrrhenian Sea. *Geophys. J. R. Astron. Soc.*, 91, 613-637.
- Anthony, J.W., Bideaux, R.A., Bladh, K.W., and Nichols, M.C. (1990). Handbook of mineralogy, volume I. Elements, sulfides, sulfosalts: Tucson, Arizona, Mineral Data Publishing, 588 p.
- Barberi, F., Gandino, A., Gioncada, A., La Torre, P., Sbrana, A., & Zenucchini C. (1994) The deep structure of the Eolian arc (Filicudi–Panarea–Vulcano sector) in light of gravity, magnetic and volcanological data. *J Volcanol Geotherm Res* 61:189–206.
- Barca, D., Belfiore, C. M., Crisci, G. M., La Russa, M. F., Pezzino, A., & Ruffolo, S. A. (2011). A new methodological approach for the chemical characterization of black crusts on building stones: a case study from the Catania city centre (Sicily, Italy). *Journal of Analytical Atomic Spectrometry*, 26(5), 1000-1011. doi: 10.1039/c0ja00226g.
- Barca, D., Crisci, G.M., & Marabini, S. (1991). Historical deposit by 'Hot Hurricane' mechanism in the Vulcano area (Southern Italy). International Conference on Active Volcanoes and Risk Mitigation, 27 August-1 September, Naples (Abstract).
- Bigazzi, G., & Bonadonna, F. (1973). Fission track dating of the obsidian of Lipari Island (Italy). *Nature* 242:322–323.
- Billi, A., Barberi, G., Faccenna, C., Neri, G., Pepe, F., & Sulli, A. (2006). Tectonics and seismicity of the Tindari Fault System, southern Italy: Crustal deformations at the transition between ongoing contractional and extensional domains located above the edge of a subducting slab. *Tectonics*, V:5, I:2, TC2006, doi:10.1029/2004TC001763.
- Bishop, J. L., Murchie, S., Pieters, C., & Zent, A. (1999). A model for generation of Martian Surface dust, soil and rock coatings: Physical vs. chemical interactions, and palagonitic plus hydrothermal alteration. NASA Ames Research Center; Moffett Field, CA United States. *The Fifth*

REFERENCES

- International Conference on Mars; SETI/NASA-ARC, MS-239-4, Moffett Field, CA 94035.*
- Borns, D. J., Adams, J. B., Curtiss, B., Farr, T. G., Palmer, F., Staley, J., & Taylor-George, S., (1980). The role of microorganisms in desert varnish formation. *Geological Society of America Abstracts with Programs*, v. 12, p. 390.
- Boyce, A.J., Fulignati, P., Sbrana, A., & Fallick, A.E. (2007). Fluids in early stage hydrothermal alteration of high-sulfidation epithermal systems: a view from the Vulcano active hydrothermal system (Aeolian Islands, Italy). *J Volcanol Geotherm Res* 166:76–90.
- Brophy, G. P., & Sheridan M. F. (1965). Sulfate studies IV: The jarosite - natrojarosite - hydronium jarosite solid solution series. *The American Mineralogist*, Vol. 50, 1595-1607.
- Calvin, W.M., King, T.V.V., & Clark, R.N. (1994). Hydrrous carbonates on Mars: Evidence from the Mariner 6/7 infrared spectrometer and groundbased tele-sopic spectra. *J. Geophys. Res.* 99, 14659–14675.
- Capaccioni, B., Coniglio, S. (1995). Varicolored and vesiculated tuffs from La Fossa volcano, Vulcano Island (Aeolian Archipelago, Italy): evidence of syndepositional alteration processes. *Bull Volcanol. Vol. 57. 61–70.*
- Chen, W., Park, A., & Ortoleva, P. (1990). Diagenesis through coupled processes: modeling approach, self-organization, and implications for exploration. *American Association of Petroleum Geologists Memoir 49, Prediction of Quality Through Chemical Modeling. pp. 103-130.*
- Chiodini, G., Cioni, R., Marini, L., Panichi, C. (1995). Origin of the fumarolic fluids of Vulcano Island, Italy and implications for volcanic surveillance. *Bull Volcanol* 57(2):99–110.
- Clocchiatti, R., Gioncada, A., Mosbah, M., & Sbrana, A. (1994). Possible deep origin of sulfur output at Vulcano. Southern Italy. In the light of melt inclusion studies. *Acta Vulcanol* 5:49–53.

REFERENCES

- Curtiss, B., Adams, J. B., & Ghiorso, M. S. (1984). Origin, development and chemistry of silica-alumina rock coatings from the semi-arid regions of the island of Hawaii. *Geochimica et Cosmochimica Acta*, 49: 49-56.
- Dana, E. S. (1932). *A Textbook of Mineralogy, with an Extended Treatise on Crystallography and Physical Mineralogy: By Edward Salisbury Dana... 3d. Ed., Rev. and Enl., by William E. Ford.* W. E. Ford (Ed.). John Wiley.
- De Astis, G., La Volpe, L., Peccerillo, A. & Civetta, L. (1997). Volcanological and petrological evolution of Vulcano Island (Aeolian Arc, southern Tyrrhenian Sea). *Journal of Geophysical Research*, 102, 8021–8050.
- De Astis, G., Ventura, G. & Vilaro, G. (2003). Geodynamic significance of the Aeolian volcanism (Southern Tyrrhenian Sea, Italy) in light of structural, seismological and geochemical data. *Tectonics*, 22, 1040–1057.
- De Astis, G., Dellino P., La Volpe L., Lucchi F., & Tranne C. A. (2006). Geological map of the island of Vulcano (Aeolian Islands). *University of Bari, University of Bologna and INGV. LAC, Firenze.*
- De Astis, G., Lucchi F., Dellino P., La Volpe L., Tranne C. A., Frezzotti M. L., & Peccerillo A. (2013). Chapter 11 Geology, volcanic history and petrology of Vulcano (central Aeolian archipelago). *Geological Society, London, Memoirs*, 37, 281-349. doi: 10.1144/M37.11
- Decelles, P.G., & Gutschick, R.C., (1983). Mississippian wood-grained chert and its significance in the western interior United States. *Journal of Sedimentary Petrology*, 53: 1175-1191.
- Deer, W. A., Howie, R. A., & Zussman, J. (Eds.). (1982). Rock-Forming Minerals: Orthosilicates, Volume 1A. *Geological Society of London.*
- Deer, W. A., Howie, R. A., & Zussman, J. (1992). An introduction to the rock-forming minerals (Vol. 2). *Hong Kong: Longman Scientific & Technical.*

REFERENCES

- De Fino, M. & La Volpe, L. (1988). Role of magma mixing during the recent activity of Fossa di Vulcano (Aeolian Islands, Italy). *Bollettino GNV*, IV, 230-241.
- Desborough, G.A., Smith, K.S., Lowers, H.A., Swayze, G.A., Hammarstrom, J.M., Diehl, S.F., Driscoll, R.L., & Leinz R.W. (2006). The use of synthetic jarosite as an analog for natural jarosite. *Seventh International Conference on Acid Rock Drainage. St. Louis, Missouri, pp. 458–475.*
- Desborough, G.A., Smith, K.S., Lowers, H.A., Swayze, G.A., & Hammarstrom, J.M. (2010). Mineralogical and Chemical Characteristics of Some Natural Jarosites. *US Geological Survey. University of Nebraska – Lincoln.*
- Dorn, R. I., & Oberlander, T. M. (1982). Rock varnish. *Progress in Physical Geography*, v. 6, p. 317-367.
- Drouet, C., & Navrotsky, A. (2003). Synthesis, characterization, and thermochemistry of K-Na-H₃O jarosites. *Geochimica et Cosmochimica Acta*, Vol. 67, No. 11, pp. 2063–2076. doi: 10.1016/S0016-7037(02)01299-1.
- Dutrizac, J. E., & Jambor, J. L. (2000) Jarosites and their application in hydrometallurgy. In *Sulfate Minerals, Crystallography, Geochemistry, and Environmental Significance* (eds. C.N. Alpers, J. L. Jambor and D. K. Nordstrom). *Mineral. Soc. Am. Rev. Mineral. Geochem.* 40, pp. 405–443.
- Ellam, R. M., Menzies, M. A., Hawkesworth, C. J., Leeman, W. P., Rosi, M., & Serri, G. (1988). The transition from calc-alkaline to potassic orogenic magmatism in the Aeolian Islands, Southern Italy. *Bulletin of Volcanology*, 50, 386–398.
- Farr, T. G. & Adams, J. B. (1984). Rock coatings in Hawaii. *Geological Society of America Bulletin*, 95, no. 9;1077-1083. doi: 10.1130/0016-7606(1984)95< 1077: RCIH>2.0.CO;2.
- Farrand, W.H., Glotch, T.D., Rice Jr., J.W., Hurowitz, J.A., & Swayze, G.A. (2009). Discovery of jarosite within the Mawrth Vallis region of

REFERENCES

- Mars: Implications for the geologic history of the region. *Icarus* 204, 478–488.
- Forni, F., Lucchi, F., Tranne, A., & Rossi, L. (2008). Un'Isola Vulcanica Che Nasce. Isola di Vulcano. *Università di Bologna Dipartimento di Scienze della Terra e Geologico-Ambientali*. From http://www.edu-geo.it/escursioni/Sicilia%201/itinerario_sc1.html.
- Frazzetta, G., La Volpe, L., & Sheridan, M. F. (1983). Evolution of the Fossa cone, Vulcano. *Journal of Volcanology and Geothermal Research*, 17(1), 329-360.
- Fu, L., Milliken, K.L., & Sharp, J.M. Jr. (1994). Porosity and permeability variations in fractured and Liesegang-banded Breathitt sandstones (Middle Pennsylvanian), eastern Kentucky: diagenetic controls and implications for modeling dual-porosity systems. *Journal of Hydrology*, 154: 351-381.
- Fulignati, P., & Sbrana, A. (1998). Presence of native gold and tellurium in the active high-sulfidation hydrothermal system of the La Fossa volcano (Vulcano, Italy). *Journal of Volcanology and Geothermal Research* 86: 187-198.
- Fulignati, P., Gioncada, A., & Sbrana, A. (1999). Rare-earth element (REE) behaviour in the alteration facies of the active magmatic hydrothermal system of Vulcano (Aeolian Islands Italy). *J Volcanol Geotherm Res* 88:325–342.
- Fulignati, P., Alessandro, S., Luperini, W., & Greco, V. (2002). Formation of rock coatings induced by the acid fumarole plume of the passively degassing volcano of La Fossa (Vulcano Island, Italy). *Journal of Volcanology and Geothermal Research* 11: 397-410.
- Gioncada, A., Clocchiatti, R., Sbrana, A., Bottazzi, P., Massare, D., & Ottolini, L. (1998). A study of melt inclusions at Vulcano (Aeolian islands, Italy): insight on the primitive magmas and on the volcanic feeding system. *Bull Volcanol* 60:286–306.
- Swayze, G., Desborough, G.A., Smith, K.S., Lowers, H.A., Hammarstrom, J.M., Diehl, S.f., Leinz, R.W., & Driscoll, R.L. (2008). Understanding contaminants associated with mineral deposits. Chapter B,

REFERENCES

- Understanding Jarosite - From Mine Waste to Mars. *U.S. Geological Survey Circular 1328*.
- Gurioli, L., Zanella, E., Gioncada, A., & Sbrana, A. (2012). The historic magmatic-hydrothermal eruption of the Breccia di Commenda, Vulcano, Italy. *Bulletin of Volcanology*. Vol. 74. 1235–1254. DOI 10.1007/s00445-012-0590-4.
- Hynek, B.M., McCollom, T.M., Marcucci, E.C., Brugman, K., & Rogers, K.L. (2013). Assessment of environmental controls on acid-sulfate alteration at active volcanoes in Nicaragua: Applications to relic hydrothermal systems on Mars. *Journal of Geophysical Research: Planets*, 118, 1–22.
- Jackson, J. A., (1997). Glossary of Geology. *American Geological Institute, Alexandria, Virginia. 4th edition. P. 366*.
- Jongmans, A. G., Groenesteijn, K., Buurman P., & Mulder. J. (1996). Surface Coatings at Costa Rican Recently Active Volcanoes. *Soil Science Society of America Journal, Vol. 60 No. 6, p. 1871-1880*.
- Keller, J. (1970). Datierung der obsidiane und bimstoffe von Lipari. *N Jb Geol Mh*, 90–101.
- Keller, J., (1980). The island of Vulcano. *Rend. Soc. It. Miner. Petrol.*, 36(1): 369-414.
- Kotler, M. (2008). One of the jarosite samples taken from the Coromandel Peninsula in New Zealand. *ASTROBIOLOGY MAGAZINE. Unlocking Martian Rocks, 07/10/08*.
- Kraft, M. , Michalski, J., & Sharp, T. (2003). Effects of pure silica coatings on thermal emission spectra of basaltic rocks: Considerations for Martian surface mineralogy. *Geophys. Res. Lett.* 30, doi:10.1029/2003GL018848.
- Krug, H.J., Brandtstadter H., & Jacob K.H., (1996). Morphological instabilities in pattern formation by precipitation and crystallization processes. *Geologische Rundschau*, 85: 19-28.

REFERENCES

- Liesegang, R. (1896). Ueber einige eigenschaften von gallerten. *Naturwissenschaftliche Wochenschrift*, 10(30), 353-362.
- Liesegang, R.E. (1913). Geologische Diffusionen. *Steinkopff*, Dresden, 180 pp.
- Liesegang, R. E., & Watanabe, M. (1923). Kapillarität und Diffusion in der Geologie. *Colloid & Polymer Science*, 32(3), 177-181.
- Malin, MC., Dzurisin, D., & Sharp, R.P. (1983). Stripping of Keanakakoi tephra on Kilauea Volcano, Hawaii. *Geol Soc Am Bull* 94:1148–1158.
- Matsukura, Y., and Kimata, M., & Yokoyama, SH. (1994). Formation of Weathering Rinds on Andesite Blocks under the Influence of Volcanic Gases around the Active Crater of Aso Volcano, Japan. *Rock Weathering and Landform Evolution*. John Wiley & Sons.
- McBride, E. F. (2003), Pseudofaults resulting from compartmentalized Liesegang bands. *Sedimentology*, 50: 725–730. doi:10.1046/j.1365-3091.2003.00572.
- McLennan, S.M. (1999). Geochemical constraints on the surface (sedimentary) mineralogy of Mars. *The Fifth International Conference on Mars, July 19-24, Pasadena, California, abstract no. 6148. 11794-2100, U.S.A.*
- Mercalli, G., & Silvestri O. (1891). L'eruzione dell'Isola di Vulcano incominciata il 3 agosto 1888 e terminata il 22 marzo 1890. *Annali dell'ufficio Centrale di Meteorologia e Geodinamica*, 10, 71–281.
- Merino, E., (1984). Survey of geochemical self-patterning phenomena. In Nicolis, G., and Baras, F. (eds.), *Chemical Instabilities*. Dordrecht: D. Reidel Publishing Company, pp. 305-328.
- Middleton, G. V., Church, M. J., Coniglio, M., Hardie, L. A., & Longstaffe, F. J. (2003). *Encyclopedia of Sediments and Sedimentary Rocks*. Kluwer Academic Publishers, Dordrecht. Pp. 221, 224.
- Naturesnippets (2014). Introduction to the wonders of nature. The picture was taken while hiking the Observation Trail at the Garden of the Gods

REFERENCES

- in southern Illinois. The post can be retrieved from:
<http://naturesnippets.com/tag/liesegang-bands>.
- Naughton, J.J., Greenberg V.A., & Gognel R. (1976). Incrustations and fumarolic condensates at Kilauea. *J Volcanol Geothermal Res* 1:141–165.
- Ostwald, WF. (1897). Studien uber die Bildung und Umwandlung fester Korper. *Zeitschrift für physikalische Chemie*, 22, 289-330.
- Ostwald, W. (1925) The theory of Liesegang rings. *Kolloid Z. Spec. no.*, 380–390.
- Pasquarè, G., Francalanci, L., Gardunom, V.H., & Tibaldi, A. (1993). Structure and geologic evolution of the Stromboli Vulcano, Aeolian Islands, Italy. *Acta Vulcanologica* 3, 79–89.
- Peccerillo, A., Frezzotti, M.L., De Astis, G., & Ventura, G. (2006). Modeling the magma plumbing system of Vulcano (Aeolian Islands, Italy) by integrated fluid-inclusion geobarometry, petrology, and geophysics. *Geology*, 34, 17–20, doi: 10.0030/G22117.1.
- Perry, R.S., & Adams, J.B. (1978). Desert varnish: evidence for cyclic deposition of manganese. *Nature*, 276, 489-491.
- Perry, R.S., Kolb, V.M., Lynne, B.Y., Sephton, M., Mcloughlin, N., Engel, M.H., Olendzenski, L., Brasier, M., & Staley, J.T. (2005). How desert varnish forms? *Astrobiology and Planetary Missions, roc. SPIE Vol. 5906*, p. 276-287.
- Phillips, Wm. Revell and Griffen, & Dana T. (1981). Optical mineralogy: The non-opaque minerals. *W.H. Freeman and Company, San Francisco*, 677 p., ISBN number 0-7167-1129-X.
- Romagnoli, C., Casalbore, D., Bortoluzzi, G., Bosman, A., Chiocci, F. L., D’Oriano, F., ... & Marani, M. (2013). Bathy-morphological setting of the Aeolian islands. In: Lucchi, F., Peccerillo, A., Keller, J., Tranne, C. A. & Rossi, P. L. (eds) The Aeolian Islands Volcanoes. *Geological Society, London, Memoirs, Vol.37*, 27–36.

REFERENCES

- Rothstein, Y. (2006). Spectroscopy of jarosite minerals, and implications for the mineralogy of Mars. *Presented to the Department of Astronomy (May 2006). Mount Holyoke College. Pp. 45.*
- Soligo, M., De Astis, G., Delitala, MC., La Volpe, L., Taddeucci, A., & Tuccimei, P. (2000). Uranium-series disequilibria in the products from Vulcano Island (Sicily, Italy): isotopic chronology and magmatological implications. *Acta Vulcanologica 12:49–59.*
- Steeffel, C. I. (2008). Geochemical Kinetics and Transport: *in* Brantley, Susan L; Kubicki, James d; White, Art F. (eds), *Kinetics of Water-Rock Interaction. Springer New York, p. 545-589.*
- Stow, D. A. V., (2009). Sedimentary rocks in the field. A color guide. *Manson publishing, pp. 103, 107.*
- Sylvester, Z. (2008). Hindered Settling random notes of a skeptical geologist. *From: <http://zsylvester.blogspot.it/2008/11/liesegang-bands-in-sandstone.html>.*
- Ventura, G. (2013). Kinematics of the Aeolian volcanism (Southern Tyrrhenian Sea) from geophysical and geological data. *In: Lucchi, F., Peccerillo, A., Keller, J., Tranne, C. A. & Rossi, P. L. (eds) The Aeolian Islands Volcanoes. Geological Society, London, Memoirs, 37, 3–11.*
- Villari, L., Donati, G., Cuerrieri, S., Ioppolo, S., Maccarrone, E., Russo, S., & Stagno, F. (1986). Studio petrologico delle piroclastiti della Fossa e di Vulcanello (Isola di Vulvano). *Boll. Gruppo Nazionale per la Vulcanologia. CNR: 531-552.*
- Warshaw, C.M. (1956). The occurrence of jarosite in underclays. *American Mineralogist, 41, 288-296.*
- Whitney, D. L., & Evans B. W. (2010). Abbreviations for names of rock-forming minerals. *American mineralogist, 95(1), 185.*
- Wray, J.J., Ehlmann, B.L., Squyres, S.W., Mustard, J.F., & Kirk, R.L. (2008). Compositional stratigraphy of clay-bearing layered deposits at Mawrth Vallis, Mars. *Geophys. Res. Lett. 35, L12202. doi:10.1029/2008GL034385.*

Appendices

APPENDICES

Appendix A.

Detailed information of samples taken from Stromboli:

No.	Sample	N	E	Height (m)	Photo
1	STR P1	38°48'03"	15°13'56,1"	118	001 - 002
2	STR P2	38°48'11"	15°13'41,1"	173	003 - 004 - 005 - 006
3	STR P3	38°48'09,4"	15°13'38,9"	199	007- 008 - 009 - 010
4	STR P4			222	013- 014 - 018- 019 - 020 - 021
5	STR P5	38°47'59,4"	15°13'36,8"	317	022 - 023
6	STR P6	38°47'56,6"	15°13'26,1"	430	035 - 036 - 037 - 038
7	STR P7	38°47'54,5"	15°13'22,5"	450	043 - 044 -045 -046
8	STR P8	38°48'08"	15°13'06,8"	470	
9	STR P9				049 - 051
10	STR P10	38°48'08"	15°13'06,8"	470	052 - 053 - 054 - 055
11	STR P11	38°47'40,11"	15°13'20,5"	610	061 - 062 - 063
12	STR P12	38°47'39,4"	15°13'14,7"	730	066 - 067 - 068 - 069 -070
13	STR P13	38°48'07,5"	15°13'31,3"	262	208 - 211
14	STR P14	38°48'10,6"	15°13'19,3"	280	217 - 218 - 219 - 220
15	STR P15	38°48'19,6"	15°12'50,1"	283	235
16	STR P16	38°48'10,0"	15°12'53,9"	441	252 - 253
17	STR P17	38°48'08,1"	15°12'54,4"	453	255 -256 - 257 - 258 - 260 - 261
18	STR P18	38°48'03,7"	15°12'57,3"	522	267
19	STR P19	38°48'03,7"	15°12'57,3"	522	277
20	STR P20	38°48'00,0"	15°12'56,7"	581	281 - 282
21	STR P21	38°47'56,2"	15°12'57,1"	663	293 - 295
22	STR P22	38°47'21,4"	15°12'50,5"	890	323
23	STR P23	38°47'24,3"	15°12'27,7"	776	341 - 342 - 343 - 344

Appendix B.

The result data of the SEM Analysis:

No.	Na2O	MgO	Al2O3	SiO2	P2O5	SO3	K2O	CaO	TiO2	FeO(tot)	MnO	Cl2O	F	Cr2O3	TOT
F010-01	4.49	1.48	17.42	59.74	0	0	6.42	3.41	0.57	6.17	0	0.3	0	0	100
F010-02	2.99	2.3	18.01	58.78	0.65	0	5.85	4.27	0.69	6.15	0	0.29	0	0	100
F010-03	1.11	0.81	8.62	24.59	8.49	18.35	6.28	1.85	0.81	29.1	0	0	0	0	100
F010-04	1.24	0.78	9.99	49.86	5.01	9.45	3.86	1.83	0.58	17.39	0	0	0	0	100
F010-05	1.03	1.18	13.4	63.26	2.07	4.99	2.74	1.34	0.39	9.61	0	0	0	0	100
F010-06	0.71	0.84	6.44	40.15	6.67	12.37	4.45	1.83	0.87	25.68	0	0	0	0	100
F010-07	0.9	1	8.02	27.69	8.05	14.97	5.53	1.91	0.75	31.18	0	0	0	0	100
F010-08	4.54	1.5	18.53	59.14	0	0	6.27	3.4	0.55	5.79	0	0.27	0	0	100
F010-09	0	33.25	0	38.81	0	0	0	0.42	0	26.9	0.62	0	0	0	100
F010-10	5.98	0	19.8	66.36	0	0	5.94	1.93	0		0	0	0	0	100
F010-11	1.21	27.73	4.47	44.96	0	0	1.6	0.38	0	19.23	0.43	0	0	0	100
F010-12	4.05	0	27.02	57.25	0	0	1.46	9.39	0	0.84	0	0	0	0	100
F010-13	3.32	1.39	18.07	59.95	0	0	6.47	3.49	0.64	6.42	0	0.25	0	0	100
F010-14	5.43	0.32	19.21	62.07	0	0.81	3.33	2.36	0.61	5.81	0	0.06	0	0	100
F010-15	0	34.19		37.77	0	0	0	0.28	0	27.22	0.53	0	0	0	100
F010-16	0	2.63	3.96	0	0	0	0		7.34	85.59	0.29	0	0	0.19	100
F014-1	2.27	1.85	11.58	50.78	0	9.51	5.47	2.01	0.61	15.74	0	0.18	0	0	100
F014-2	5.04	2.64	17.85	56.01	1.03	0.42	5.71	4.06	0.78	6.07	0	0.39	0	0	100
F014-3	0	0	0	0	2.33	32.68	11.69	0	0	43.29	0	0	0	0	90
F014-5	0.75	0.84	2.92	13.58	1.92	31.78	8.72	0.33	0.6	38.01	0	0.53	0	0	100
F014-6	1.52	1.87	10.38	39.01	1.13	16.43	6.76	1.65	0.59	20.2	0	0.45	0	0	100

No.	Na2O	MgO	Al2O3	SiO2	P2O5	SO3	K2O	CaO	TiO2	FeO(tot)	MnO	Cl2O	F	Cr2O3	TOT
F014-7	0	0	0	0	0	0	0	0	0	100	0	0	0	0	100
F014-8	3.64	2.45	17.92	58.83	0.78	0	6.14	3.28	0.85	5.77	0	0.35	0	0	100
F014-9	0.96	2.03	7.81	48.19	1.21	11.9	5.05	1.91	0.92	19.57	0	0.44	0	0	100
F014-10	1.14	15.04	4.02	52.64	0	0	0	19.26	0.59	7.31	0	0	0	0	100
F014-11	1.16	14.89	4.85	51.81	0	0	0	19.33	0.62	7.34	0	0	0	0	100
F014-14	1.1	15.53	3.58	52.77	0	0	0.18	19.68	0.46	6.49	0	0	0	0.21	100
F014-15	1.19	15.37	3.42	52.83	0	0	0	18.69	0.51	7.98	0	0	0	0	100
F014-16	1.87	1.72	6.92	30.18	3.05	21.09	7.27	0.93	0.59	26.38	0	0	0	0	100
F014-17	1.09	14.74	2.82	53.68	0	0	0	20.02	0.35	6.87	0.42	0	0	0	100
F014-18	1.51	16.36	5.04	53.6	0	0	0	16.64	0.48	6.13	0.24	0	0	0	100
F014-19	0.75	15.91	2.9	53.49	0	0	0	18.59	0.39	7.65	0.32	0	0	0	100
F014-20	7.89	0	20.96	64.74	0	0	3.19	2.36	0	0.86	0	0	0	0	100
F014-21	1.47	13.69	5.27	51.97	0	1.26	0.73	15.61	0.52	9.14	0.33	0	0	0	100
F014-22	0.79	4.15	7.11	8.33	0	1.05	0.65	0.52	6.12	70.38	0.5	0	0	0.4	100
F014-23	4.54	1.38	18.25	58.53	0	1.4	5.95	2.2	0.61	7.14	0	0	0	0	100
F014-25	5.83	2.88	17.99	55.52	1.34	1.66	5.28	2.8	0.56	5.67	0	0.46	0	0	100
F014-26	1.25	13.9	4.81	52.36	0	1.34	0.71	16.04	0.56	9.05	0	0	0	0	100
F014-27	0.89	13.95	4.67	52.62	0	1.26	0.64	16.07	0.69	9.21	0	0	0	0	100
F014-28	1.04	0	2.72	87.77	0	2.48	1.29	0.54	0	4.16	0	0	0	0	100
F014-29	1.03	1.27	4.36	85.43	0	1.84	1.02	0.5	0.6	2.79	0	1.14	0	0	100
F014-30	1.09	4.9	8.12	6.91	0	0	0.49	0.5	5.13	71.89	0	0	0	0.96	100
F014-31	4.74	2.59	17.5	55.29	0	0.9	6.75	3.62	0.79	7.45	0	0.37	0	0	100
F014-32	1.36	14.15	5.68	52.22	0	0	0.55	15.56	0.64	9.84	0	0	0	0	100
F015-01	1.12	1.32	6.09	23.74	3.81	22.35	7.27	0.52	0.51	33.27	0	0	0	0	100
F015-02	0.71	1.07	6.96	62	2.4	9.34	4.39	0.69	0.31	12.13	0	0	0	0	100

No.	Na2O	MgO	Al2O3	SiO2	P2O5	SO3	K2O	CaO	TiO2	FeO(tot)	MnO	Cl2O	F	Cr2O3	TOT
F015-03	0.8	1.2	6.19	30.81	3.64	19.77	6.97	0.47	0.56	29.27	0	0.32	0	0	100
F015-04	1	1.12	5.21	36.17	3.35	19.19	5.83	0.38	0.43	27.02	0	0.31	0	0	100
F015-05	0.54	0.89	4.68	56.29	2.39	12.97	4.6	0.47	0.38	16.57	0	0.22	0	0	100
F015-06	1.55	1.29	8.01	50.51	2.08	11.9	6.15	0.6	0.32	17.47	0	0.11	0	0	100
F015-07	4.11	2.13	16.78	59.56	0.86	0.68	6.15	2.95	0.57	5.87	0	0.33	0	0	100
F015-08	1.52	1.48	5.45	22.28	2.23	12.77	3.85	0.32	0.22	49.74	0	0.15	0	0	100
F015-09	0	4.66	7.4	0	0	0	0	0	6.79	81.15	0	0	0	0	100
F015-10	0	2.59	1.58	0	0	0	0	0	6.76	88.24	0.82	0	0	0	100
F015-11	1.27	14.26	4.95	51.2	0	0	0	19.21	0.73	8.39	0	0	0	0	100
F015-12	4.82	0	28.38	54.95	0	0	1.07	9.91	0	0.87	0	0	0	0	100
F015-13	4.69	2.99	18.26	55.86	0	0	5.9	4.54	0.63	6.79	0	0.33	0	0	100
F015-14	6.84	0	20.7	64.14	0	0	5	1.85	0	1.47	0	0	0	0	100
F015-15	1.08	14.77	3.57	52.83	0	0	0	19.02	0.36	8.26	0.11	0	0	0	100
F015-16	7.28	0	22.56	62.89	0	0	3.18	3.29	0	0.82	0	0	0	0	100
F015-17	7.19	0	25.51	59.29	0	0	0.75	6.46	0	0.8	0	0	0	0	100
F015-18	7.32	0	23.68	60.1	0	0	1.36	5.94	0	1.61	0	0	0	0	100
F015-19	4.29	1.74	17.79	52.71	1.12	5.64	7.14	1.23	0.47	7.7	0	0.18	0	0	100
F185(6)	0.73	0	4.35	21.31	1.16	28.05	4.94	0	0	35.86	0	0	3.58	0	100
F185(7)	3.59	0	12.32	67.58	0	3.59	6.97	0	0	5.95	0	0	0	0	100
F185(8)	0.3	0	3.04	13.64	0.4	47.6	2.28	0	0	32.73	0	0	0	0	100
F185(10)	1.63	0	5.78	20.31	0	5.14	1.65	0	0	65.5	0	0	0	0	100
F185(11)	5.17	0	13.33	66.22	0	2.5	6.55	0	0	6.24	0	0	0	0	100
F185(12)	0	0	5.27	82.22	0	4.34	2.31	0	0	5.86	0	0	0	0	100
F186(3)	0	0	3.79	17.29	3.65	30.27	8.22	0	0	33.66	0	0	3.12	0	100
F186(4)	0	0	3.9	19.52	2.42	24.33	5.49	0	0	29.21	0	0	15.12	0	100

No.	Na2O	MgO	Al2O3	SiO2	P2O5	SO3	K2O	CaO	TiO2	FeO(tot)	MnO	Cl2O	F	Cr2O3	TOT
F186(5)	0	0	3.5	18.05	0	27.43	7.73	0	0	38.81	0	0	4.49	0	100
F186(6)	0	0	4.73	23.04	3.41	28.17	6.09	0	0	34.56	0	0	0	0	100
F186(7)	0	0	3.08	17.07	2.8	29.12	7.11	0	0	37.85	0	0	2.96	0	100
F186(8)	0	0	2.54	85.15	0	0	3.01	0	0	9.29	0	0	0	0	100
F186(10)	0	2.3	16.98	54.26	0	0	5.42	0	0	11.5	0	0	9.54	0	100
F186(13)	0	0	4.87	89.15	0	0	2.24	0	0	3.74	0	0	0	0	100
F186(14)	0	0	2.98	95.75	0	0	1.27	0	0	0	0	0	0	0	100
F186(16)	4.89	1.26	16.45	55.64	0.43	0	6.99	4.69	0.72	8.59	0	0.34	0	0	100
F186(17)	1.2	1.23	6.46	30.51	3.13	21.05	7.92	0	0.62	27.88	0	0	0	0	100
F186(18)	3.43	0	16.58	57.18	0	1.09	4.7	3.76	0	5.79	0	0.19	7.28	0	100
F186(19)	4.59	0	19.41	59.39	0	0	4.41	3.01	0.87	8.32	0	0	0	0	100
F186(20)-P1	5.27	0	19.13	61.05	0	0	5.81	4.92	0	3.1	0	0	0.72	0	100
F186(20)-P2	4.88	0	19.99	61.61	0	0	5.63	4.67	0	3.23	0	0	0	0	100.01
F186(20)-P3	5.39	0	19.21	62.48	0	0	5.5	4.45	0	2.97	0	0	0	0	100
F186(20)-P4	6.45	0	19.07	61.71	0	0	2.86	3.56	0.62	5.73	0	0	0	0	100
F186(20)-P5	5.73	0	18.21	59.46	0	0	4.67	3.42	1.32	7.18	0	0	0	0	99.99
F186(20)-P6	0	0.47	2.1	59.87	0	0	0	37.55	0	0	0	0	0	0	99.99
F186(21)	3.07	1.25	10.47	45.27	0.58	9.61	5.83	3.4	0	19.92	0	0.6	0	0	100
F186(22)P1	6.03	0.29	18.45	56.17	0	0	4.45	4.78	0	9.83	0	0	0	0	100
F186(22)P2	4.81	0	21.82	58.1	0	0	4.98	5.66	0	4.64	0	0	0	0	100.01
F186(22)P3	4.09	0.14	18.61	58.86	0.24	0	8.96	0	0	6.74	0	0	0	2.38	100.02
F186(24)	4.92	1.41	16.91	56.02	0	0	7.24	4.38	0.47	8.33	0	0.32	0	0	100
F186(25)	5.48	1.32	16.86	57.25	0	0	6.59	3.62	0.67	8.22	0	0	0	0	100
F186(26)	2.92	0.95	10.26	46.72	1.27	10.15	7.69	0	0	19.31	0	0.72	0	0	100
F186(27)	4.12	1.08	9.99	46.44	1.14	10.42	6.88	0	0	19.48	0	0.45	0	0	100

No.	Na2O	MgO	Al2O3	SiO2	P2O5	SO3	K2O	CaO	TiO2	FeO(tot)	MnO	Cl2O	F	Cr2O3	TOT
F186(28)	3.44	1.54	11.14	60.97	0	2.73	4.24	4.61	0	11.09	0	0.25	0	0	100
F186(35)	3.3	2.93	10.55	59.73	0	1.76	7.6	9.99	0	0	0	4.15	0	0	100
F186(37)	3.81	1.85	11.05	61.02	0.18	2.09	4.38	5.05	0	10.34	0	0.22	0	0	100
F186(40)	3	1.61	11.13	61.15	0	3.17	4.61	4.93	0	10.05	0	0.37	0	0	100
F186(42)	2.85	1.19	9.74	58.52	0	6.81	5.03	2.62	0	12.98	0	0.28	0	0	100
F186(45)	4.04	1.83	12.03	45.51	0	9.44	6.2	3.86	0	16.7	0	0.4	0	0	100
F186(46)	3.45	1.45	11.29	47.41	0	10.1	6	3.51	0	16.19	0	0.6	0	0	100
F186(47)	3.53	1.7	11.45	45.03	0	10.51	6.29	3.92	0	17.56	0	0	0	0	100
F186(48)	2.77	1.54	8.34	41.24	0	16.14	7.78	0	0	21.74	0	0.45	0	0	100
F186(51)	2.83	5.05	8.57	47.92	0	4.44	9.32	0	0	18.67	0	3.21	0	0	100
F186(52)	1.79	7.61	5.12	44.02	0	1.45	1.31	12.53	0	25.99	0	0.18	0	0	100
F186(53)	2.52	6.12	6.87	43.47	0	0	1.91	10	0.54	28.57	0	0	0	0	100
F186(54)	4.29	3.27	10.98	49.29	0	5.05	4.72	6.75	0	15.24	0	0.4	0	0	100
F186(55)	3.85	3.22	11.18	50.18	0	3.89	4.63	6.88	0	16.17	0	0	0	0	100
F186(56)	3.54	2.75	11.38	49.25	0	5.32	4.88	6.6	0	15.88	0	0.4	0	0	100
F186(57)	4.1	1.22	13.07	46.5	0	8.86	6.21	3.91	0	15.36	0	0.78	0	0	100
F186(58)	4.5	1.28	13.65	48.38	0	7.09	6.38	3.83	0	14.58	0	0.31	0	0	100
F186(59)	5.96	1.61	15.15	53.77	0	2.72	6.48	4.39	0	9.63	0	0.29	0	0	100
F186(60)	2.92	2.21	9.81	46.93	0	10.37	5.29	4.96	0	17.5	0	0	0	0	100
F186(63)	3.04	2.37	8.89	46.21	0	11.58	5.49	4.45	0	17.97	0	0	0	0	100
F186(64)	2.89	2.26	9.27	46.9	0	11.29	5.4	4.25	0	17.75	0	0	0	0	100
F186(65)	2.74	0.87	9.21	48.09	0	13.43	6.67	0	0	18.99	0	0	0	0	100
F186(66)	2.43	0.65	6.15	45.2	0	15.45	6.35	0	0	23.77	0	0	0	0	100
F186(83)	9.86	3.03	1.46	75.44	0	0	0	9.6	0	0.62	0	0	0	0	100
F186(84)	12.47	3.04	1.46	73.44	0	0	0	9.24	0	0.35	0	0	0	0	100

No.	Na2O	MgO	Al2O3	SiO2	P2O5	SO3	K2O	CaO	TiO2	FeO(tot)	MnO	Cl2O	F	Cr2O3	TOT
F186(87)	10.19	3.02	1.6	75.31	0	0	0	9.39	0	0.48	0	0	0	0	100
F186(88)	5.39	0	27.35	52.8	0	0	1.08	12.34	0	1.04	0	0	0	0	100
F186(89)	0	0	1.32	90.14	0	2.73	0.87	0	0	4.51	0	0.43	0	0	100
F186(90)	0	0	1.03	92.93	0	2.21	0.72	0	0	2.84	0	0.26	0	0	100
F186(91)	8.1	0	22.38	61.35	0	0	2.32	4.79	0	1.06	0	0	0	0	100
F186(92)	2.6	0.64	9.89	53.55	1.04	8.2	4.43	1.99	0.56	16.68	0	0.43	0	0	100
F186(93)	4.36	0	27.33	52.57	0	0	1.01	12.98	0	1.75	0	0	0	0	100
F186(94)	6.89	---	19.75	58.66	0	0	3.05	4.47	0.83	6.04	0	0.31	0	0	100
F186(98)	0	0	1.61	94.83	0	1.14	0.94	0	0	1.23	0	0.24	0	0	100
F186(99)	5.45	0	26.85	52.95	0	0	1.11	12.13	0	1.52	0	0	0	0	100
F186(100)	2.72	0.98	10.1	43.94	0.93	12.34	6.14	2.99	0.72	18.67	0	0.46	0	0	100
F186(101)	5.21	0.97	16.17	56.33	0.47	0.36	6.75	4.08	0.95	8.39	0	0.31	0	0	100
F186(102)	2.78	0.85	10.08	43.55	1.77	12.83	5.92	2.89	0.43	18.52	0	0.39	0	0	100
F186(103)	5.33	1.02	16.34	56.67	0.4	0	6.62	3.9	1.04	8.34	0	0.34	0	0	100
F186(104)	4.52	1.2	16.44	56.78	0.4	0	6.72	4.86	0.8	7.98	0	0.3	0	0	100
F186(105)	0	0	1.06	96.56	0	0.63	0.56	0	0	1.05	0	0.15	0	0	100
F186(106)	4.59	1	16.34	56.76	0.31	0	6.87	4.55	1	8.25	0	0.34	0	0	100
F186(107)	4.35	1.15	16.38	56.76	0.54	0.4	6.59	4.39	0.97	8.13	0	0.32	0	0	100
F186(108)	4.48	1.04	16.24	56.82	0.28	0	6.74	4.63	0.97	8.5	0	0.3	0	0	100
F186(109)	4.53	1.09	16.22	56.61	0.48	0	6.62	4.94	0.76	8.4	0	0.35	0	0	100
F186(112)	4.49	1.19	16.48	56.37	0.47	0	6.8	4.95	0.97	7.95	0	0.33	0	0	100
F186(113)	5.47	0	27.03	53.17	0	0	1.22	11.94	0	1.17	0	0	0	0	100
F186(114)	4.49	1.19	16.58	56.13	0.33	0	6.67	5.14	0.91	8.3	0	0.25	0	0	100
F186(115)	4.9	1.08	16.53	56.69	0.54	0	5.9	5.05	0.72	8.23	0	0.38	0	0	100
F186(116)	4.46	1.19	16.42	56.22	0.52	0	6.31	4.95	1.22	8.31	0	0.4	0	0	100

No.	Na2O	MgO	Al2O3	SiO2	P2O5	SO3	K2O	CaO	TiO2	FeO(tot)	MnO	Cl2O	F	Cr2O3	TOT
F186(117)	2.64	1.08	14.17	47	0.54	8.82	5.18	4.45	0.76	14.96	0	0.4	0	0	100
F186(118)	4.45	1.01	16.42	57.85	0.45	0	6.61	4.24	0.82	7.82	0	0.32	0	0	100
F186(119)	4.64	1.08	16.27	56.34	0.45	0	6.87	4.79	0.88	8.31	0	0.37	0	0	100
F186(120)	4.61	1.16	16.26	56.13	0.57	0	6.79	5.17	0.77	8.23	0	0.31	0	0	100
F186(121)	4.69	1.38	16.19	55.38	0.5	0.7	6.62	4.98	0.84	8.42	0	0.29	0	0	100
F186(122)	4.56	1.28	16.45	56.31	0.38	0	6.76	4.73	0.95	8.24	0	0.35	0	0	100
F186(123)	4.34	1.27	16.27	56.54	0.43	0	6.58	5.2	0.76	8.19	0	0.41	0	0	100
F186(124)	4.72	1.16	16.09	56.58	0.48	0	6.49	5.13	0.84	8.18	0	0.33	0	0	100
F186(125)	5.1	0	27.51	52.02	0	0	1.09	12.88	0	1.39	0	0	0	0	100
F186(126)	4.64	1.23	16.54	56.63	0.4	0	6.94	4.64	0.89	7.83	0	0.26	0	0	100
F186(127)	4.52	1.3	16.41	56.04	0.45	0	6.51	5.31	0.9	8.18	0	0.38	0	0	100
F040-01	0.46	0.87	7.2	35.92	3.67	22.11	5.86	0.58	0.33	22.96	0.04	0	0	0	100
F040-02	0.21	0.75	9.1	20.2	4.76	26.68	7.32	0.57	0.55	29.74	0.12	0	0	0	100
F040-03	0.33	0.4	6.35	18.91	5.45	25.88	7.23	0.85	0.46	34.09	0.04	0	0	0	99.99
F040-04	0.37	0.78	7.66	23.98	4.62	25.6	7.06	0.58	0.46	28.9	0	0	0	0	100.01
F040-05	0.48	0.83	8.04	28.16	4.26	23.64	6.62	0.86	0.5	26.61	0	0	0	0	100
F040-06	0.2	0.46	9.06	11.23	5.62	29.1	7.7	1.07	0.43	35.12	0	0	0	0	99.99
F040-07	0.3	0.45	9	12.74	5.42	29.11	8.02	0.74	0.24	33.9	0.05	0	0	0	99.97
F040-08	0.21	0.45	7.91	12.15	5.67	29.14	7.78	0.92	0.36	35.41	0.01	0	0	0	100.01
F040-09	0.12	0.39	8.04	12.52	5.52	30.25	7.86	0.57	0.22	34.48	0.02	0	0	0	99.99
F040-10	0.23	0.78	7.51	15.21	5.36	28.86	7.74	0.51	0.26	33.5	0.04	0	0	0	100
F040-11	0.26	0.42	8.47	12.14	5.72	28.31	7.74	0.77	0.42	35.75	0	0	0	0	100
F040-12	0.26	0.46	7.27	11.95	6.02	27.24	7.17	1.32	0.7	37.6	0	0	0	0	99.99
F040-13	0.24	0.53	6.73	10.95	6.06	28	7.65	1.21	0.62	37.88	0.13	0	0	0	100
F040-14	0.3	0.47	4.78	12.29	6.31	27.05	7.57	1.02	0.65	39.45	0.12	0	0	0	100.01

No.	Na2O	MgO	Al2O3	SiO2	P2O5	SO3	K2O	CaO	TiO2	FeO(tot)	MnO	Cl2O	F	Cr2O3	TOT
F040-15	0.29	0.44	5.26	10.97	6.03	29.94	7.95	0.82	0.57	37.7	0.02	0	0	0	99.99
F040-16	0.23	0.27	4.4	12.74	6.11	29.04	7.56	0.79	0.7	38.16	0	0	0	0	100
F040-17	0.24	0.28	4.37	17.76	5.78	27.02	6.84	0.96	0.64	36.11	0	0	0	0	100
F040-18	0.24	0.25	3.53	22.75	5.55	24.7	6.56	0.73	0.85	34.72	0.11	0	0	0	99.99
F040-19	0.16	0.26	3.52	30.51	5.03	22	5.68	0.7	0.72	31.41	0	0	0	0	99.99
F040-20	0.24	0.33	4.78	16.72	5.76	27.25	7.2	1.07	0.62	36.03	0.01	0	0	0	100.01
F040-21	0.39	0.91	7.02	54.78	2.63	12.36	3.97	0.93	0.54	16.46	0	0	0	0	99.99
F040-22	0.56	0.53	5.88	40.86	3.65	18.33	5.67	1.05	0.63	22.83	0	0	0	0	99.99
F040-23	0.2	0.36	7.32	30.91	4.34	23.07	5.99	0.54	0.17	27.1	0	0	0	0	100
F040-24	0.24	0.49	4.29	56.83	3.11	11.06	3.35	0.54	0.51	19.42	0.15	0	0	0	99.99
F040-25	0.15	0.43	3.07	51.96	3.49	14.1	3.95	0.54	0.48	21.82	0	0	0	0	99.99
F040-26	0.18	0.29	4.46	12.36	6.1	29.59	7.74	0.54	0.61	38.14	0	0	0	0	100.01
F040-27	0.3	0.57	7.27	13.19	8.57	22.48	7.76	1.16	0.51	38.09	0.09	0	0	0	99.99
F040-28	0.43	0.59	5.85	9.25	8.97	23.36	8.47	1.02	0.89	41.17	0	0	0	0	100
F040-29	0.45	0.94	7.95	33.94	3.04	19.03	6.67	0.71	0.22	26.98	0.06	0	0	0	99.99
F040-30	0.44	0.46	7.5	30.9	3.28	20.95	7.03	0.48	0.36	28.59	0	0	0	0	99.99
F043-01	1.56	1.48	8.41	30.91	11.59	17.22	5.40	2.07	0.86	20.31	0.19	0	0	0	100
F043-02	2.29	0.66	8.12	49.16	5.55	12.28	5.41	1.19	0.46	14.68	0.20	0	0	0	100
F043-03	0.30	1.28	6.18	33.63	13.52	13.68	4.79	1.51	0.90	23.92	0.29	0	0	0	100
F043-04	0.80	1.77	23.36	47.14	3.68	5.55	6.50	1.35	0.53	9.01	0.31	0	0	0	100
F043-05	1.61	1.51	6.71	50.59	6.52	11.92	4.79	2.25	0.00	14.10	0.00	0	0	0	100
F043-06	0.64	0.63	4.30	39.48	9.73	13.95	4.49	2.43	0.51	23.54	0.29	0	0	0	100
F043-07	0.48	0.74	6.09	27.73	8.16	19.03	6.80	1.73	0.49	28.40	0.33	0	0	0	100
F043-08	0.46	0.87	5.36	31.89	10.69	14.48	5.45	2.51	0.00	27.96	0.33	0	0	0	100
F043-09	1.78	0.83	9.25	61.65	2.78	6.98	4.23	1.31	0.44	10.59	0.16	0	0	0	100

No.	Na2O	MgO	Al2O3	SiO2	P2O5	SO3	K2O	CaO	TiO2	FeO(tot)	MnO	Cl2O	F	Cr2O3	TOT
F043-10	4.16	0.55	15.17	63.13	1.30	3.78	4.76	1.58	0.50	4.94	0.13	0	0	0	100
F041-01	0.23	0.42	4.77	52.68	3.11	12.81	4.36	0.42	0.36	20.83	0.01	0	0	0	100
F041-02	0.10	0.50	4.75	21.06	6.49	22.54	6.48	0.21	0.58	37.18	0.11	0	0	0	100
F041-03	0.52	0.28	3.50	81.06	1.04	3.56	1.80	0.30	0.30	7.64	0.00	0	0	0	100
F041-04	0.35	0.34	3.56	59.76	2.83	8.99	3.30	0.42	0.62	19.84	0.00	0	0	0	100
F041-05	0.87	0.57	6.68	72.04	1.35	4.52	2.99	1.32	0.32	9.28	0.06	0	0	0	100
F041-06	0.76	0.40	5.56	54.52	3.06	10.88	4.21	0.47	0.47	19.66	0.01	0	0	0	100
F041-07	1.08	0.40	7.01	40.00	4.08	14.61	5.01	1.32	0.62	25.86	0.01	0	0	0	100
F041-08	0.42	0.74	4.47	43.34	1.99	17.62	6.07	0.50	0.37	24.39	0.09	0	0	0	100
F041-09	0.43	0.56	4.2	44.93	1.66	16.84	6.06	0.29	0.34	24.69	0	0	0	0	100
F041-10	0.44	0.70	3.61	44.99	1.53	17.34	5.89	0.70	0.35	24.31	0.13	0	0	0	100
F041-11	0.51	0.60	4.44	47.85	1.43	15.63	5.75	0.49	0.59	22.63	0.08	0	0	0	100
F041-12	0.71	1.11	5.35	34.41	1.16	20.13	7.28	1.46	0.41	27.95	0.03	0	0	0	100
F041-13	0.55	0.93	5.31	44.65	1.47	17.00	5.87	0.96	0.44	22.76	0.07	0	0	0	100
F041-14	0.00	0.00	8.29	47.28	4.41	17.21	5.76	0.00	0.00	17.04	0.00	0	0	0	100
F041-15	0.00	0.00	4.33	9.43	10.87	30.06	7.44	0.00	0.94	36.92	0.00	0	0	0	100
F041-16	0	0	4.47	44.45	5.92	15.65	5.07	0	0.89	23.55	0	0	0	0	100
F042-01	0	0.85	4.72	41.54	5.86	16.97	4.16	1.26	1.15	23.5	0	0	0	0	100.01
F042-02	0.13	0.99	5.56	46.17	3.3	15.98	4.14	0.75	1.02	21.96	0	0	0	0	100
F042-03	1.04	2.02	6.5	35.89	3.39	22.34	5.26	1.34	0.38	21.84	0	0	0	0	100
F042-04	0.62	1.05	6.06	29.76	4.54	23.74	6.6	0.9	0.8	25.92	0	0	0	0	99.99
F042-05	0.63	1.22	7.21	43.72	1.58	17.09	5.52	1.42	1.58	20.04	0	0	0	0	100.01
F042-06	0.72	0	5.53	61.51	3.43	11.5	3.27	0.64	0.72	12.69	0	0	0	0	100.01
F042-07	0.28	0.62	5.14	32.21	3.35	22.88	6.7	0.56	0.67	27.59	0	0	0	0	100
F042-08	0	0.46	6.24	18.52	4.33	29.11	8.02	0.53	0.89	31.91	0	0	0	0	100.01

No.	Na2O	MgO	Al2O3	SiO2	P2O5	SO3	K2O	CaO	TiO2	FeO(tot)	MnO	Cl2O	F	Cr2O3	TOT
F042-09	0.84	1.68	7.78	23.03	4.19	24.03	6.67	0.46	0.83	30.48	0	0	0	0	99.99
F042-10	0.65	1.54	14.49	23.1	2.91	23.1	9.24	1.22	0.8	22.95	0	0	0	0	100
F042-11	0.99	1.91	7.01	59.47	2.04	10.32	4.32	1.27	0.57	12.1	0	0	0	0	100
F042-12	0.59	1.08	8.22	23	6.17	23.66	6.98	0.65	0.92	28.53	0	0	0	0	99.8
Vulcanello Px	0.4	13.68	3.17	48.19	0.04	0	0.01	22.5	0.49	8.5	0.26	0.02	0	0	97.26
Vulcanello Px	0.44	13.59	3.8	48.17	0.07	0.06	0.07	22.03	0.71	8.55	0.32	0	0	0	97.81
Vulcanello Px	0.37	14.29	2.83	50.01	0.02	0.04	0.01	22.1	0.44	8.08	0.38	0	0	0	98.57
Vulcanello Px	0.32	14.7	2.98	51.4	0	0	0.03	21.71	0.37	7.97	0.22	0	0	0	99.7
Vulcanello Px	0.43	14.44	1.95	52.31	0	0	0	20.62	0.24	9.01	0.35	0	0	0	99.35
Luccia Px	1.07	14.11	7.12	53.03	0.43	0.38	0.38	16.66	0.95	5.58	0.29	0.18	0	0	100.18
Luccia Px	1.07	14.32	4.51	54.09	0.33	0.45	0.23	18.55	0.66	5.14	0.64	0.18	0	0	100.17
Luccia Px	0.94	13.57	2.56	53.56	0.47	0.43	0.33	19.97	0.71	6.86	0.6	0	0	0	100
Luccia Px	0.68	15.12	3.72	52.47	0.26	0.52	0.45	17.34	0.64	8.06	0.74	0	0	0	100
Luccia Px	1.78	10.08	7.28	53.55	0.82	0.43	1.68	13.16	0.73	9.82	0.67	0	0	0	100
Lentia Px	0.47	13.56	3.53	49.35	0.01	0.11	0.04	22.1	0.7	8.72	0.32	0	0	0	98.91
Lentia Px	0.44	13.92	3.49	49.29	0	0	0	22.33	0.68	8.63	0.15	0	0	0	98.93
Lentia Px	0.41	14.26	3.38	49.18	0.02	0	0.02	21.91	0.53	7.56	0.28	0	0	0	97.55
Lentia Px	0.39	14.53	2.71	49.66	0.04	0	0.02	22.02	0.46	8.25	0.34	0	0	0	98.42
Lentia Px	0.48	13.51	3.55	49.16	0	0.01	0.06	21.93	0.57	8.46	0.23	0	0	0	97.96
Lentia Px	0	13.89	4.82	51.34	0.42	0.07	0.2	21.28	0	7.99	0	0	0	0	100.01
Saraceno Px	0.87	14.69	4.73	51.71	0	0	0.26	20.48	0.72	6.33	0.2	0	0	0	99.99
Saraceno Px	1.04	14.53	3.76	52.09	0	0	0.3	20.29	0.61	7.06	0.32	0	0	0	100
Saraceno Px	0.77	14.49	5.52	51.51	0	0	0.06	19.51	0.63	7.28	0.23	0	0	0	100
Saraceno Px	0.69	16.02	4.21	52.22	0.31	0.5	0.33	19.88	0.69	4.72	0.43	0.12	0	0	100.12
Saraceno Px	0.93	14.87	4.44	51.53	0.45	0.3	0.32	18.54	0.69	7.29	0.64	0.11	0	0	100.11

No.	Na2O	MgO	Al2O3	SiO2	P2O5	SO3	K2O	CaO	TiO2	FeO(tot)	MnO	Cl2O	F	Cr2O3	TOT
Saraceno Px	0.8	14.22	4.81	51.45	0.39	0.41	0.22	19.07	0.66	7.44	0.53	0.21	0	0	100.21
Vulcanello Feld	4.31	0.08	28.16	54.08	0.00	0.00	1.37	11.14	0.00	0.86	0.00	0	0	0	100.00
Vulcanello Feld	6.85	0.05	21.59	62.58	0.04	0.00	3.42	4.64	0.02	0.81	0.00	0	0	0	100.00
Vulcanello Feld	6.02	0.07	23.79	60.04	0.05	0.00	1.85	6.98	0.08	1.11	0.00	0	0	0	100.00
Vulcanello Feld	6.20	0.09	24.37	59.09	0.05	0.00	1.54	7.61	0.04	0.89	0.11	0	0	0	100.00
Vulcanello Feld	4.31	0.07	27.77	54.34	0.00	0.00	1.11	11.60	0.00	0.79	0.00	0	0	0	100.00
Vulcanello Feld	4.68	0.06	27.94	53.87	0.00	0.00	1.30	11.30	0.02	0.81	0.00	0	0	0	100.00
Vulcanello Feld	4.29	0.07	27.51	55.08	0.00	0.00	1.47	10.60	0.04	0.94	0.00	0	0	0	100.00
Vulcanello Feld	5.82	0.07	21.33	62.28	0.00	0.00	6.12	3.38	0.03	0.94	0.02	0	0	0	100.00
Vulcanello Feld	4.48	0.05	28.16	53.78	0.00	0.00	1.22	11.52	0.00	0.72	0.06	0	0	0	100.00
Vulcanello Feld	2.86	0.66	15.23	66.49	0.00	0.00	10.21	1.58	0.37	2.52	0.08	0	0	0	100.00
Vulcanello Feld	2.94	0.38	15.17	68.97	0.00	0.00	8.03	1.02	0.56	2.91	0.03	0	0	0	100.00
Luccia Feld	6.19	0.61	19.68	65.02	0.33	0.00	6.23	0.77	0.29	0.67	0.19	0	0	0	100.00
Luccia Feld	5.92	0.50	19.86	65.23	0.25	0.00	6.40	0.88	0.21	0.59	0.16	0	0	0	100.00
Luccia Feld	5.32	0.68	18.39	66.69	0.24	0.00	7.06	0.52	0.20	0.61	0.29	0	0	0	100.00
Luccia Feld	5.27	0.51	18.38	66.78	0.38	0.00	6.73	0.70	0.26	0.81	0.18	0	0	0	100.00
Luccia Feld	5.46	0.47	18.21	66.85	0.27	0.00	6.82	0.79	0.27	0.58	0.26	0	0	0	100.00
Luccia Feld	5.41	0.63	18.64	65.99	0.30	0.00	6.69	0.98	0.36	0.82	0.17	0	0	0	100.00
Lentia Feld	4.71	0.09	27.26	55.23	0.02	0.00	1.53	10.24	0.00	0.85	0.06	0	0	0	100.00
Lentia Feld	4.30	0.08	27.61	53.84	0.05	0.00	1.20	11.66	0.04	1.22	0.00	0	0	0	100.00
Lentia Feld	4.23	0.08	28.36	53.34	0.04	0.00	1.00	12.05	0.05	0.84	0.00	0	0	0	100.00
Lentia Feld	3.86	0.00	19.46	64.40	0.00	0.00	11.14	0.72	0.04	0.39	0.00	0	0	0	100.00
Saraceno Feld	6.22	0.07	21.44	63.28	0.00	0.00	5.02	2.56	0.45	0.95	0.00	0	0	0	100.00
Saraceno Feld	5.48	0.76	20.18	63.02	0.27	0.00	8.11	1.10	0.36	0.72	0.00	0	0	0	100.00
Saraceno Feld	5.03	0.43	20.30	65.07	0.12	0.00	7.22	1.16	0.06	0.56	0.05	0	0	0	100.00

No.	Na2O	MgO	Al2O3	SiO2	P2O5	SO3	K2O	CaO	TiO2	FeO(tot)	MnO	Cl2O	F	Cr2O3	TOT
Saraceno Feld	4.17	0.83	29.33	52.53	0.44	0.00	0.91	10.40	0.35	0.92	0.11	0	0	0	100.00
Saraceno Feld	5.38	1.25	19.03	63.81	0.26	0.00	6.47	1.82	0.48	1.13	0.35	0	0	0	100.00
Saraceno Feld	5.30	0.81	27.53	54.64	0.31	0.00	1.33	8.30	0.29	1.26	0.23	0	0	0	100.00
Vulcanello/vetro	4.66	2.17	17.34	54.46	0.4	0.11	6.4	4.91	0.55	6.61	0.15	0.26	0.22	0	98.24
Vulcanello/vetro	4.49	2.15	17.73	54.69	0.46	0	6.5	4.72	0.68	6.68	0.05	0.28	0	0	98.43
Vulcanello/vetro	5.11	1.23	17.55	55.19	0.29	0.4	5.49	3.63	0.66	6.58	0.15	0.06	0.09	0	96.43
Vulcanello/vetro	4.8	1.65	17.32	54.85	0.42	0.04	7.1	3.58	0.6	6.14	0.17	0.27	0.13	0	97.07
Vulcanello/vetro	4.19	2.16	17.57	53.67	0.43	0	6.58	4.86	0.57	6.35	0.11	0.3	0	0	96.79
Vulcanello/vetro	4.27	1.93	17.81	54.9	0.38	0.02	6.42	4.64	0.57	6.34	0.15	0.17	0	0	97.6
Vulcanello/vetro	3.82	2.22	17.99	54.96	0	0.06	6.36	5.14	0.65	6.85	0.09	0	0.37	0	98.51
Vulcanello/vetro	4.45	2.24	17.22	54.28	0	0.01	6.45	4.95	0.64	6.66	0.15	0	0	0	97.05
Vulcanello/vetro	4.47	2.12	17.21	54.11	0	0.06	6.37	4.93	0.59	6.69	0.1	0	0	0	96.65
Vulcanello vetro Cos	5.03	2.46	18.25	56.54	0	0.02	7.05	5.33	0.42	6.43	0	0	0	0	101.53
Vulcanello vetro Cos	4.63	2.37	17.46	54.21	0	0.27	6.94	1.62	1.05	6.99	0	0	0	0	95.54
Vulcanello vetro Cos	3.11	1.85	16.63	52.19	0	0.05	6.52	3.47	1.01	6.85	0	0	0	0	91.68
Vulcanello vetro Cos	5.18	2.07	17.88	55.34	0	0.09	6.77	5.26	0.59	6.85	0	0	0	0	100.03
Vulcanello vetro Cos	4.12	2.1	17.26	54.19	0	0.01	6.5	5.31	0.59	6.24	0	0	0	0	96.32
Vulcanello vetro Cos	5.35	1.87	17.25	53.87	0	0.03	6.66	5	0.72	6.66	0	0	0	0	97.41
Vulcanello vetro Cos	5.22	2.08	17.33	54.79	0	0.05	5.98	4.63	0.55	7.02	0	0	0	0	97.65
Vulcanello vetro Cos	2.87	1.97	18.06	57.08	0	0.04	5.77	4.85	0.38	6.45	0	0	0	0	97.47
Vulcanello vetro Cos	4.75	1.1	17.62	52.85	0	0.27	5.49	5.9	0.21	5.41	0	0	0	0	93.6
Vulcanello vetro Cos	4.47	1.99	17.53	54.56	0	0.09	6.41	4.6	0.61	6.54	0	0	0	0	96.8
EGS510/Luccia/vetro	5.03	2.12	18.77	57.57	0.46	0.24	5.6	3.53	0.86	5.44	0.37	0	0	0	99.99
EGS510/Luccia/vetro	4.83	2.45	18.69	57.98	1.01	0.24	5.65	3.38	0.78	4.24	0.43	0.42	0	0	100.1
EGS510/Luccia/vetro	3.97	1.9	18.9	59.8	0.36	0.15	5.99	3.09	0.67	4.95	0.22	0.37	0	0	100.37

No.	Na2O	MgO	Al2O3	SiO2	P2O5	SO3	K2O	CaO	TiO2	FeO(tot)	MnO	Cl2O	F	Cr2O3	TOT
EGS510/Luccia/vetro	3.97	2.24	18.64	57.9	0.57	0.25	6.32	3.58	0.8	5.72	0	0.39	0	0	100.38
EGS510/Luccia/vetro	3.34	2.1	17.83	57.92	0.85	0.27	6.39	3.75	0.76	6.38	0.39	0.38	0	0	100.36
EGS510/Luccia/vetro	3.98	2.11	17.35	60.45	0.64	0.21	5.51	3.28	0.78	5.43	0.27	0.3	0	0	100.31
EGS510/Luccia/vetro	4.29	2.3	18.86	58.13	0.67	0.22	5.84	3.22	0.62	5.59	0.26	0.31	0	0	100.31
Lentia vetro	4.35	1.72	17.25	54.08	0.39	0	7.08	3.97	0.54	6.11	0.09	0.24	0.28	0	96.1
Lentia vetro	4.2	1.68	17.29	55.88	0.41	0	7.12	3.83	0.59	5.66	0.18	0.2	0	0	97.04
Lentia vetro	4.35	1.64	17.41	55.1	0.4	0.09	6.85	3.7	0.6	6.42	0.11	0.25	0.01	0	96.93
Lentia vetro	3.98	1.69	17.15	55.15	0.42	0	6.51	4.22	0.66	6.31	0.13	0.23	0.88	0	97.33
Lentia vetro	2.68	0.91	17.2	58.37	0.3	0.27	5.68	2.98	0.51	4.8	0.07	0.22	0.3	0	94.29
Lentia vetro	3.25	0.59	15.78	58.43	0.4	0.73	5.19	3.03	0.67	4.4	0.19	0.32	1.08	0	94.06
Lentia vetro	4.55	2.21	16.79	54.52	0.45	0	6.24	4.81	0.68	6.41	0.14	0.23	0.16	0	97.19
Lentia vetro	4.6	2.21	16.91	54.43	0.46	0.01	5.86	4.67	0.66	6.24	0.12	0.2	0.12	0	96.49
Lentia vetro	4.4	2.2	16.73	54.58	0.48	0	6.46	4.65	0.63	6.43	0.15	0.2	0.06	0	96.97
Lentia vetro	3.93	2.07	16.88	53.85	0.43	0	6.77	4.61	0.73	6.64	0.15	0.34	0	0	96.4
Lentia vetro	4.44	2.3	17.28	53.88	0.48	0.05	6.4	4.62	0.65	6.48	0.06	0.25	0	0	96.89
Lentia vetro	4.18	2.17	16.69	54.78	0.42	0.04	6.43	4.71	0.61	6.41	0.13	0.22	0.12	0	96.91
Lentia vetro	4.05	2.48	16.78	53.12	0.55	0.02	6.24	4.88	0.57	6.82	0.11	0.2	0.13	0	95.95
Lentia vetro	4.42	1.81	17.02	55.09	0.47	0.04	6.87	4.08	0.65	6.41	0.16	0.36	0.04	0	97.42
Lentia vetro	4.44	1.26	17.32	56.11	0.4	0.36	6.49	3.01	0.52	5.11	0	0.15	0.6	0	95.77
Lentia vetro	3.83	0.74	16.58	56.16	0.38	1.26	7.09	2.58	0.56	5.76	0.08	0.13	0.56	0	95.71
Lentia vetro	4.49	0.54	15.63	60.69	0.37	0.05	5.16	2.36	0.41	4.62	0.09	0.07	0.86	0	95.34
Lentia vetro	3.64	0.49	15.67	55.94	0.3	2.47	5.28	1.38	0.65	6.36	0.06	0.07	2	0	94.31
Lentia vetro	4.46	1.83	17.05	54.79	0.43	0.05	6.91	4.21	0.59	6.17	0.1	0.25	0	0	96.84
Lentia vetro	4.27	1.85	16.84	53.9	0.43	0	6.82	4.06	0.6	6.23	0.19	0.3	0.1	0	95.59
Lentia vetro	4.44	1.67	17.32	55.6	0.39	0.06	6.83	3.78	0.69	6.26	0.12	0.29	1.3	0	98.75

No.	Na2O	MgO	Al2O3	SiO2	P2O5	SO3	K2O	CaO	TiO2	FeO(tot)	MnO	Cl2O	F	Cr2O3	TOT
Saraceno vetro-Cs	4.67	2.78	18.52	57.8	0.57	0	5.8	4.01	0.73	5.11	0	0	0	0	99.99
Saraceno vetro-Cs	4.57	2.6	18.45	57.68	0.72	0.12	5.91	3.83	0.77	5.33	0	0	0	0	99.98
Saraceno vetro-Cs	4.57	2.63	18.32	57.51	0.69	0.23	5.81	4.06	0.6	5.59	0	0	0	0	100.01
Saraceno vetro-Cs	5.49	2.55	18.02	55.86	0	0.28	8.04	3.9	0.6	5.18	0.07	0	0	0	99.99
Saraceno vetro-Cs	5.35	2.53	18.15	57.03	0	0.67	6.07	4.12	0.54	5.25	0.28	0	0	0	99.99
Saraceno vetro	4.44	1.71	18.5	58.18	0.25	0.11	6.34	3.86	0.66	5.95	0	0	0	0	100
Saraceno vetro	3.7	1.85	18.26	57.53	0.22	0.07	6.67	4.51	0.78	6.41	0	0	0	0	100
Saraceno vetro	4.58	1.93	18.24	56.95	0.22	0	6.56	4.48	0.72	6.33	0	0	0	0	100.01
Saraceno vetro	4.32	2.28	18.03	56.19	0.3	0.2	6.59	4.55	0.85	6.69	0	0	0	0	100
Saraceno vetro/roccia	3.83	3.01	21.32	51.53	0.22	0	2.23	10.18	0.63	6.5	0.55	0	0	0	100
Saraceno vetro/roccia	4.43	3.75	16.49	58.78	0	0	4.75	6.1	0.72	4.61	0.36	0	0	0	99.99
Saraceno vetro/roccia	1.75	5.33	13.05	52.41	2.88	2.58	3.53	1.45	0.74	16.02	0.27	0	0	0	100.01

Appendix C.

The result data of the Microprobe Analysis:

No.	Na2O	MgO	Al2O3	SiO2	P2O5	SO3	K2O	CaO	TiO2	FeO(tot)	MnO	Cl2O	Cr2O3	TOT
S1-1	0.22	0.44	4.22	54.02	0.96	9.81	2.79	0.25	0.26	15.04	0.03	0.18	0.01	88.24
S1-2	0.49	0.82	7.27	48.35	1.61	11.90	4.71	1.06	0.39	18.22	0.06	0.23	0.00	95.10
S1-3	0.83	0.88	5.84	41.48	1.81	13.51	4.47	1.11	0.30	19.72	0.04	0.17	0.00	90.15
S1-4	0.44	1.43	5.90	36.86	1.98	11.75	4.36	0.51	0.34	29.60	0.08	0.21	0.02	93.47
S1-5	0.32	0.86	3.82	41.68	1.46	9.48	3.32	0.38	0.29	28.92	0.06	0.17	0.00	90.77
S1-6	0.84	0.47	8.19	27.82	1.80	21.41	6.19	1.14	0.45	26.07	0.03	0.38	0.04	94.83
S1-7	0.65	0.43	4.85	23.52	2.43	20.69	6.46	0.59	0.29	28.77	0.04	0.49	0.00	89.22
S1-8	0.56	0.65	5.38	24.01	2.16	15.21	5.58	0.38	0.86	35.64	0.07	0.31	0.02	90.84
S1-9	0.51	0.60	5.24	31.97	2.02	14.31	4.78	0.56	0.44	25.09	0.06	0.33	0.03	85.93
S1-10	0.45	0.49	5.72	32.16	2.77	14.97	5.48	0.70	0.40	23.74	0.04	0.28	0.04	87.25
S1-11	1.20	0.34	7.92	51.51	2.01	9.45	4.87	0.92	0.28	12.82	0.01	0.17	0.04	91.54
S1-12	0.77	0.86	10.87	47.73	1.86	8.99	4.15	2.80	0.41	13.08	0.06	0.24	0.03	91.85
S1-13	0.27	0.45	3.29	56.02	1.32	8.84	3.00	0.40	0.22	10.35	0.00	0.14	0.02	84.33
S1-14	0.52	0.39	3.73	33.05	2.30	16.07	5.53	0.52	0.39	26.98	0.01	0.28	0.00	89.78
S1-15	0.21	0.45	3.33	64.80	0.90	5.70	2.29	0.31	0.22	9.32	0.02	0.16	0.02	87.73
S1-16	0.54	0.46	3.82	58.17	1.44	9.19	3.32	0.29	0.38	15.76	0.01	0.20	0.02	93.61
S1-17	0.56	0.54	5.48	42.07	2.10	15.52	5.03	0.47	0.59	21.87	0.04	0.27	0.02	94.56
S1-18	1.32	0.50	7.62	44.04	1.38	7.10	5.15	0.25	4.05	19.91	0.04	0.15	0.07	91.59
S1-19	0.87	0.51	5.20	40.40	1.95	12.21	5.08	0.43	0.58	20.73	0.05	0.48	0.01	88.50
S1-20	1.59	0.36	11.47	49.65	1.00	7.54	8.39	0.49	0.26	10.53	0.02	0.43	0.00	91.72
S1-21	0.68	1.00	6.32	31.65	2.18	18.64	6.67	0.29	0.97	25.21	0.00	0.39	0.01	93.99
S1-22	0.85	0.52	6.05	28.15	2.12	19.92	6.32	0.42	0.40	25.41	0.05	0.44	0.00	90.66

No.	Na2O	MgO	Al2O3	SiO2	P2O5	SO3	K2O	CaO	TiO2	FeO(tot)	MnO	Cl2O	Cr2O3	TOT
S1-23	1.71	1.13	7.76	36.13	1.40	13.85	6.99	1.31	0.38	20.78	0.06	0.40	0.00	91.89
S1-24	0.80	0.77	3.52	17.49	1.25	15.02	5.03	0.39	1.73	43.69	0.20	0.33	0.04	90.26
S1-25	0.94	0.58	5.91	37.83	1.44	15.64	5.34	1.04	0.31	20.68	0.02	0.39	0.00	90.12
S1-26	0.74	0.50	4.81	32.55	1.49	19.42	5.65	0.60	0.87	25.14	0.04	0.44	0.05	92.30
S1-27	0.56	0.61	4.34	34.70	1.91	18.44	5.51	0.30	0.89	28.19	0.02	0.45	0.00	95.90
S1-28	0.48	0.47	4.62	16.70	2.74	24.63	7.22	0.41	0.55	32.26	0.01	0.49	0.05	90.62
S1-29	0.53	0.47	5.15	18.45	2.87	22.00	6.61	0.41	0.51	32.25	0.05	0.43	0.01	89.74
S1-30	0.75	0.48	5.25	21.89	2.90	21.43	6.46	0.54	0.47	27.15	0.05	0.40	0.03	87.81
S1-31	0.64	0.45	4.99	39.10	2.37	15.43	4.86	0.48	0.67	21.18	0.01	0.39	0.00	90.57
S1-32	1.80	0.20	11.45	55.89	1.56	6.61	7.98	0.24	0.39	6.09	0.00	0.57	0.04	92.82
S1-33	0.59	0.41	5.76	52.12	1.71	9.29	4.50	0.28	0.45	13.67	0.03	0.46	0.00	89.27
S1-34	0.97	0.32	5.27	48.85	1.53	10.45	4.29	0.76	0.42	16.94	0.04	0.49	0.00	90.33
S1-35	0.82	0.88	5.69	47.26	1.40	8.89	5.14	0.52	0.71	16.26	0.03	0.40	0.01	88.01
S1-36	1.08	8.49	7.61	42.38	0.92	6.82	6.70	0.47	6.61	13.25	0.02	0.41	0.00	94.77
S1-37	0.82	8.10	8.22	42.28	0.69	4.16	7.07	0.31	5.42	10.24	0.05	0.18	0.03	87.56
S1-38	1.01	0.66	14.39	51.60	0.97	6.98	4.38	0.95	0.50	13.61	0.02	0.53	0.00	95.59
S1-39	1.14	0.43	12.06	43.33	1.65	9.77	5.69	0.64	0.63	17.78	0.07	0.65	0.04	93.87
S1-40	0.52	0.41	7.25	30.32	2.01	14.77	5.47	0.65	0.39	27.56	0.05	0.48	0.01	89.89
S1-41	1.00	0.69	8.23	43.45	1.61	12.08	5.29	0.90	0.41	18.06	0.05	0.41	0.03	92.22
S1-42	0.37	0.31	3.10	42.33	2.08	14.86	4.71	0.36	0.68	22.25	0.05	0.35	0.02	91.47
S1-43	0.31	0.11	1.67	59.64	1.31	11.49	3.38	0.20	0.25	12.46	0.04	0.27	0.01	91.14
S1-44	0.61	0.27	2.87	37.76	1.89	16.48	5.55	0.42	0.90	25.57	0.02	0.40	0.00	92.74
S1-45	1.64	0.65	9.91	48.05	1.33	10.50	5.44	1.29	0.51	12.63	0.01	0.45	0.00	92.41
S1-46	0.51	0.45	2.65	34.64	1.89	18.09	5.52	0.41	0.32	24.47	0.00	0.48	0.03	89.45
S1-47	0.68	0.78	4.18	56.35	1.39	10.12	3.77	0.71	0.26	13.92	0.02	0.59	0.01	92.79

No.	Na2O	MgO	Al2O3	SiO2	P2O5	SO3	K2O	CaO	TiO2	FeO(tot)	MnO	Cl2O	Cr2O3	TOT
S1-48	2.55	1.64	14.65	51.92	0.91	3.81	6.39	3.57	0.62	8.38	0.12	0.37	0.00	94.93
S1-49	0.79	0.63	7.47	54.27	1.20	6.59	3.89	1.74	0.45	11.61	0.04	0.32	0.03	89.03
S1-50	0.46	0.42	4.91	52.72	0.93	6.79	3.01	0.57	0.36	12.97	0.01	0.34	0.04	83.52
S1-51	0.87	0.30	5.98	65.40	0.81	5.74	3.60	0.46	0.24	10.23	0.00	0.25	0.01	93.88
S1-52	0.93	0.37	6.49	71.06	0.51	3.58	3.51	0.54	0.21	6.56	0.00	0.19	0.02	93.96
S1-53	0.94	0.35	4.99	70.59	0.60	4.78	2.44	0.46	0.18	7.31	0.02	0.13	0.00	92.79
S1-54	0.84	0.39	3.17	70.74	0.69	5.47	2.06	0.23	0.50	7.38	0.02	0.27	0.00	91.75
S1-55	0.55	0.76	3.27	60.07	0.73	5.75	2.73	0.22	4.82	8.90	0.02	0.35	0.03	88.20
S1-56	0.82	0.60	5.83	29.06	1.73	19.55	6.40	0.78	0.41	26.31	0.04	0.52	0.04	92.08
S1-57	0.46	0.73	4.53	35.48	1.40	17.23	5.31	0.68	0.74	23.79	0.00	0.42	0.01	90.76
S1-58	0.45	0.46	3.75	26.53	1.99	20.48	6.23	0.36	0.47	29.21	0.05	0.47	0.02	90.48
S1-59	0.15	0.50	1.60	51.72	1.15	12.37	3.32	0.20	0.33	13.10	0.05	0.56	0.00	85.04
S1-60	0.80	0.50	5.49	27.87	2.68	17.06	6.03	0.78	0.49	28.29	0.01	0.45	0.00	90.46
S2-1	1.23	0.47	7.51	52.25	1.45	8.37	4.57	0.64	0.26	13.53	0.05	0.18	0.00	90.51
S2-2	0.55	0.37	5.25	24.74	2.59	20.55	7.38	0.47	0.26	30.24	0.04	0.32	0.02	92.76
S2-3	0.38	0.34	4.56	20.91	2.38	22.09	7.22	0.31	0.23	30.28	0.01	0.32	0.01	89.04
S2-4	0.21	0.48	4.44	37.92	1.93	17.73	5.31	0.27	0.32	21.61	0.04	0.23	0.00	90.49
S2-5	0.33	0.69	5.22	39.58	1.85	17.59	5.10	0.30	0.58	23.98	0.05	0.24	0.00	95.52
S2-6	0.26	0.97	4.91	37.98	1.74	18.54	5.50	0.67	0.43	25.41	0.11	0.23	0.01	96.75
S2-7	0.25	1.10	4.50	29.39	1.67	21.81	6.42	0.70	0.40	29.22	0.10	0.31	0.03	95.90
S2-8	0.16	0.77	3.26	40.01	1.08	18.06	5.03	0.41	0.34	22.16	0.12	0.27	0.00	91.67
S2-9	0.12	0.74	2.34	63.32	0.70	10.02	2.96	0.31	0.28	10.17	0.02	0.14	0.04	91.15
S2-10	0.28	0.96	2.67	54.66	1.01	10.93	3.30	0.93	0.31	15.27	0.07	0.17	0.02	90.56
S2-11	0.30	0.74	3.48	38.44	1.52	19.17	5.48	0.29	0.73	28.73	0.12	0.25	0.01	99.26
S2-12	0.40	0.55	3.84	23.50	1.85	24.66	7.13	0.31	0.31	32.27	0.10	0.34	0.00	95.25

No.	Na2O	MgO	Al2O3	SiO2	P2O5	SO3	K2O	CaO	TiO2	FeO(tot)	MnO	Cl2O	Cr2O3	TOT
S2-13	0.26	0.46	3.76	23.98	1.92	22.89	7.11	0.35	0.22	28.90	0.10	0.32	0.01	90.28
S2-14	0.29	0.39	3.45	25.06	1.92	22.75	6.75	0.27	0.27	28.53	0.03	0.36	0.04	90.10
S2-15	0.32	0.35	3.00	17.56	1.67	26.09	7.27	0.33	0.36	31.51	0.04	0.45	0.03	88.97
S2-16	0.25	0.45	4.36	18.99	1.94	24.98	6.60	0.35	0.44	28.09	0.08	0.56	0.01	87.11
S2-17	0.23	0.43	4.63	17.85	2.57	24.71	5.82	0.28	0.48	30.23	0.06	0.49	0.00	87.78
S2-18	0.20	0.61	4.27	11.84	3.03	26.71	6.18	0.27	0.35	34.62	0.04	0.33	0.01	88.47
S2-19	0.14	0.81	4.07	8.71	3.23	26.37	6.17	0.27	0.34	35.75	0.07	0.29	0.02	86.24
S2-20	0.21	0.49	3.97	11.23	2.87	26.75	6.64	0.32	0.27	32.20	0.05	0.29	0.03	85.32
S2-21	0.18	0.51	3.36	21.35	2.10	24.23	5.82	0.27	0.21	27.50	0.06	0.29	0.00	85.88
S2-22	0.16	0.50	3.32	29.09	1.43	23.27	5.68	0.19	0.15	24.91	0.06	0.32	0.02	89.10
S2-23	0.08	0.46	2.53	52.96	0.70	13.83	3.59	0.12	0.07	13.41	0.01	0.19	0.00	87.96
S2-24	0.51	0.54	4.22	39.51	1.19	18.96	5.27	0.30	0.15	22.93	0.06	0.28	0.00	93.91
S2-25	0.38	0.48	4.19	33.21	1.28	22.15	5.86	0.32	0.18	25.97	0.07	0.30	0.02	94.40
S2-26	0.24	0.36	3.64	27.34	1.55	23.31	6.10	0.21	0.12	27.70	0.09	0.30	0.00	90.98
S2-27	0.23	0.37	4.12	36.98	1.52	19.94	5.76	0.26	0.25	23.86	0.06	0.25	0.00	93.59
S2-28	0.29	0.67	6.25	44.19	1.21	13.98	5.41	0.90	0.32	19.54	0.02	0.26	0.04	93.07
S2-29	0.24	0.40	5.01	28.09	1.11	18.84	6.01	0.29	0.25	30.57	0.04	0.32	0.02	91.21
S2-30	0.39	0.57	3.66	24.93	0.98	24.08	6.83	0.24	0.28	30.65	0.06	0.42	0.06	93.14
S2-31	0.30	0.56	3.58	37.59	0.96	20.06	5.99	0.25	0.40	23.40	0.04	0.40	0.04	93.58
S2-32	0.30	0.45	4.20	34.04	1.21	20.31	5.94	0.38	0.80	24.63	0.05	0.32	0.02	92.66
S2-33	0.34	0.42	4.36	33.16	1.32	21.23	5.93	0.30	0.54	26.59	0.05	0.31	0.02	94.56
S2-34	0.12	0.50	4.22	44.59	1.10	15.89	4.53	0.26	0.37	18.36	0.06	0.25	0.01	90.27
S2-35	0.11	0.74	4.22	51.99	0.90	10.42	3.16	0.41	0.30	12.72	0.05	0.25	0.01	85.29
S2-36	0.11	0.51	3.26	49.33	0.75	8.71	3.01	0.33	0.23	9.95	0.00	0.31	0.03	76.53
S2-37	0.09	0.36	2.71	37.61	0.70	8.17	2.69	0.22	0.16	9.76	0.04	0.44	0.01	62.95

No.	Na2O	MgO	Al2O3	SiO2	P2O5	SO3	K2O	CaO	TiO2	FeO(tot)	MnO	Cl2O	Cr2O3	TOT
S2-38	0.23	0.53	5.24	38.61	1.12	12.31	4.24	0.53	0.31	18.63	0.04	0.33	0.03	82.15
S2-39	0.48	0.49	6.09	41.87	1.28	15.24	5.22	0.64	0.39	21.18	0.00	0.26	0.00	93.13
S2-40	0.96	0.49	7.65	44.97	1.18	13.67	4.39	1.34	0.30	17.95	0.02	0.23	0.00	93.13
S3-1	0.37	13.94	3.68	49.84	0.04	0.03	0.09	22.04	0.68	7.56	0.13	0.01	0.11	98.52
S3-2	0.37	14.07	3.46	50.36	0.04	0.05	0.10	22.23	0.58	6.97	0.08	0.01	0.36	98.67
S3-3	0.46	13.42	3.83	51.17	0.09	0.48	0.31	20.63	0.69	7.80	0.14	0.03	0.32	99.35
S3-4	0.30	6.14	3.78	52.34	0.85	6.97	1.47	11.49	0.80	14.82	0.04	0.08	0.19	99.27
S3-5	0.12	1.54	3.68	49.55	1.27	12.41	3.00	1.52	0.38	18.19	0.02	0.14	0.08	91.90
S3-6	0.16	1.22	4.50	41.79	1.83	17.30	4.07	0.75	0.36	28.19	0.09	0.18	0.00	100.44
S3-7	0.20	0.99	5.17	35.90	1.93	19.56	5.26	0.36	0.33	29.89	0.09	0.19	0.00	99.87
S3-8	0.22	0.86	6.17	42.25	1.71	20.44	5.40	0.49	0.43	23.25	0.15	0.21	0.04	101.62
S3-9	0.32	0.82	5.96	40.63	1.49	18.97	5.05	0.52	0.33	22.03	0.03	0.21	0.06	96.43
S3-10	0.50	0.50	7.06	34.49	1.10	21.25	4.52	0.67	0.21	25.40	0.00	0.33	0.06	96.10
S3-11	0.17	0.85	2.72	11.25	0.86	28.80	5.23	0.30	0.25	43.34	0.00	0.48	0.06	94.30
S3-12	0.11	0.77	2.77	6.51	0.93	30.32	3.53	0.30	0.11	45.69	0.02	0.48	0.01	91.56
S3-13	0.10	0.84	3.74	8.15	1.71	30.62	3.33	0.46	0.24	42.88	0.07	0.42	0.09	92.66
S3-14	0.13	0.87	4.43	18.01	1.39	25.77	4.86	0.51	0.27	33.71	0.11	0.37	0.16	90.58
S3-15	0.27	0.87	5.10	34.41	1.33	19.03	4.80	0.43	0.31	18.41	0.02	0.29	0.06	85.33
S3-16	0.16	0.93	4.96	52.42	0.92	12.97	2.98	0.61	0.32	14.41	0.05	0.16	0.01	90.90
S3-17	0.43	1.71	6.30	53.51	1.01	10.29	3.59	1.26	0.50	16.85	0.18	0.17	0.02	95.82
S3-18	0.28	1.16	6.65	57.48	1.21	9.04	3.06	0.99	0.42	14.10	0.14	0.15	0.06	94.74
S3-19	0.18	1.20	7.93	43.90	1.38	10.75	3.62	1.65	0.45	16.91	0.01	0.20	0.00	88.17
S3-20	0.21	2.25	5.52	44.92	1.12	12.73	3.79	1.69	0.46	16.77	0.11	0.21	0.07	89.85
S3-21	0.12	1.22	4.75	59.24	0.73	6.68	2.08	0.88	0.42	10.34	0.12	0.15	0.06	86.77
S3-22	0.19	1.29	5.23	60.82	1.20	7.88	2.65	1.14	0.37	14.44	0.03	0.17	0.02	95.43

No.	Na2O	MgO	Al2O3	SiO2	P2O5	SO3	K2O	CaO	TiO2	FeO(tot)	MnO	Cl2O	Cr2O3	TOT
S3-23	0.20	0.83	3.86	59.23	1.59	8.90	3.19	0.50	0.31	15.10	0.19	0.17	0.00	94.08
S3-24	0.22	0.82	3.21	61.64	1.12	6.62	2.94	0.47	0.29	11.90	0.16	0.22	0.11	89.71
S3-25	0.81	0.68	7.41	68.47	0.37	2.96	0.95	2.41	0.13	7.20	0.08	0.22	0.00	91.69
S3-26	2.80	0.29	21.65	59.48	0.11	0.99	1.02	9.51	0.07	1.36	0.00	0.08	0.00	97.36
S3-27	2.31	0.16	26.10	56.92	0.05	0.13	1.01	11.14	0.04	1.29	0.06	0.01	0.00	99.21
S3-28	1.76	0.45	12.86	71.08	0.30	1.19	0.77	5.15	0.09	3.35	0.09	0.10	0.06	97.26
S3-29	0.21	0.56	3.36	69.16	0.75	4.35	1.28	0.56	0.23	7.71	0.04	0.13	0.01	88.35
S3-30	0.23	0.70	3.63	52.81	1.12	10.39	3.55	0.49	0.33	21.97	0.03	0.17	0.00	95.43
S3-31	0.42	1.09	8.54	48.37	1.13	11.33	4.89	2.18	0.61	11.28	0.10	0.28	0.00	90.24
S3-32	0.23	0.55	4.89	55.95	1.34	11.41	3.30	1.04	0.38	16.04	0.08	0.19	0.03	95.43
S3-33	0.28	0.39	2.89	31.21	2.41	21.21	5.85	0.37	0.46	31.69	0.06	0.30	0.02	97.14
S3-34	0.35	0.75	3.01	27.13	2.37	20.85	6.92	0.88	0.58	29.87	0.14	0.31	0.07	93.23
S3-35	0.28	0.75	2.47	51.32	1.86	12.00	3.47	1.00	0.38	21.88	0.05	0.19	0.01	95.66
S3-36	0.25	0.55	2.80	44.10	2.27	16.44	4.87	0.43	0.50	25.29	0.14	0.23	0.04	97.90
S3-37	0.22	0.50	3.44	42.84	2.36	15.98	4.89	0.30	0.29	25.16	0.09	0.19	0.02	96.28
S3-38	0.33	0.84	4.31	40.64	2.39	15.55	5.37	0.35	0.45	28.02	0.24	0.18	0.00	98.67
S3-39	0.25	0.44	3.46	48.84	2.17	13.17	3.96	0.33	0.68	21.39	0.13	0.19	0.00	95.01
S3-40	0.50	0.51	6.56	37.43	2.42	14.85	4.15	0.81	0.64	23.63	0.05	0.20	0.03	91.77
S3-41	0.25	0.85	5.51	30.54	2.67	18.03	5.30	0.56	0.62	28.15	0.11	0.27	0.00	92.87
S3-42	0.31	0.64	6.14	49.66	1.96	12.58	4.02	0.73	0.41	18.49	0.09	0.17	0.09	95.29
S3-43	0.64	1.25	4.72	56.68	1.26	8.61	3.15	2.19	0.35	14.99	0.10	0.13	0.07	94.14
S3-44	0.93	1.10	6.50	61.33	1.04	5.12	2.25	2.98	0.39	12.00	0.13	0.10	0.06	93.92
S3-45	0.98	0.51	7.69	59.42	1.04	6.89	3.06	0.91	0.39	10.57	0.11	0.12	0.08	91.76
S3-46	0.43	0.56	4.30	67.01	1.06	5.99	1.82	0.43	0.26	10.21	0.00	0.09	0.04	92.20
S3-47	0.25	0.56	3.86	60.43	1.64	10.21	2.69	0.41	0.42	20.88	0.06	0.15	0.00	101.55

No.	Na2O	MgO	Al2O3	SiO2	P2O5	SO3	K2O	CaO	TiO2	FeO(tot)	MnO	Cl2O	Cr2O3	TOT
S3-48	0.17	0.51	3.27	64.95	1.29	8.01	2.71	0.28	1.10	15.01	0.09	0.14	0.13	97.65
S3-49	0.31	0.32	4.05	40.03	0.05	0.01	4.39	0.64	0.52	0.34	0.00	0.00	0.04	50.69
S3-50	0.15	0.77	4.79	49.02	1.43	11.34	4.02	0.68	0.36	20.00	0.02	0.17	0.08	92.85
S3-51	0.34	0.74	4.19	45.17	1.02	5.87	4.60	0.45	0.38	11.89	0.06	0.13	0.01	74.85
S3-52	0.36	0.74	6.43	41.47	1.71	14.28	5.11	0.55	0.58	24.00	0.09	0.23	0.02	95.58
S3-53	0.32	0.57	6.51	48.40	1.46	15.98	4.83	0.34	0.58	20.12	0.04	0.20	0.10	99.46
S3-54	0.24	0.67	5.47	58.69	1.28	12.42	3.20	0.48	0.41	13.68	0.09	0.20	0.10	96.94
S3-55	0.45	1.94	7.27	59.34	0.91	7.27	2.65	3.44	0.75	7.98	0.00	0.18	0.02	92.21
S3-56	0.61	1.30	10.33	55.65	1.07	5.39	4.53	2.56	0.55	9.49	0.04	0.21	0.00	91.72
S3-57	0.61	0.61	6.77	47.86	1.62	10.93	3.64	0.99	0.35	18.26	0.14	0.22	0.03	92.04
S3-58	1.43	0.37	9.51	51.62	1.17	10.49	4.21	1.00	0.30	9.50	0.11	0.22	0.15	90.07
S3-59	1.01	0.47	7.96	49.60	1.55	12.09	4.60	0.59	0.40	18.31	0.11	0.21	0.00	96.91
S3-60	0.81	0.71	5.73	37.04	1.82	15.77	5.78	0.50	3.21	34.37	0.16	0.26	0.10	106.27
S3-61	0.78	0.59	5.18	39.35	1.47	12.34	4.67	0.50	3.11	24.13	0.16	0.22	0.01	92.52
S3-62	0.39	1.00	3.71	35.89	1.46	11.38	4.44	0.33	2.10	35.85	0.14	0.22	0.01	96.90
S3-63	0.10	1.53	3.09	36.53	0.82	5.70	2.03	0.20	0.79	36.99	0.38	0.10	0.15	88.41
S3-64	0.25	0.95	5.02	62.43	0.85	6.11	2.15	0.51	0.63	9.71	0.15	0.11	0.00	88.88
S3-65	0.19	0.56	4.50	62.98	1.16	8.78	2.99	0.34	0.82	14.23	0.08	0.12	0.00	96.74
S3-66	0.32	0.84	4.51	46.95	1.84	17.12	5.43	0.34	0.35	28.92	0.15	0.24	0.00	107.01
S3-67	0.40	0.69	4.41	40.47	1.95	17.99	6.19	0.40	0.32	25.37	0.00	0.27	0.06	98.51
S3-68	0.30	0.55	4.11	31.98	2.02	17.09	5.91	0.32	0.28	28.12	0.09	0.28	0.00	91.05
S3-69	0.22	0.79	3.48	38.34	1.58	15.16	4.14	0.24	0.23	19.18	0.10	0.28	0.04	83.78
S3-70	0.20	0.68	5.70	32.11	2.02	17.16	4.27	0.33	0.29	27.69	0.09	0.29	0.07	90.88
S3-71	0.23	0.54	6.79	36.97	1.57	15.63	3.87	0.35	0.33	21.75	0.00	0.30	0.00	88.32
S3-72	0.28	0.89	8.58	57.14	0.87	6.49	2.85	1.42	0.62	8.60	0.10	0.25	0.07	88.17

No.	Na2O	MgO	Al2O3	SiO2	P2O5	SO3	K2O	CaO	TiO2	FeO(tot)	MnO	Cl2O	Cr2O3	TOT
S3-73	0.18	0.84	5.76	66.31	0.63	5.73	2.00	0.77	0.59	8.19	0.15	0.19	0.06	91.40
S3-74	0.13	0.83	2.92	75.73	0.46	4.17	1.17	0.25	0.13	4.54	0.00	0.20	0.00	90.53
S3-75	0.08	0.72	2.58	75.38	0.53	4.19	0.82	0.20	0.19	4.81	0.00	0.25	0.00	89.75
S3-76	0.29	1.05	4.13	37.32	2.08	14.70	5.11	0.41	0.35	31.59	0.11	0.26	0.00	97.40
S3-77	0.20	0.44	5.59	35.68	1.99	14.32	3.99	0.41	0.51	29.63	0.07	0.24	0.00	93.07
S3-78	0.45	0.39	4.16	32.81	1.66	16.84	4.86	0.38	0.46	21.67	0.06	0.31	0.00	84.06
S3-79	0.30	0.35	4.97	41.53	1.55	15.38	4.01	0.44	0.47	16.62	0.11	0.30	0.01	86.03
S3-80	0.29	0.41	7.03	51.10	1.35	10.55	6.63	0.38	0.42	16.07	0.06	0.19	0.04	94.52
S3-81	0.28	0.28	10.09	53.79	1.24	8.61	6.48	0.22	0.39	17.38	0.03	0.11	0.01	98.91
S3-82	0.27	0.18	12.93	61.50	0.79	5.57	7.79	0.20	0.32	12.80	0.10	0.09	0.01	102.54
S3-83	0.22	0.23	10.27	60.27	1.00	6.11	5.59	0.19	0.26	13.96	0.00	0.10	0.02	98.21
S3-84	0.25	0.42	7.92	46.16	1.77	14.77	4.63	0.25	0.34	22.70	0.14	0.24	0.00	99.58
S3-85	0.45	0.74	6.82	24.76	1.98	22.43	7.33	0.31	0.45	34.88	0.09	0.33	0.05	100.61
S3-86	0.40	0.79	8.06	27.14	2.11	23.52	7.55	0.41	0.83	33.44	0.06	0.42	0.06	104.79
S3-87	0.34	0.51	7.39	22.61	2.29	25.40	8.22	0.39	0.52	31.27	0.08	0.41	0.02	99.45
S3-88	0.32	0.43	5.42	33.16	1.97	21.03	6.48	0.26	0.44	26.19	0.03	0.39	0.00	96.11
S3-89	0.35	0.39	5.25	31.01	1.93	20.01	6.10	0.29	0.53	29.67	0.11	0.46	0.07	96.16
S3-90	0.24	0.37	4.83	39.21	1.71	20.95	4.33	0.29	0.38	22.02	0.10	0.47	0.01	94.92
S3-91	0.28	0.43	4.61	47.69	1.50	15.57	4.36	0.22	0.56	17.53	0.06	0.40	0.00	93.21
S3-92	0.34	0.43	5.34	34.63	2.35	19.41	5.35	0.38	0.96	31.61	0.15	0.33	0.02	101.28
S3-93	0.14	0.35	4.29	42.96	2.10	16.00	4.31	0.29	0.53	21.08	0.04	0.34	0.02	92.44
S3-94	0.20	0.31	2.88	54.20	1.95	10.81	3.81	0.21	0.42	17.80	0.03	0.31	0.13	93.05
S3-95	0.16	0.38	3.45	39.16	2.56	15.88	3.79	0.29	0.91	27.20	0.06	0.29	0.04	94.16
S3-96	0.13	0.42	4.37	31.32	2.63	18.98	4.47	0.38	0.96	29.34	0.00	0.32	0.00	93.33
S3-97	0.16	0.31	4.62	34.35	2.41	19.24	4.55	0.34	1.97	23.06	0.13	0.34	0.00	91.48

No.	Na2O	MgO	Al2O3	SiO2	P2O5	SO3	K2O	CaO	TiO2	FeO(tot)	MnO	Cl2O	Cr2O3	TOT
S3-98	0.10	0.30	4.07	38.18	2.11	16.72	3.68	0.26	1.74	18.60	0.04	0.28	0.00	86.08
S3-99	0.17	0.26	4.54	44.53	2.03	13.14	4.05	0.28	1.09	20.39	0.14	0.26	0.01	90.90
S3-100	0.16	0.57	4.14	31.10	1.41	10.45	2.50	0.20	0.42	44.41	0.33	0.18	0.00	95.88
S3-101	0.11	0.71	3.10	44.29	1.28	7.30	2.39	0.24	0.86	20.38	0.17	0.13	0.10	81.05
S3-102	0.12	0.80	3.30	46.70	1.33	8.60	2.77	0.22	0.79	15.34	0.04	0.16	0.20	80.36
S3-103	0.39	0.94	4.12	31.08	2.54	18.87	6.54	0.63	0.64	32.18	0.04	0.31	0.05	98.33
S3-104	0.57	0.67	4.46	24.31	2.18	19.51	6.82	0.56	0.49	31.64	0.02	0.33	0.04	91.60
S3-105	0.50	0.66	5.56	30.52	2.45	19.67	5.62	0.64	0.56	35.46	0.10	0.31	0.00	102.04
S3-106	0.32	1.69	3.62	29.88	1.68	18.31	5.20	2.40	0.37	29.13	0.12	0.33	0.00	93.05
S3-107	0.64	0.95	6.87	34.16	1.71	18.21	5.40	0.90	0.61	25.91	0.09	0.27	0.07	95.78
S3-108	1.41	0.99	7.60	48.75	1.10	10.02	5.00	1.61	0.46	16.52	0.09	0.17	0.00	93.73
S3-109	0.67	1.18	5.48	50.59	1.16	11.02	3.81	0.98	0.33	13.59	0.11	0.13	0.02	89.06
S3-110	0.40	0.82	5.32	42.36	2.01	17.97	4.93	0.49	0.30	28.97	0.04	0.24	0.00	103.86
S3-111	0.43	1.24	6.29	32.83	2.57	21.52	7.39	0.75	0.39	35.49	0.12	0.27	0.04	109.32
S3-112	0.47	2.35	6.33	37.51	2.08	16.97	6.14	3.17	0.52	27.63	0.24	0.21	0.00	103.62
S3-113	0.34	0.99	6.38	45.69	1.92	13.34	5.11	0.66	0.29	19.72	0.08	0.14	0.00	94.66
S3-114	0.24	0.58	5.73	47.27	1.87	13.53	4.68	0.51	0.38	19.98	0.04	0.15	0.03	94.99
S3-115	0.17	0.88	4.46	50.93	1.59	11.98	3.89	0.40	0.32	22.65	0.16	0.15	0.00	97.58
S3-116	0.27	1.14	5.23	47.72	1.53	15.18	4.94	0.46	0.37	22.45	0.25	0.19	0.03	99.75
S3-117	0.68	1.85	6.27	36.45	1.71	14.63	6.23	1.39	0.48	26.16	0.09	0.22	0.03	96.19
S3-118	0.75	1.53	11.28	46.68	1.09	10.31	4.02	1.71	0.58	11.45	0.04	0.26	0.12	89.82
S3-119	0.66	1.51	10.57	44.09	1.29	13.63	4.05	1.64	0.60	14.06	0.04	0.27	0.06	92.48
S3-120	1.44	1.99	17.41	54.00	0.72	2.07	3.82	4.33	0.77	7.50	0.12	0.31	0.03	94.51
S3-121	1.56	2.11	18.52	58.00	0.70	0.22	2.45	4.90	0.75	6.99	0.13	0.31	0.02	96.66
S3-122	1.23	2.08	18.37	59.17	0.74	0.55	2.31	4.68	0.73	7.07	0.18	0.32	0.02	97.45

No.	Na2O	MgO	Al2O3	SiO2	P2O5	SO3	K2O	CaO	TiO2	FeO(tot)	MnO	Cl2O	Cr2O3	TOT
S3-123	0.34	1.06	12.90	54.33	0.97	4.74	2.22	2.38	0.70	9.45	0.19	0.28	0.02	89.59
S3-124	0.28	0.74	8.27	58.74	1.07	9.58	3.18	0.65	0.59	14.33	0.15	0.23	0.05	97.85
S3-125	0.31	0.65	5.02	65.86	0.94	8.16	3.12	0.53	0.40	9.24	0.06	0.15	0.03	94.47
S3-126	0.31	0.66	5.49	54.83	1.25	9.02	3.74	0.46	0.38	12.23	0.11	0.16	0.00	88.64
S3-127	0.17	1.91	6.26	37.09	0.89	9.22	3.18	0.40	2.91	44.51	0.15	0.21	0.26	107.16
S3-128	0.14	2.09	4.92	21.75	0.88	7.73	1.68	0.22	3.04	43.21	0.32	0.12	0.47	86.58
S3-129	0.14	0.63	3.25	57.95	1.06	11.04	1.80	0.34	0.35	12.53	0.16	0.22	0.03	89.51
S3-130	0.10	0.43	2.04	80.62	0.30	3.80	0.71	0.14	0.16	1.78	0.15	0.23	0.03	90.49
S3-131	0.74	0.37	5.82	80.25	0.31	1.70	1.89	0.29	0.24	1.69	0.00	0.14	0.00	93.45
S3-132	0.76	0.60	6.84	59.76	1.43	7.43	3.66	0.50	0.34	15.20	0.02	0.10	0.11	96.74
S3-133	0.46	0.80	4.99	49.18	1.54	13.83	4.78	0.53	0.36	21.07	0.13	0.20	0.07	97.94
S3-134	0.20	0.97	3.58	52.85	1.17	12.65	2.92	0.35	0.27	16.92	0.03	0.19	0.00	92.11
S3-135	0.25	2.36	4.91	52.54	0.98	11.13	3.56	0.61	0.53	13.70	0.04	0.18	0.02	90.81
S3-136	0.26	1.01	5.77	31.44	1.32	17.45	5.55	0.43	0.25	29.71	0.00	0.24	0.00	93.43
S3-137	0.45	1.04	6.59	35.23	1.35	17.63	5.42	0.32	0.22	28.44	0.13	0.23	0.00	97.05
S3-138	0.32	0.75	5.08	23.95	1.56	24.32	5.64	0.45	0.25	33.57	0.02	0.30	0.00	96.21
S3-139	0.33	0.66	5.07	30.64	1.26	22.99	5.29	0.78	0.40	24.36	0.19	0.32	0.04	92.33
S3-140	0.29	0.79	5.62	45.79	1.53	17.13	4.09	0.71	0.80	23.20	0.00	0.22	0.00	100.16
S3-141	0.20	0.78	6.72	51.01	1.29	12.25	3.88	0.85	0.46	17.17	0.05	0.22	0.10	94.97
S3-142	0.25	0.71	11.02	55.07	0.88	7.21	2.53	0.43	0.45	12.07	0.11	0.25	0.00	90.98
S3-143	0.22	0.97	7.04	67.35	0.52	5.44	1.77	0.37	0.30	6.70	0.02	0.08	0.00	90.80
S3-144	0.11	0.70	4.36	73.68	0.42	2.79	1.05	0.36	0.15	4.59	0.00	0.05	0.01	88.27
S3-145	0.05	0.34	3.00	69.68	1.03	1.23	0.49	0.28	0.21	22.16	0.01	0.04	0.04	98.57
S3-146	0.04	0.15	2.05	69.90	0.80	0.87	0.36	0.27	0.13	14.40	0.13	0.02	0.06	89.17
S3-147	0.01	0.17	3.56	82.84	0.14	0.11	0.57	0.27	0.03	0.92	0.00	0.03	0.00	88.65

No.	Na2O	MgO	Al2O3	SiO2	P2O5	SO3	K2O	CaO	TiO2	FeO(tot)	MnO	Cl2O	Cr2O3	TOT
S3-148	0.04	0.22	4.85	86.14	0.00	0.03	0.35	0.32	0.00	0.41	0.01	0.03	0.00	92.40
S3-149	0.01	0.22	5.52	86.34	0.01	0.06	0.29	0.37	0.01	0.45	0.00	0.03	0.00	93.31
S3-150	0.05	0.21	6.24	86.04	0.01	0.05	0.25	0.44	0.02	0.20	0.00	0.02	0.00	93.52
S3-151	0.00	0.17	6.06	86.46	0.01	0.02	0.27	0.44	0.03	0.28	0.00	0.02	0.00	93.76
S3-152	0.03	0.17	11.13	80.63	0.01	0.09	0.31	0.57	0.00	0.42	0.00	0.05	0.04	93.44
S3-153	0.01	0.23	24.35	61.22	0.01	0.19	0.31	0.58	0.00	0.63	0.04	0.14	0.01	87.70
S3-154	0.03	0.32	17.18	63.43	0.01	0.11	0.37	0.82	0.00	0.30	0.00	0.09	0.04	82.71
S3-155	0.00	0.34	18.22	64.15	0.00	0.23	0.27	0.80	0.00	0.48	0.06	0.11	0.00	84.65
S3-156	0.02	0.39	18.10	70.22	0.02	0.20	0.30	0.98	0.01	0.27	0.00	0.12	0.00	90.64
S3-157	0.04	0.34	24.17	65.65	0.00	0.27	0.28	0.77	0.00	0.61	0.00	0.14	0.06	92.33
S3-158	0.03	0.43	14.95	72.06	0.01	0.11	0.24	1.25	0.03	0.40	0.06	0.03	0.07	89.65
S3-159	0.00	0.40	17.40	68.81	0.00	0.15	0.24	0.89	0.00	0.42	0.00	0.03	0.03	88.37
S3-160	0.00	0.37	22.39	66.80	0.04	0.34	0.22	0.63	0.00	0.49	0.00	0.06	0.00	91.35
F186-M-1	0.00	3.87	5.73	0.13	0.00	0.01	0.05	0.02	6.11	75.79	0.38	0.01	0.41	92.52
F186-M-2	0.03	3.87	5.80	0.16	0.00	0.03	0.06	0.02	5.94	75.44	0.39	0.00	0.37	92.10
F186-M-3	3.23	1.94	17.47	54.74	0.66	0.42	5.89	4.44	0.70	7.19	0.15	0.31	0.00	97.14
F186-M-4	0.05	0.07	4.45	9.82	0.88	5.97	2.10	0.19	0.20	11.25	0.01	0.62	0.00	35.61
F186-M-5	0.23	2.92	2.84	53.03	1.15	9.33	2.54	5.01	0.31	14.06	0.08	0.18	0.05	91.74
F186-M-6	0.34	0.46	3.98	41.42	1.54	16.00	5.00	0.24	0.57	21.58	0.01	0.30	0.01	91.44
F186-M-7	0.53	0.38	6.54	32.47	2.23	16.66	5.88	0.44	0.42	27.27	0.01	0.26	0.02	93.10
F186-M-8	2.20	0.77	13.78	60.89	0.46	3.45	2.58	5.01	0.25	4.94	0.03	0.07	0.00	94.44
F186-M-9	0.07	0.14	9.30	59.38	0.10	1.16	0.51	0.13	0.47	9.47	0.01	0.16	0.00	80.90
F186-M-10	4.13	1.22	17.18	57.82	0.48	0.35	4.30	3.88	0.61	5.82	0.12	0.23	0.02	96.17
F186-M-11	0.75	0.77	9.47	59.36	0.68	5.26	3.27	0.68	0.44	8.03	0.03	0.31	0.00	89.05
F186-M-12	0.33	7.71	3.07	52.91	0.49	5.53	1.56	11.43	0.53	10.89	0.09	0.12	0.03	94.69

No.	Na2O	MgO	Al2O3	SiO2	P2O5	SO3	K2O	CaO	TiO2	FeO(tot)	MnO	Cl2O	Cr2O3	TOT
F186-M-13	1.65	0.49	8.62	47.61	0.95	7.93	5.02	0.94	0.21	10.47	0.02	0.69	0.00	84.60
F186-M-14	0.45	0.50	5.06	66.97	0.72	5.90	2.76	0.43	0.17	7.10	0.04	0.13	0.01	90.25
F186-M-15	0.26	0.36	1.37	18.97	0.67	3.68	1.45	0.20	0.12	53.00	0.06	0.08	0.04	80.25
F186-M-16	0.79	0.60	4.21	43.18	1.42	8.33	3.74	0.48	0.19	26.53	0.06	0.17	0.00	89.70
F186-M-17	1.34	1.30	9.10	43.07	0.78	5.08	4.68	1.01	0.40	7.98	0.00	1.17	0.00	75.92
F186-M-18	0.56	0.77	4.15	76.23	0.50	2.85	2.00	0.55	0.24	5.38	0.04	0.16	0.00	93.43
F186-M-19	0.36	0.53	13.62	36.15	1.20	6.31	3.41	0.87	0.81	17.03	0.02	0.27	0.01	80.60
F186-M-20	0.73	0.80	10.80	39.07	2.49	17.85	4.93	0.88	0.48	14.93	0.01	0.40	0.09	93.46
F186-M-21	0.32	0.38	3.58	46.43	1.17	6.48	2.52	0.47	0.58	10.10	0.02	0.76	0.01	72.83
F186-M-22	0.38	0.12	1.85	90.67	0.30	1.89	0.77	0.09	0.09	1.42	0.01	0.24	0.01	97.84
F186-M-23	0.61	0.47	6.14	45.80	1.48	12.02	4.32	0.77	0.34	16.33	0.00	0.45	0.03	88.76
F186-M-24	1.00	0.41	3.14	82.41	0.10	5.35	1.51	2.41	0.63	1.04	0.05	1.66	0.00	99.71
F186-M-25	0.56	0.50	4.65	25.35	2.16	19.26	5.99	0.82	0.52	27.93	0.06	0.49	0.01	88.31
F186-M-26	0.57	0.65	5.39	46.78	1.50	11.47	4.18	0.44	0.54	16.57	0.07	0.15	0.00	88.31
F186-M-27	2.24	0.49	9.25	52.69	1.27	8.45	4.90	1.18	0.39	11.80	0.04	0.13	0.01	92.85
F186-M-28	0.24	0.75	5.93	42.79	1.67	13.45	4.46	0.31	0.27	19.41	0.03	0.17	0.04	89.52
F186-M-29	0.32	4.84	4.83	50.05	1.38	7.46	2.64	7.10	0.46	13.19	0.11	0.10	0.03	92.52
F186-M-30	0.60	0.60	9.81	42.45	0.98	16.40	4.78	0.97	0.40	14.85	0.06	0.23	0.04	92.16
F186-M-31	0.31	0.96	3.42	33.19	1.21	18.96	5.17	1.06	0.25	22.12	0.07	0.30	0.00	87.01
F186-M-32	0.24	0.16	2.18	72.51	0.90	7.27	2.16	0.20	0.23	7.28	0.02	0.15	0.03	93.33
F186-M-33	1.39	0.73	7.64	45.49	1.47	9.18	4.97	0.92	0.37	16.92	0.05	0.20	0.00	89.32
F186-M-34	1.57	0.43	9.17	43.35	2.00	12.37	6.14	0.94	0.43	15.44	0.00	0.14	0.02	92.01
F186-M-35	1.28	0.82	7.48	41.51	1.79	10.59	5.05	2.15	0.54	17.38	0.05	0.15	0.04	88.84
F186-M-36	2.72	0.91	16.94	56.05	0.81	1.32	4.03	3.60	0.66	5.66	0.06	0.26	0.01	93.04
F186-M-37	3.14	0.54	15.88	56.92	0.69	2.72	4.17	2.46	0.67	6.13	0.03	0.13	0.02	93.49

No.	Na2O	MgO	Al2O3	SiO2	P2O5	SO3	K2O	CaO	TiO2	FeO(tot)	MnO	Cl2O	Cr2O3	TOT
F186-M-38	3.01	0.37	18.10	57.32	0.62	0.77	4.24	2.37	0.79	5.18	0.06	0.25	0.00	93.08
F186-M-39	0.06	0.04	1.60	19.62	0.67	4.96	1.69	0.13	0.22	13.47	0.00	0.68	0.01	43.15
F186-M-40	0.01	0.02	0.79	10.81	2.26	13.28	3.54	0.22	0.26	13.87	0.05	0.74	0.02	45.84
F186-M-41	0.25	0.29	2.95	50.54	1.95	11.91	3.51	0.27	0.36	16.52	0.01	0.09	0.01	88.66
F186-M-42	0.00	0.00	0.28	3.45	1.00	6.33	1.11	0.08	0.16	9.73	0.07	1.07	0.00	23.29
F186-M-43	0.63	0.59	4.09	32.15	1.55	18.24	5.40	0.56	0.24	26.23	0.09	0.23	0.02	90.01
F186-M-44	0.73	0.65	6.83	44.63	1.24	10.03	4.32	1.16	0.26	15.50	0.05	0.25	0.01	85.66
F186-M-45	0.26	0.47	2.59	33.48	1.31	17.99	4.80	0.40	0.31	24.46	0.10	0.21	0.05	86.42
F186-M-46	0.45	0.58	4.12	44.39	1.52	13.27	4.00	0.44	0.37	23.93	0.10	0.32	0.01	93.50
F186-M-47	0.44	0.55	6.42	38.38	1.61	15.27	5.08	0.70	0.19	20.33	0.05	0.20	0.00	89.22
F186-M-48	1.01	0.77	7.97	53.66	1.08	7.90	5.55	0.55	0.30	13.29	0.03	0.13	0.00	92.24
F186-M-49	2.79	1.25	14.16	52.47	0.56	2.84	4.10	2.17	0.66	7.36	0.07	0.16	0.00	88.60
F186-M-50	3.59	0.69	13.70	48.86	0.82	3.97	4.04	2.13	0.45	7.41	0.04	0.27	0.02	85.99
F186-M-51	0.07	0.09	3.19	35.41	0.63	1.44	0.91	0.42	0.16	15.43	0.02	1.98	0.01	59.76
F186-M-52	1.53	1.21	8.41	46.53	1.44	8.54	5.92	2.51	0.32	15.06	0.07	0.10	0.02	91.66
F186-M-53	0.60	0.56	6.87	40.81	2.04	10.82	5.07	0.85	0.83	21.65	0.05	0.17	0.04	90.35
F186-M-54	1.50	0.83	10.09	49.03	1.13	9.30	5.15	2.02	0.43	14.78	0.08	0.29	0.00	94.63
F186-M-55	0.34	3.73	4.40	39.08	0.70	8.72	2.44	4.28	0.48	16.08	0.07	0.25	0.00	80.58
F186-M-56	0.32	0.68	4.28	31.46	2.71	15.93	4.72	1.02	0.59	27.51	0.03	0.20	0.00	89.45
F186-M-57	0.16	0.89	4.68	32.05	1.61	7.73	2.83	0.40	1.69	35.56	0.08	0.16	0.14	87.98
F186-M-58	0.53	0.68	6.75	39.00	2.50	13.71	4.75	0.99	0.49	21.80	0.06	0.27	0.04	91.58
F186-M-59	0.16	0.19	4.32	26.73	1.18	5.78	2.84	0.53	0.46	14.17	0.00	0.50	0.02	56.87
F186-M-60	0.34	0.44	5.27	45.24	1.53	9.45	3.28	0.62	0.43	16.44	0.04	0.23	0.04	83.35
F186-M-61	3.76	0.24	13.18	52.72	1.23	6.51	5.15	1.32	0.47	9.04	0.04	0.18	0.00	93.84
F186-M-62	0.79	0.18	7.01	21.51	3.16	16.90	5.66	0.54	0.43	28.77	0.04	0.31	0.03	85.32

No.	Na2O	MgO	Al2O3	SiO2	P2O5	SO3	K2O	CaO	TiO2	FeO(tot)	MnO	Cl2O	Cr2O3	TOT
F186-M-63	0.28	0.28	2.84	44.16	2.45	13.45	4.76	0.39	2.05	20.62	0.01	0.19	0.00	91.48
F186-M-64	0.72	0.20	5.72	21.56	3.55	20.37	6.67	0.58	0.59	29.82	0.00	0.17	0.01	89.95
F186-M-65	0.27	0.36	3.58	35.16	2.40	15.47	4.94	0.35	0.48	25.49	0.03	0.21	0.05	88.80
F186-M-66	0.75	0.34	6.46	47.81	2.18	9.61	5.96	0.48	0.47	15.78	0.00	0.19	0.00	90.03
F186-M-67	0.24	0.40	4.06	36.66	3.35	16.90	5.32	0.43	0.45	24.56	0.00	0.18	0.04	92.58
F186-M-68	0.54	0.39	6.81	48.17	1.53	8.92	3.58	0.85	0.39	18.26	0.02	0.12	0.00	89.58
F186-M-69	0.18	0.33	4.23	43.58	2.16	15.92	4.52	0.30	0.50	19.45	0.03	0.14	0.03	91.37
F186-M-70	0.17	0.16	2.89	43.78	1.47	10.72	3.34	0.32	0.73	15.48	0.01	0.19	0.00	79.25
F186-M-71	4.34	2.04	17.51	55.31	0.71	0.04	6.11	4.26	0.68	6.75	0.14	0.28	0.00	98.17
F186-M-72	4.22	2.07	17.80	55.79	0.67	0.04	5.65	4.42	0.70	6.66	0.16	0.27	0.00	98.45
F186-M-73	0.21	0.21	4.24	34.59	2.99	15.30	5.25	0.39	0.55	24.77	0.02	0.26	0.03	88.82
F186-M-74	0.17	0.52	4.85	32.16	3.28	17.61	4.83	0.42	0.52	26.05	0.02	0.17	0.00	90.60
F186-M-75	0.21	0.28	4.98	43.77	2.57	13.29	3.98	0.48	0.63	20.23	0.00	0.15	0.01	90.58
F186-M-76	0.03	0.04	2.19	7.25	0.62	6.55	1.52	0.13	0.16	6.42	0.02	0.98	0.02	25.95
F186-M-77	0.07	0.22	1.30	74.40	0.09	0.98	0.45	0.03	0.49	1.24	0.01	0.18	0.00	79.45
F186-M-78	0.12	0.12	2.25	41.62	2.45	11.27	3.71	0.21	0.76	18.13	0.04	0.15	0.06	80.88
F186-M-79	0.02	0.04	0.45	1.71	0.17	1.08	0.10	0.03	0.08	3.30	0.00	0.62	0.00	7.60
F186-M-80	0.00	0.00	0.03	0.18	0.00	0.12	0.05	0.02	0.00	0.11	0.00	1.31	0.00	1.83
F186-M-81	0.24	0.50	2.23	67.17	0.91	5.97	2.14	0.17	0.53	6.11	0.04	0.07	0.02	86.10
F186-M-82	0.36	0.25	5.79	16.02	2.36	15.97	4.75	0.55	0.57	22.29	0.03	0.39	0.02	69.36
F186-M-83	0.01	0.00	0.30	0.89	0.06	0.34	0.18	0.02	0.00	0.39	0.00	0.92	0.00	3.10
F186-M-84	0.20	0.33	4.63	30.47	2.60	18.55	5.56	0.38	0.47	28.51	0.04	0.19	0.05	91.99
F186-M-85	0.07	0.78	2.54	59.30	0.34	4.52	1.66	0.66	0.31	6.64	0.01	0.14	0.02	76.99
F186-M-86	0.96	0.29	5.99	58.01	0.91	4.91	3.18	0.69	1.59	15.09	0.05	0.12	0.00	91.79
F186-M-87	0.40	0.90	5.44	43.78	0.86	14.67	4.19	1.02	0.55	17.84	0.00	0.29	0.02	89.96

No.	Na2O	MgO	Al2O3	SiO2	P2O5	SO3	K2O	CaO	TiO2	FeO(tot)	MnO	Cl2O	Cr2O3	TOT
F186-M-88	0.39	0.63	3.64	25.36	1.08	20.45	6.37	0.37	0.32	33.28	0.08	0.40	0.05	92.43
F186-M-89	0.29	0.54	5.08	22.54	2.18	20.82	6.26	0.67	0.46	26.55	0.07	0.34	0.02	85.82
F186-M-90	0.10	0.35	1.72	65.21	0.60	6.09	1.97	0.25	0.17	8.05	0.05	0.11	0.01	84.67
F186-M-91	1.31	0.52	9.29	55.76	0.95	7.25	5.16	0.48	0.56	10.75	0.03	0.08	0.01	92.15
F186-M-92	0.52	9.27	5.74	48.19	0.50	3.89	1.54	15.48	0.52	9.48	0.18	0.10	0.06	95.48
F186-M-93	0.17	0.51	3.74	49.25	1.31	10.29	3.38	0.29	0.27	12.88	0.03	0.13	0.06	82.31
F186-M-94	0.40	2.18	4.90	32.68	1.87	13.97	4.56	0.86	0.53	26.60	0.11	0.18	0.00	88.85
F186-M-95	0.42	0.63	4.88	32.45	1.84	17.65	6.04	0.51	0.27	26.28	0.06	0.30	0.01	91.34
F186-M-96	0.26	0.61	4.20	47.63	1.63	17.30	4.15	0.32	0.18	18.56	0.00	0.21	0.01	95.07
F186-M-97	0.60	0.56	6.82	42.20	1.17	13.73	5.14	0.50	0.31	22.27	0.08	0.21	0.00	93.58
F186-M-98	0.62	1.33	6.00	30.24	1.90	17.34	5.83	1.59	0.46	21.89	0.04	0.30	0.02	87.56
F186-M-99	0.43	1.17	5.11	36.41	1.30	18.86	5.63	1.16	0.30	21.13	0.02	0.25	0.05	91.82
F186-M-100	2.17	0.73	9.62	36.91	0.33	2.27	2.85	2.01	0.35	5.05	0.02	0.42	0.01	62.75
F186-L-1	3.57	2.17	17.38	55.84	0.64	0.02	6.26	4.66	0.75	6.65	0.14	0.28	0.00	98.36
F186-L-2	2.96	0.17	16.82	64.14	0.36	0.43	5.78	2.38	0.50	4.75	0.04	0.19	0.00	98.53
F186-L-3	4.05	2.38	17.69	55.64	0.64	0.04	5.63	4.84	0.71	6.76	0.11	0.28	0.00	98.77
F186-L-4	3.82	0.09	28.90	52.36	0.02	0.00	0.92	12.32	0.04	0.83	0.00	0.00	0.00	99.30
F186-L-5	3.88	0.08	28.84	52.62	0.03	0.00	0.99	12.05	0.03	0.85	0.00	0.01	0.01	99.40
F186-L-6	0.00	0.00	0.00	0.40	0.00	0.02	0.03	0.06	0.00	0.15	0.00	1.12	0.02	1.82
F186-L-7	0.00	0.00	0.10	2.48	0.00	0.09	0.16	0.07	0.01	0.78	0.00	0.53	0.00	4.23
F186-L-8	0.25	0.36	3.72	35.28	1.66	16.62	5.41	0.30	0.17	24.17	0.05	0.28	0.04	88.31
F186-L-9	0.15	0.84	2.44	46.31	0.36	6.46	2.03	2.01	0.24	13.59	0.04	0.23	0.01	74.70
F186-L-10	0.56	0.56	6.52	48.70	2.61	12.93	4.39	0.62	0.34	20.58	0.04	0.20	0.00	98.05
F186-L-11	1.64	0.78	7.46	49.61	1.98	9.81	4.91	0.89	0.42	18.01	0.03	0.37	0.02	95.93
F186-L-12	1.91	0.78	12.34	49.08	1.08	5.83	4.32	1.99	0.41	11.17	0.08	0.13	0.00	89.11

No.	Na2O	MgO	Al2O3	SiO2	P2O5	SO3	K2O	CaO	TiO2	FeO(tot)	MnO	Cl2O	Cr2O3	TOT
F186-L-13	0.25	1.84	2.79	77.49	0.54	0.25	0.75	2.91	0.77	4.99	0.02	0.21	0.00	92.81
F186-L-14	1.97	0.56	10.59	31.90	2.07	14.49	7.56	0.79	0.30	21.99	0.05	0.18	0.00	92.45
F186-L-15	0.08	2.65	3.42	0.81	0.11	0.97	0.36	0.05	3.35	79.48	0.34	0.03	0.00	91.63
F186-L-16	0.20	0.42	1.93	8.49	0.37	2.86	1.07	0.38	0.66	8.44	0.03	0.77	0.00	25.63
F186-L-17	0.12	0.20	7.20	36.69	0.37	2.66	1.27	0.41	5.41	6.16	0.03	1.41	0.01	61.95
F186-L-18	3.32	1.96	16.54	52.32	0.83	3.86	5.58	3.56	0.62	10.14	0.12	0.30	0.00	99.16
F186-L-19	2.66	0.30	18.41	51.16	0.12	0.09	4.31	1.81	0.69	6.95	0.01	0.13	0.00	86.65
F186-L-20	1.29	0.83	8.43	37.65	1.10	14.65	6.06	1.50	0.35	19.69	0.05	0.26	0.00	91.86
F186-L-21	2.32	1.87	13.08	44.80	0.75	1.09	5.67	4.32	0.65	6.97	0.12	0.28	0.02	81.94
F186-L-22	0.02	0.00	0.08	0.44	0.00	0.04	0.07	0.01	0.01	0.28	0.00	0.57	0.00	1.52
F186-L-23	0.04	0.07	16.04	20.43	1.37	16.81	5.08	0.24	0.18	24.26	0.01	0.33	0.03	84.87
F186-L-24	0.20	0.31	3.23	31.14	1.57	14.23	4.44	0.47	0.24	23.95	0.06	0.31	0.02	80.17
F186-L-25	0.53	0.40	5.80	46.56	1.19	11.46	3.98	0.64	0.30	17.21	0.01	0.27	0.04	88.39
F186-L-26	0.05	0.09	36.65	48.28	0.01	0.11	0.11	0.15	0.02	4.29	0.01	0.15	0.02	89.94
F186-L-27	0.03	0.02	1.12	14.40	0.23	2.74	1.12	0.06	0.07	9.04	0.01	0.74	0.00	29.57
F186-L-28	0.26	0.18	12.33	72.39	0.03	0.06	2.63	1.27	0.00	0.31	0.01	0.01	0.00	89.47
F186-L-29	0.14	0.18	3.20	38.63	0.20	2.96	1.88	0.27	0.10	11.84	0.02	0.31	0.01	59.75
F186-L-30	5.19	0.63	15.91	58.72	0.34	3.46	6.53	1.15	0.18	3.59	0.01	0.10	0.00	95.81
F186-L-31	1.81	0.55	15.49	45.54	0.60	7.80	3.73	4.90	0.11	11.52	0.02	0.19	0.00	92.26
F186-L-32	0.29	0.44	3.30	64.76	0.52	5.76	2.53	0.28	0.65	9.11	0.05	0.14	0.02	87.86
F186-L-33	0.70	0.41	8.84	37.89	2.35	14.37	6.13	0.86	0.39	20.01	0.05	0.17	0.00	92.16
F186-L-34	0.52	1.95	7.48	36.82	0.90	6.60	3.88	1.01	0.49	16.08	0.04	0.31	0.04	76.12
F186-L-35	0.50	9.08	5.28	40.55	0.49	8.44	3.03	12.62	0.42	14.75	0.12	0.21	0.12	95.62
F186-L-36	0.40	4.31	7.22	45.05	0.55	7.61	2.86	7.65	0.43	14.93	0.12	0.21	0.03	91.36
F186-L-37	0.16	0.79	4.38	57.67	0.71	4.72	1.54	0.63	0.78	8.62	0.07	0.23	0.00	80.30

No.	Na2O	MgO	Al2O3	SiO2	P2O5	SO3	K2O	CaO	TiO2	FeO(tot)	MnO	Cl2O	Cr2O3	TOT
F186-L-38	0.01	0.08	8.16	16.65	0.53	3.60	1.67	0.19	0.06	5.05	0.01	0.54	0.01	36.56
F186-L-39	3.54	0.41	15.08	47.21	0.34	0.58	5.05	1.33	3.12	23.59	0.16	0.05	0.02	100.47
F186-L-40	1.87	1.04	10.67	32.99	0.93	4.56	4.49	2.22	0.52	12.41	0.10	0.36	0.00	72.16
F186-L-41	0.23	5.49	18.14	45.99	0.17	1.71	0.61	8.22	0.46	10.28	0.08	0.14	0.01	91.55
F186-L-42	0.82	0.93	7.65	37.09	1.80	16.75	5.44	0.81	0.73	22.02	0.04	0.28	0.00	94.37
F186-L-43	4.26	1.08	17.29	52.51	1.09	1.41	3.80	5.12	0.46	6.24	0.05	0.18	0.00	93.49
F186-L-44	0.13	0.37	2.82	42.98	0.35	8.35	4.39	0.27	0.09	13.34	0.05	0.10	0.03	73.27
F186-L-51	0.39	0.42	3.88	52.94	0.47	11.85	3.98	0.50	0.10	13.53	0.02	0.20	0.00	88.28
F186-L-52	0.41	0.97	5.49	36.67	1.15	16.35	5.19	0.67	0.29	22.27	0.10	0.25	0.04	89.85
F186-L-53	0.41	2.09	4.39	55.68	0.82	6.74	2.60	1.89	0.32	12.75	0.06	0.15	0.04	87.95
F186-L-54	1.06	0.39	6.52	45.19	1.05	9.62	4.27	0.59	1.09	19.36	0.01	0.23	0.01	89.39
F186-L-55	1.64	1.45	12.02	43.02	0.99	9.48	6.08	2.63	0.59	11.25	0.09	0.29	0.03	89.55
F186-L-56	3.27	0.97	13.77	54.53	0.70	5.29	6.86	3.02	0.37	5.07	0.06	0.12	0.00	94.03
F186-L-57	2.16	0.33	11.07	49.30	1.05	10.45	6.57	1.35	0.25	14.05	0.01	0.12	0.00	96.72
F186-L-58	0.80	0.60	4.39	17.49	1.33	10.34	4.30	1.02	4.56	31.72	0.04	0.32	0.03	76.95
F186-L-59	0.17	0.83	3.95	57.26	1.09	9.10	3.12	0.31	0.46	10.94	0.00	0.11	0.02	87.36
F186-L-60	0.15	0.09	9.26	20.18	0.58	4.57	1.68	0.19	0.13	11.14	0.03	1.03	0.00	49.03
F186-L-61	1.26	0.86	9.00	41.25	1.63	10.36	5.72	1.89	0.56	17.33	0.08	0.47	0.05	90.47
F186-L-62	0.39	0.74	5.07	27.69	2.06	19.69	6.04	0.55	0.43	29.47	0.06	0.28	0.05	92.53
F186-L-63	0.59	0.72	5.21	19.09	1.83	23.52	7.35	0.45	0.40	29.93	0.04	0.32	0.02	89.47
F186-L-64	0.37	0.55	1.17	75.14	0.00	0.15	0.14	2.85	0.00	0.53	0.03	0.02	0.00	80.96
F186-L-65	1.58	1.07	9.37	26.26	0.91	15.43	6.20	0.85	0.49	21.75	0.00	0.59	0.04	84.54
F186-L-66	1.80	8.64	12.82	52.09	0.69	3.22	7.49	0.75	0.30	6.87	0.00	0.19	0.00	94.86
F186-L-67	0.45	0.30	5.53	13.80	1.18	21.81	6.73	0.30	0.42	27.19	0.03	0.43	0.04	78.21
F186-L-68	0.72	1.24	9.00	28.98	1.98	15.88	6.60	1.85	0.58	22.87	0.08	0.44	0.00	90.21

No.	Na2O	MgO	Al2O3	SiO2	P2O5	SO3	K2O	CaO	TiO2	FeO(tot)	MnO	Cl2O	Cr2O3	TOT
F186-L-69	2.18	1.87	15.40	47.64	0.72	5.48	5.93	3.74	0.66	9.80	0.08	0.33	0.00	93.82
F186-L-70	0.61	0.96	5.66	9.39	0.83	21.69	5.75	0.36	0.35	32.05	0.03	0.45	0.04	78.18
F186-L-71	0.01	0.00	0.03	0.16	0.00	0.00	0.02	0.10	0.00	0.07	0.00	1.11	0.00	1.51
F186-L-72	0.62	1.11	9.06	29.43	0.99	16.59	6.07	2.01	0.42	22.69	0.08	0.41	0.05	89.52
F186-L-73	2.61	0.47	17.34	55.60	0.53	2.56	4.77	2.32	0.67	6.49	0.09	0.46	0.03	93.93
F186-L-74	0.00	0.00	0.64	9.37	0.11	0.77	0.74	0.24	0.07	2.02	0.01	1.35	0.00	15.32
F186-L-75	0.16	0.22	4.80	45.91	0.13	2.59	1.69	0.41	0.11	2.42	0.01	0.56	0.01	59.03
F186-L-76	0.33	0.19	5.37	40.30	0.58	9.85	3.61	0.30	0.20	11.15	0.31	0.30	0.00	72.49
F186-L-77	0.22	0.46	3.59	65.69	0.53	8.48	3.11	0.31	0.14	11.22	0.00	0.21	0.03	93.99
F186-L-78	4.01	2.24	18.69	58.11	0.68	0.16	6.36	4.44	0.69	6.64	0.10	0.28	0.03	102.43
F186-L-79	3.57	2.09	17.75	55.71	0.67	0.65	6.26	4.48	0.69	6.78	0.14	0.30	0.00	99.09
F186-L-80	3.89	1.96	18.14	56.83	0.69	0.14	5.97	4.03	0.71	6.43	0.12	0.34	0.00	99.25
F186-L-81	0.26	0.12	2.23	31.50	0.02	0.24	0.51	0.21	0.09	2.36	0.18	0.28	0.00	37.99
F186-L-82	1.35	1.28	12.06	38.26	1.04	8.52	5.92	2.76	0.52	19.80	0.08	0.35	0.00	91.94
F186-L-83	0.25	0.33	4.98	64.53	0.30	4.20	2.72	0.91	0.11	5.65	0.02	0.18	0.02	84.21
F186-L-84	0.46	0.44	4.24	10.20	1.65	26.64	7.30	0.28	0.23	34.03	0.02	0.57	0.03	86.09
F186-L-85	0.01	0.00	0.00	0.02	0.00	0.01	0.00	0.02	0.00	0.07	0.00	1.11	0.00	1.24
F186-L-86	1.80	0.83	9.24	33.50	1.61	16.52	6.65	1.42	0.49	22.69	0.06	0.42	0.00	95.23
F186-L-87	3.66	2.11	17.63	55.45	0.68	0.06	6.37	4.59	0.69	6.77	0.12	0.28	0.02	98.42
F186-L-88	3.64	1.85	16.46	56.86	0.64	1.09	5.44	3.18	0.69	6.28	0.10	0.44	0.00	96.67
F186-L-90	0.27	0.66	4.69	29.92	1.48	20.93	5.61	0.89	0.27	26.94	0.06	0.35	0.05	92.12
F186-L-93	0.03	0.02	0.47	3.50	0.04	0.34	0.46	0.16	0.05	2.98	0.02	0.46	0.00	8.53
F186-L-94	0.88	0.32	7.02	51.43	1.18	10.06	5.47	0.54	0.24	13.84	0.00	0.32	0.00	91.30
F186-L-95	0.00	0.00	0.08	2.09	0.01	0.24	0.30	0.14	0.01	0.62	0.00	0.47	0.02	3.98
F186-L-96	3.35	2.10	17.60	54.87	0.68	0.35	6.34	4.42	0.70	6.76	0.10	0.26	0.00	97.53

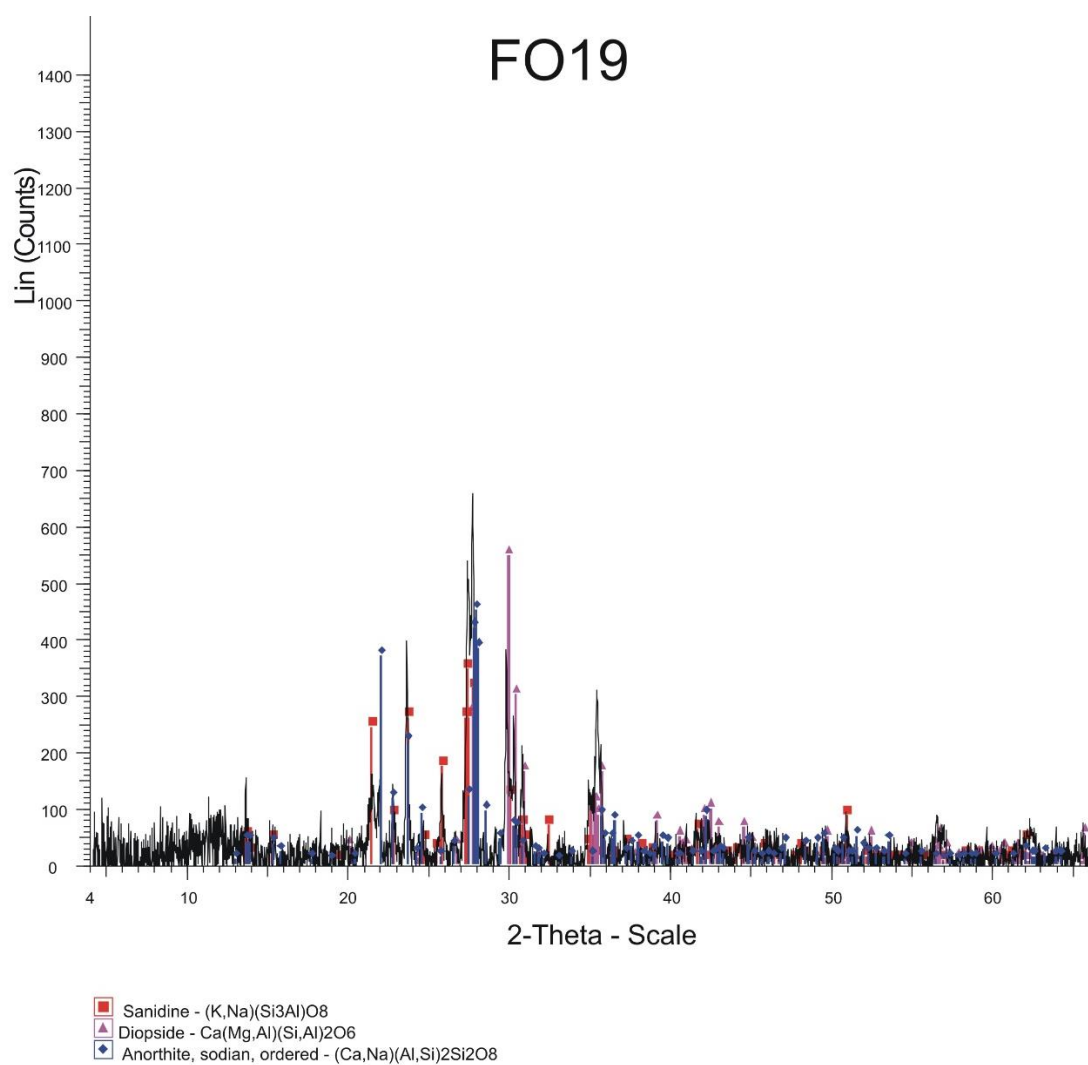
No.	Na2O	MgO	Al2O3	SiO2	P2O5	SO3	K2O	CaO	TiO2	FeO(tot)	MnO	Cl2O	Cr2O3	TOT
F186-L-97	0.02	0.01	0.61	1.90	0.10	1.45	0.44	0.05	0.03	1.12	0.00	1.59	0.00	7.31
F186-L-98	0.86	1.61	6.96	25.07	0.01	0.12	0.46	2.59	0.63	6.58	0.03	0.26	0.00	45.18
F186-L-99	0.95	0.68	8.23	28.06	2.29	15.56	6.30	1.37	0.42	21.52	0.03	0.25	0.00	85.66
F186-L-100	1.08	1.68	8.69	61.72	0.47	3.70	3.58	1.06	1.08	8.38	0.04	0.07	0.00	91.54
F186-L-101	2.93	0.26	12.85	62.15	0.61	0.94	3.45	2.25	0.87	5.78	0.03	0.06	0.01	92.19
F186-L-102	0.20	0.51	6.32	17.71	1.66	22.79	6.53	0.50	0.40	30.35	0.08	0.54	0.03	87.62
F186-L-103	0.04	0.03	7.61	13.92	0.19	0.17	0.08	0.06	0.27	8.26	0.06	0.93	0.00	31.63
F186-L-104	0.40	0.25	6.45	10.65	2.45	25.01	7.38	0.42	0.40	30.74	0.04	0.26	0.03	84.47
F186-L-105	0.57	17.40	2.77	50.73	0.02	0.08	0.10	19.23	0.42	8.30	0.28	0.04	0.03	99.97
F186-L-106	0.00	0.00	0.02	0.08	0.01	0.01	0.02	0.01	0.00	0.06	0.00	1.23	0.00	1.45
F186-L-107	1.50	0.38	10.34	51.27	0.97	10.42	5.40	0.91	0.21	14.55	0.02	0.15	0.02	96.13
F186-L-108	1.18	1.24	12.63	40.55	1.48	5.93	5.84	2.96	0.60	13.76	0.09	0.29	0.00	86.54
F186-L-109	0.21	0.23	4.96	18.73	1.60	7.94	4.54	1.64	0.54	17.10	0.05	0.30	0.03	57.87
F186-L-110	0.45	0.69	12.33	39.30	0.74	3.34	3.07	1.13	1.06	14.45	0.06	0.25	0.03	76.89
F186-L-111	0.44	14.48	3.33	49.91	0.03	0.04	0.04	21.66	0.57	8.16	0.21	0.03	0.00	98.89
F186-L-112	0.44	13.88	3.47	53.05	0.03	0.02	0.04	21.37	0.47	7.96	0.22	0.01	0.03	100.98
F186-L-113	0.02	0.09	25.89	41.24	0.01	0.30	0.19	0.13	0.08	7.14	0.01	0.12	0.02	75.24
F186-L-114	0.01	0.00	0.01	0.12	0.01	0.02	0.03	0.00	0.00	0.18	0.01	0.66	0.00	1.04
F186-L-115	0.47	0.76	5.30	44.36	1.73	12.15	4.62	1.07	0.27	19.07	0.03	0.16	0.00	89.99
F186-L-116	3.07	0.16	9.77	39.26	2.49	11.48	5.19	0.66	0.38	20.39	0.00	0.23	0.01	93.09
F186-L-117	0.19	0.19	2.52	76.56	0.80	4.73	1.80	0.16	0.52	8.33	0.00	0.09	0.00	95.90
F186-L-118	3.74	0.21	15.06	55.91	0.70	4.52	5.85	1.62	0.25	5.73	0.01	0.08	0.00	93.69
F186-L-119	0.00	0.00	0.01	0.23	0.00	0.00	0.01	0.09	0.00	0.06	0.00	1.12	0.00	1.52
F186-L-120	2.62	7.05	0.39	50.54	0.02	0.01	0.10	18.85	0.55	18.75	0.48	0.00	0.00	99.37
F186-L-121	0.56	0.48	4.47	12.91	1.43	22.98	7.13	0.51	0.51	32.33	0.08	0.43	0.02	83.83

No.	Na2O	MgO	Al2O3	SiO2	P2O5	SO3	K2O	CaO	TiO2	FeO(tot)	MnO	Cl2O	Cr2O3	TOT
F186-L-122	0.29	0.67	4.61	41.88	1.10	14.59	4.53	0.64	0.39	19.71	0.08	0.20	0.01	88.70
F186-L-123	2.49	0.36	17.63	51.06	0.45	2.79	1.53	7.97	0.14	4.26	0.01	0.17	0.00	88.87
F186-L-124	3.60	1.31	14.47	49.21	2.14	9.99	7.55	0.65	0.74	25.25	0.14	0.19	0.00	115.24
F186-L-125	0.35	0.82	6.94	44.96	1.79	8.40	3.19	1.68	0.60	16.21	0.03	0.28	0.00	85.25
F186-L-126	4.34	0.23	14.22	59.20	0.68	4.28	5.47	1.08	0.24	5.47	0.00	0.08	0.02	95.31
F186-L-127	0.29	0.23	3.30	18.26	2.68	18.55	5.41	0.34	0.82	29.99	0.02	0.45	0.02	80.36
F186-L-128	0.45	0.13	4.41	19.79	3.08	15.27	5.58	0.27	0.52	30.37	0.30	0.38	0.04	80.59
F186-L-129	0.95	0.59	5.42	29.74	3.01	16.77	6.23	0.35	0.67	26.44	0.06	0.21	0.02	90.45
F186-L-130	0.47	6.85	3.69	38.29	1.19	11.66	3.19	9.66	0.59	18.57	0.18	0.24	0.03	94.61
F186-L-131	0.40	1.34	4.88	19.36	3.39	19.91	5.86	1.78	0.57	29.25	0.06	0.19	0.03	87.02
F186-L-132	0.20	0.21	3.91	21.03	2.89	18.01	5.12	0.32	0.31	21.67	0.00	0.62	0.03	74.32
F186-L-133	0.00	0.00	0.05	0.42	0.00	0.19	0.07	0.02	0.01	0.28	0.00	0.85	0.00	1.91
F186-L-134	0.55	1.33	5.35	43.57	1.86	12.24	5.07	0.51	0.33	15.54	0.06	0.16	0.05	86.62
F186-L-135	0.03	0.01	0.84	3.22	0.18	2.47	0.67	0.08	0.04	1.48	0.00	0.72	0.01	9.75
F186-L-136	1.61	0.51	13.15	58.52	0.89	3.78	5.70	1.56	0.58	8.06	0.04	0.25	0.00	94.64
F186-L-137	0.51	0.43	3.52	27.43	1.99	19.04	6.06	0.26	0.39	29.16	0.02	0.75	0.03	89.59
F186-L-138	3.80	0.06	18.98	61.11	0.82	1.73	9.37	1.75	0.58	1.62	0.01	0.15	0.00	99.98
F186-L-139	1.07	0.46	7.17	42.37	1.55	12.49	5.07	0.66	0.32	17.77	0.04	0.32	0.00	89.30
F186-L-140	1.30	0.76	8.26	32.48	1.38	10.26	5.24	0.84	0.21	17.87	0.02	0.57	0.01	79.19
F186-L-141	0.03	0.01	0.20	0.90	0.01	0.06	0.07	0.03	0.02	0.40	0.00	1.06	0.00	2.78
F186-L-142	5.39	0.33	16.43	56.06	0.48	2.82	5.07	1.00	0.10	3.67	0.04	0.14	0.00	91.52
F186-L-143	0.00	0.01	0.02	0.09	0.01	0.00	0.03	0.00	0.01	0.09	0.00	1.63	0.00	1.90
F186-L-144	0.48	13.97	3.90	49.49	0.00	0.02	0.04	21.64	0.69	8.45	0.21	0.00	0.01	98.89
F186-L-145	0.47	0.76	6.32	41.04	1.77	13.34	5.01	0.47	0.30	19.04	0.03	0.26	0.00	88.81
F186-L-146	2.79	1.61	17.45	56.08	0.56	0.06	8.66	3.67	0.62	6.34	0.14	0.28	0.01	98.26

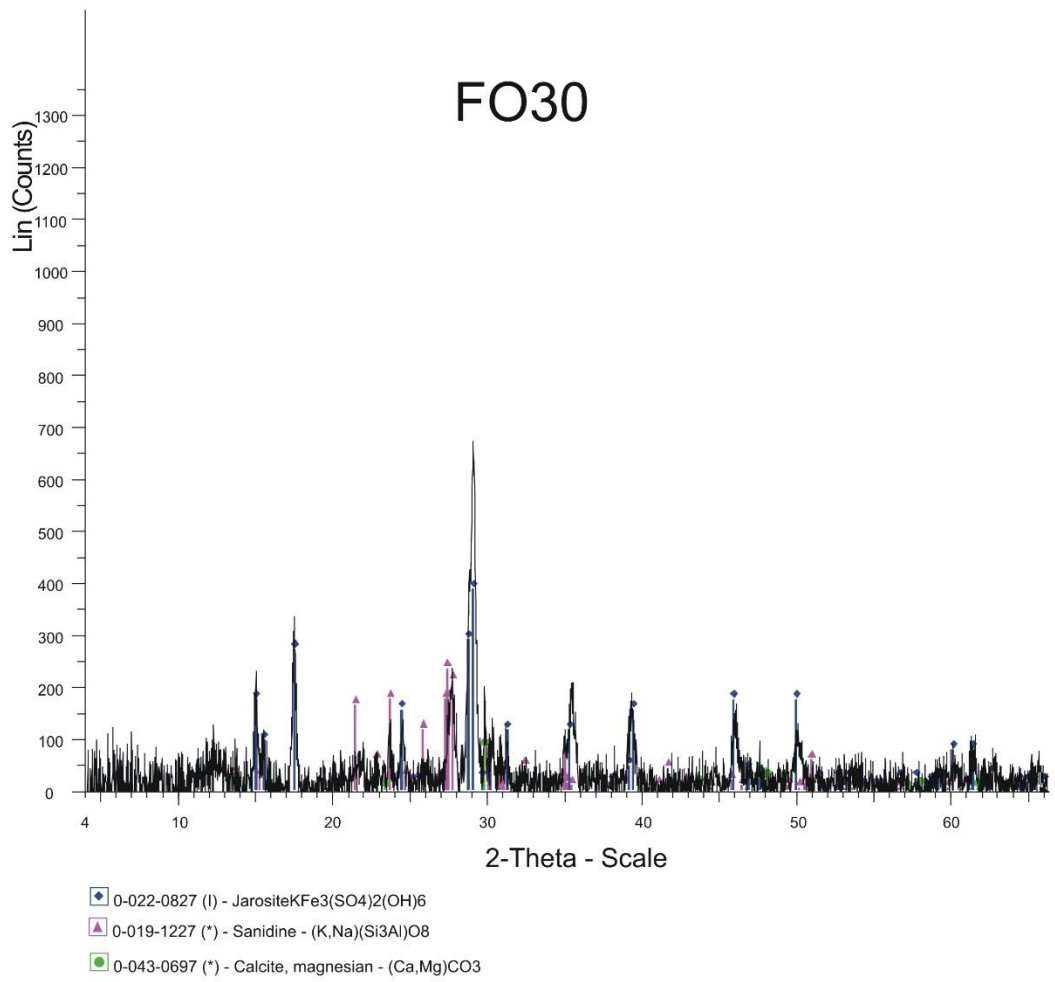
No.	Na2O	MgO	Al2O3	SiO2	P2O5	SO3	K2O	CaO	TiO2	FeO(tot)	MnO	Cl2O	Cr2O3	TOT
F186-L-147	0.45	0.51	5.85	41.04	2.08	13.97	4.82	0.60	0.39	22.33	0.02	0.30	0.02	92.38
F186-L-148	0.73	0.22	4.79	36.78	2.32	16.09	5.80	0.38	0.81	21.74	0.04	0.43	0.01	90.15
F186-L-149	0.42	0.36	3.09	30.61	1.68	19.63	5.61	0.34	0.50	26.67	0.02	0.38	0.01	89.32
F186-L-150	2.10	0.29	8.05	38.32	1.44	13.16	5.42	1.13	0.93	17.39	0.03	0.88	0.03	89.17
F186-L-151	0.39	0.48	4.17	18.90	1.68	23.53	7.11	0.41	0.49	31.58	0.03	0.46	0.02	89.24
F186-L-152	0.45	14.34	3.23	49.93	0.01	0.01	0.03	21.37	0.55	9.05	0.30	0.00	0.03	99.31
F186-L-153	0.08	0.06	1.21	11.75	0.46	6.73	1.84	0.10	0.08	4.01	0.01	0.63	0.00	26.96
F186-L-154	1.11	0.13	5.75	34.83	0.90	8.26	3.79	0.47	0.14	8.81	0.03	0.43	0.02	64.66
F186-L-155	6.08	0.04	21.25	62.15	0.09	0.24	5.40	3.59	0.19	1.08	0.00	0.01	0.04	100.16
F186-L-156	1.67	0.57	7.47	38.74	1.24	10.58	3.21	1.66	0.34	22.82	0.08	0.24	0.02	88.63
F186-L-157	0.59	0.71	5.18	39.31	1.46	13.84	5.03	1.04	0.40	19.51	0.04	0.36	0.03	87.49
F186-L-158	1.95	0.99	16.28	57.50	0.68	0.96	6.17	2.40	0.81	6.09	0.09	0.68	0.00	94.60
F186-L-159	0.57	0.59	8.76	63.98	0.44	1.18	2.83	0.71	0.98	5.21	0.07	0.27	0.03	85.61
F186-L-160	2.86	0.33	11.91	45.87	2.34	9.84	6.41	1.11	0.34	13.60	0.02	0.15	0.00	94.79
F186-L-161	5.74	0.35	15.52	55.99	1.24	5.51	3.01	2.28	0.18	5.66	0.00	0.15	0.05	95.67
F186-L-162	0.53	0.45	5.40	33.88	1.79	13.82	5.47	0.43	0.42	22.88	0.04	0.39	0.01	85.49
F186-L-163	0.07	0.09	2.88	7.75	1.94	3.78	1.46	0.32	0.15	11.32	0.08	1.05	0.01	30.90
F186-L-164	0.39	0.63	7.97	38.72	2.31	13.08	4.59	1.26	0.40	19.68	0.03	0.19	0.04	89.29
F186-L-165	0.09	0.46	4.02	42.99	0.72	3.72	1.46	0.23	0.18	6.14	0.01	0.43	0.00	60.43
F186-L-166	0.97	0.39	8.30	40.23	2.45	10.16	4.50	0.71	0.32	19.17	0.00	0.24	0.00	87.44
F186-L-167	0.32	0.32	6.64	34.93	2.18	12.34	4.10	0.49	0.29	20.83	0.03	0.25	0.01	82.73
F186-L-168	0.10	0.04	0.56	8.23	1.04	3.09	1.16	0.21	0.04	6.51	0.02	1.17	0.00	22.15
F186-L-169	0.01	0.00	0.05	0.08	0.00	0.01	0.02	0.04	0.00	0.04	0.02	1.24	0.00	1.51

Appendix D.

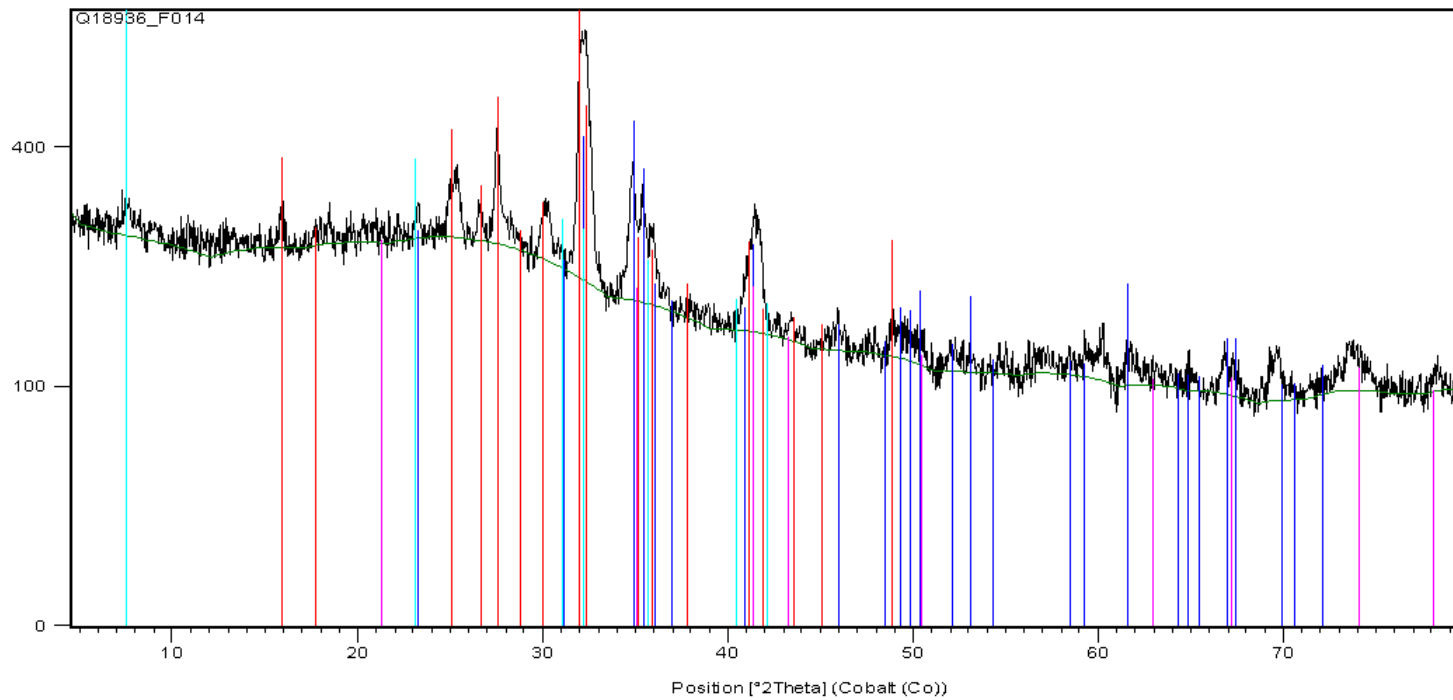
The results of the XRD and Micro-XRD Analysis:



XRD result of Sample F019.

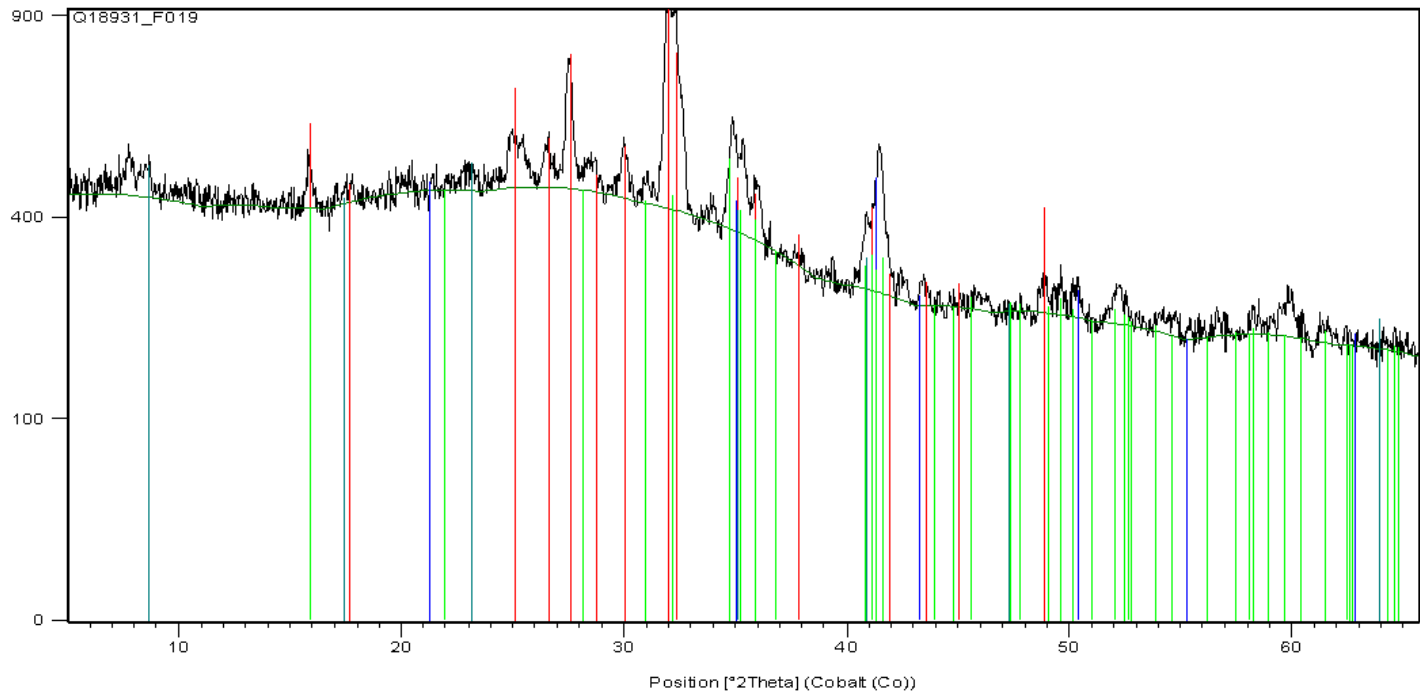


XRD result of Sample F030.



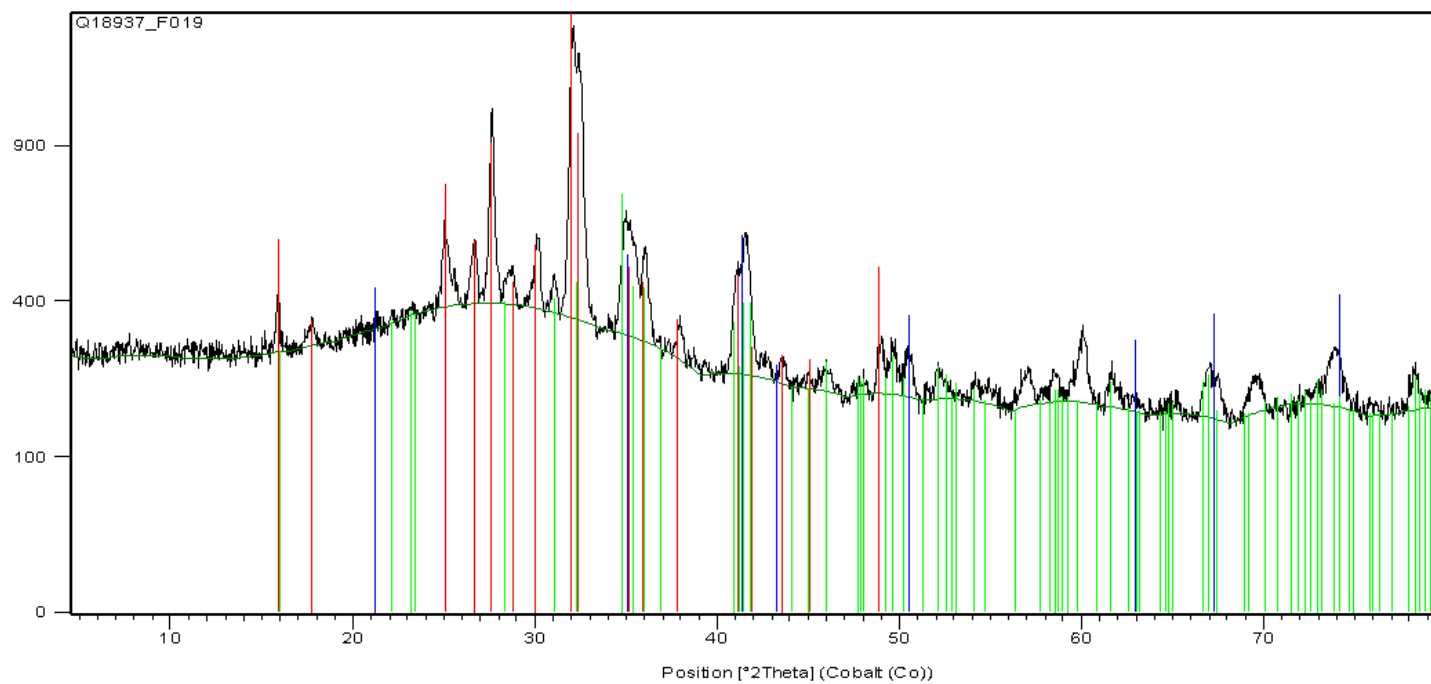
Peak List
00-010-0357; (Na, K)(Si ₃ Al)O ₈ ; Sanidine potassium, disordered, syn
00-009-0460; Ca Mg (Si O ₃) ₂ ; Diopside
00-019-0629; Fe +2 Fe ₂ +3 O ₄ ; Magnetite, syn
00-013-0259; Na _{0.3} (Al, Mg) ₂ Si ₄ O ₁₀ (OH) ₂ ·xH ₂ O; Montmorillonite-14A

Micro-XRD result of Sample F014.



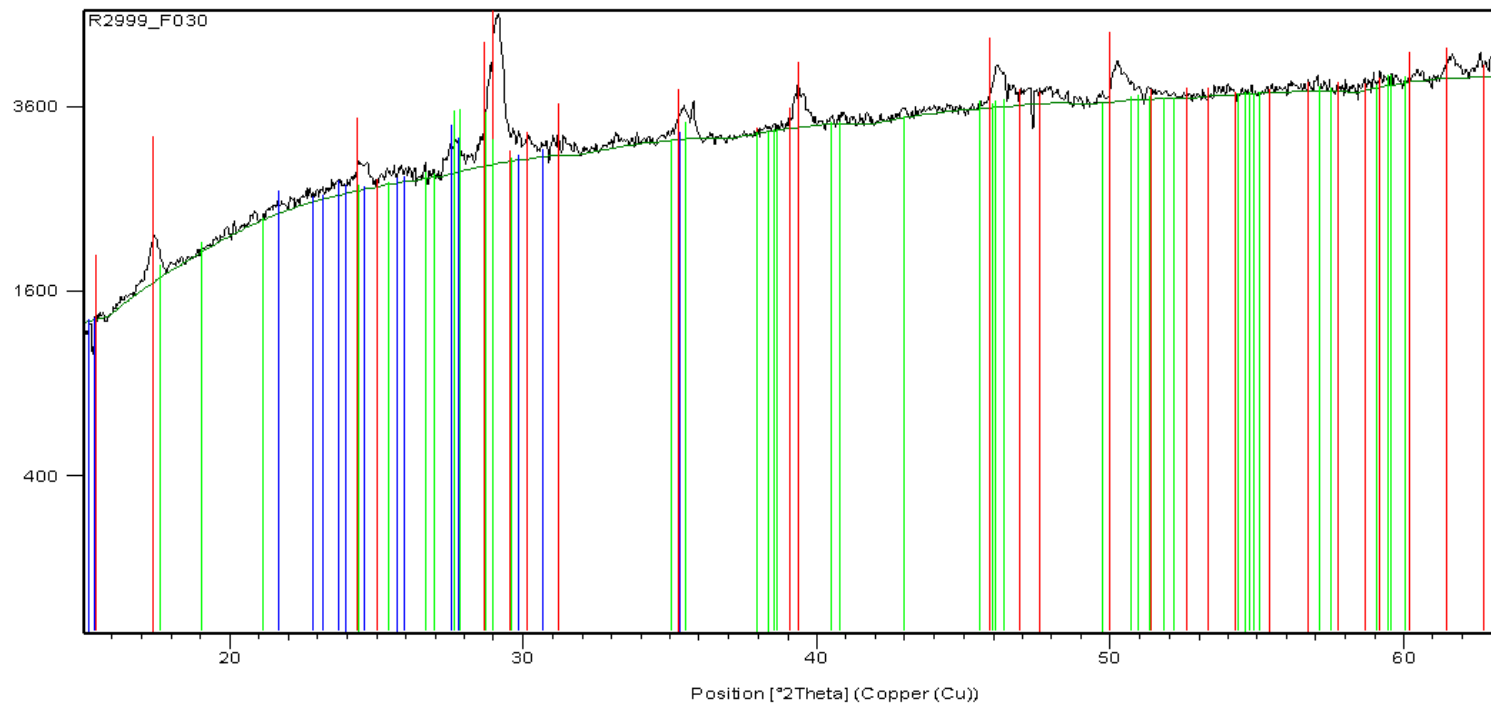
Peak List
00-010-0357; (Na, K)(Si ₃ Al)O ₈ ; Sanidine, potassian, disordered, syn
01-089-0688; Fe ₃ O ₄ ; Magnetite, syn
01-088-0848; (Mg, Fe, Ti, Al)(Ca, Na, Mg)(Si, Al) ₂ O ₆ ; Augite
00-002-0037; AlSi ₂ O ₆ (OH) ₂ ; Montmorillonite

Micro-XRD result of Sample F019.



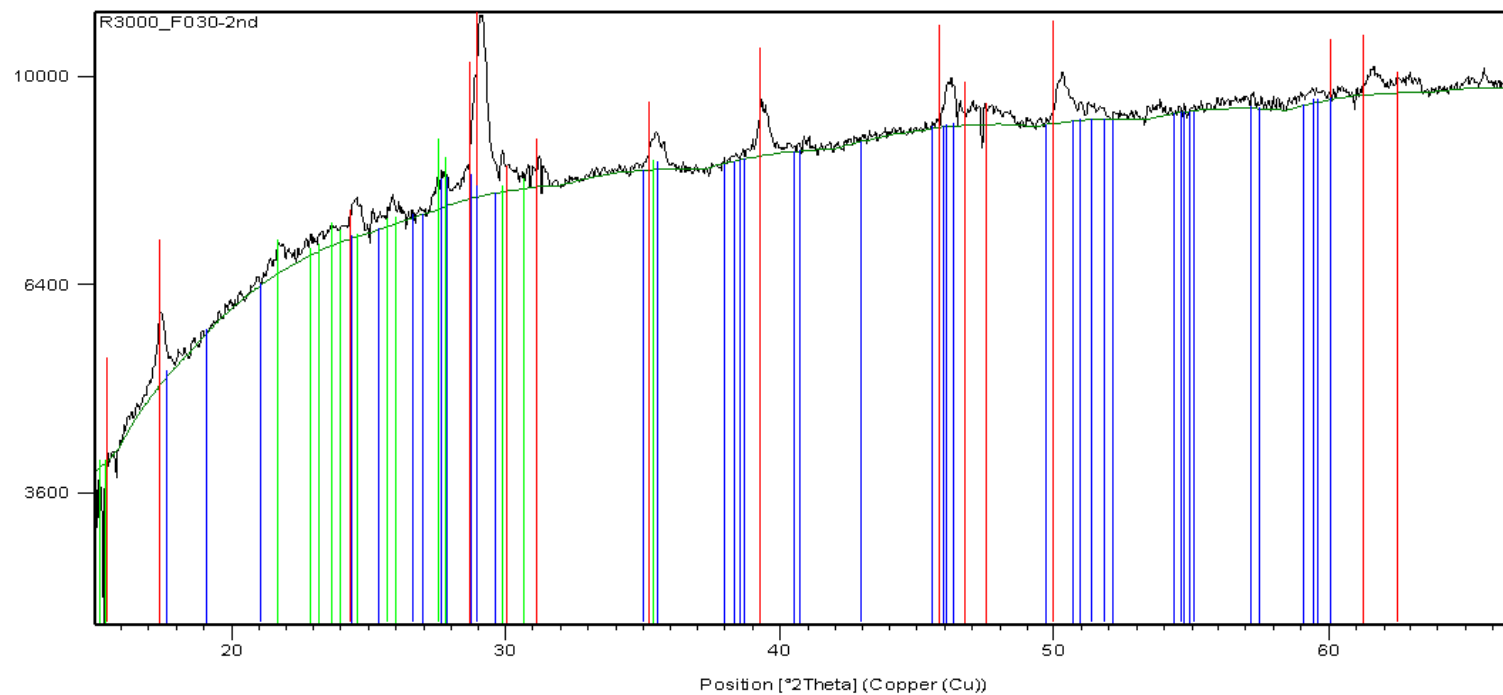
Phase	Color
00-010-0357; (Na, K)(Si ₃ Al)O ₈ ; Sanidine, potassium, disordered, syn	Red
00-007-0322; FeO · Fe ₂ O ₃ ; Magnetite	Blue
01-088-0838; (Mg, Fe, Al, Ti, Cr)(Ca, Fe, Na, Mg)(Si, Al) ₂ O ₆ ; Augite	Green

Micro-XRD result of Sample F019-b.



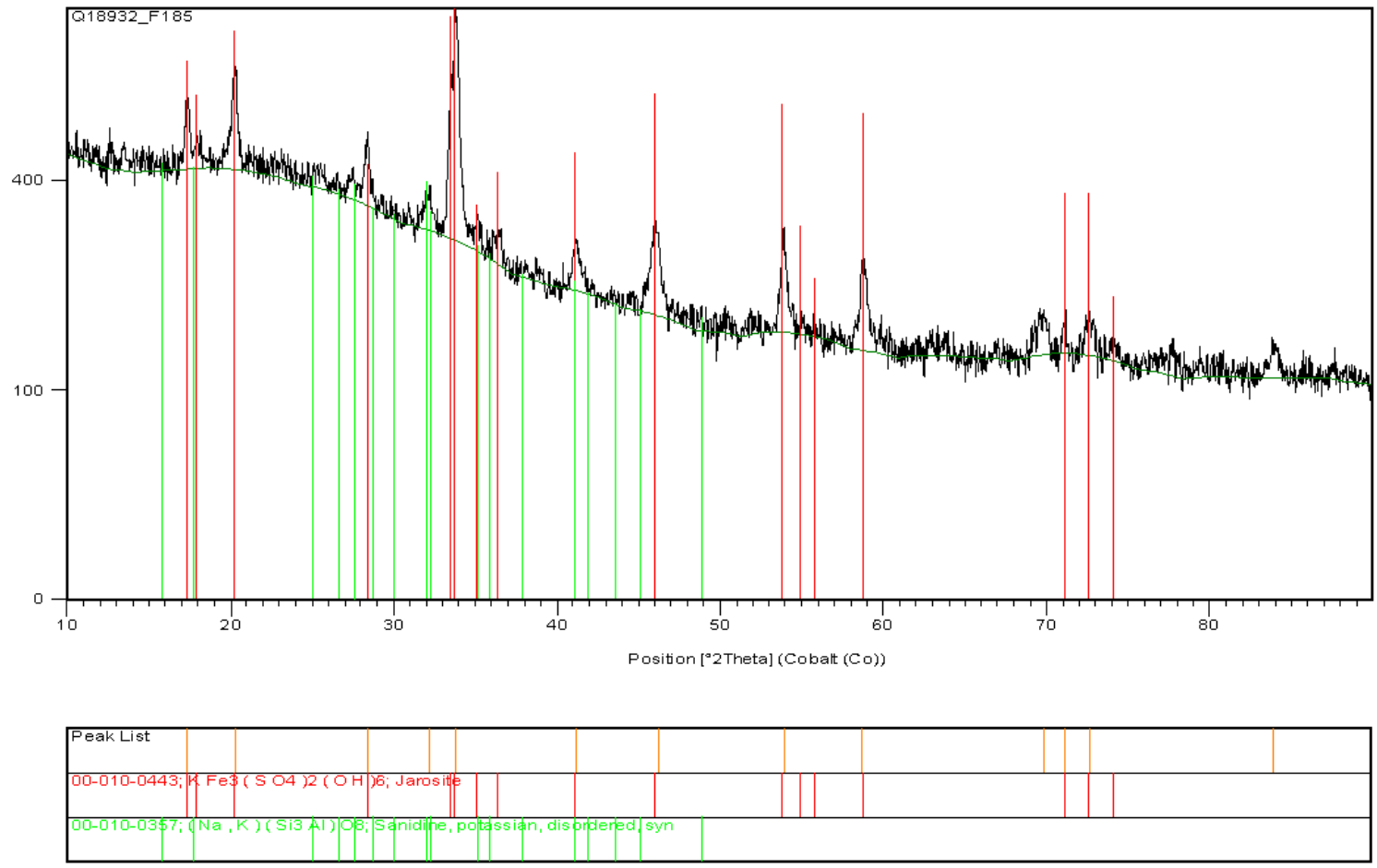
Peak List
00-022-0827; $K_2Fe_3(SO_4)_2(OH)_6$; Jarosite, syn
00-042-1352; $Al_4(P_2O_7)_3(OH)_3$; Tribillite
00-010-0361; $Na_{0.71}K_{0.29}Al_3Si_3O_{10}$; Anorthoclase, syn

Micro-XRD result of Sample F030.

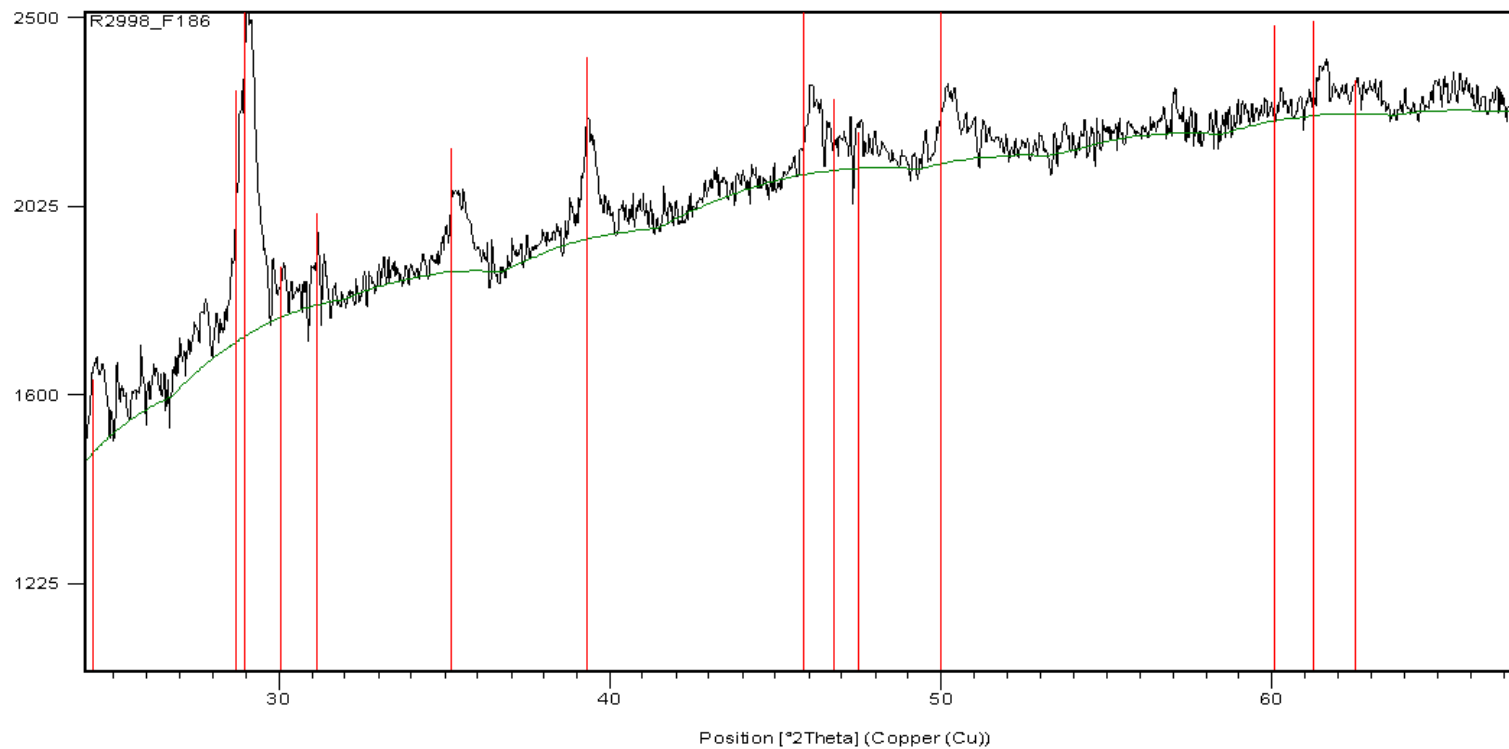


Reference	Chemical Formula	Phase Name
00-010-0443	$K_2Fe_3(SO_4)_2(OH)_6$	Jarosite
00-042-1352	$Al_4(P_2O_7)_3(OH)_3$	Triblerite
00-010-0361	$Na_0.71K_{0.29}Al_3(SO_4)_3$	Anorthoclase, syn

Micro-XRD result of Sample F030-b.

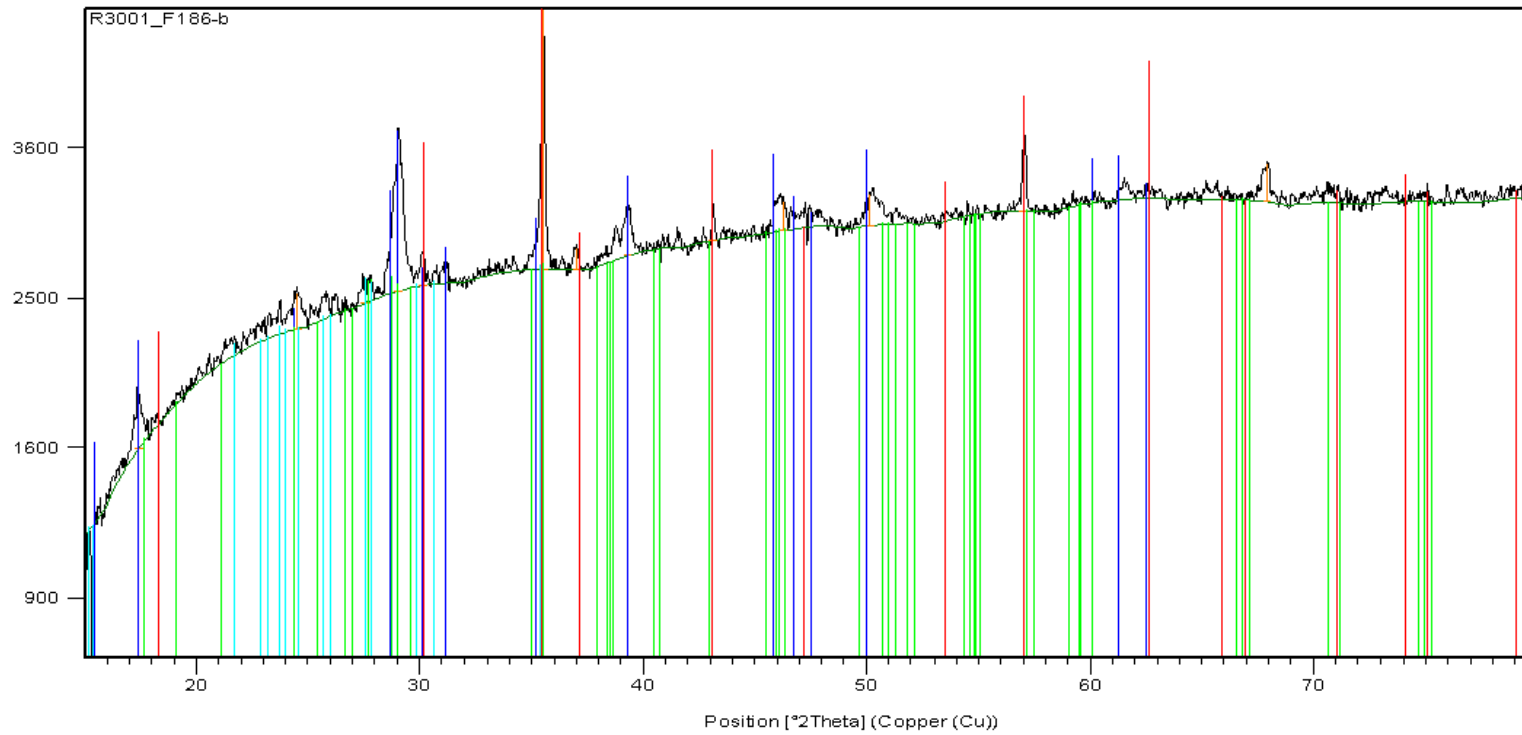


Micro-XRD result of Sample F185.



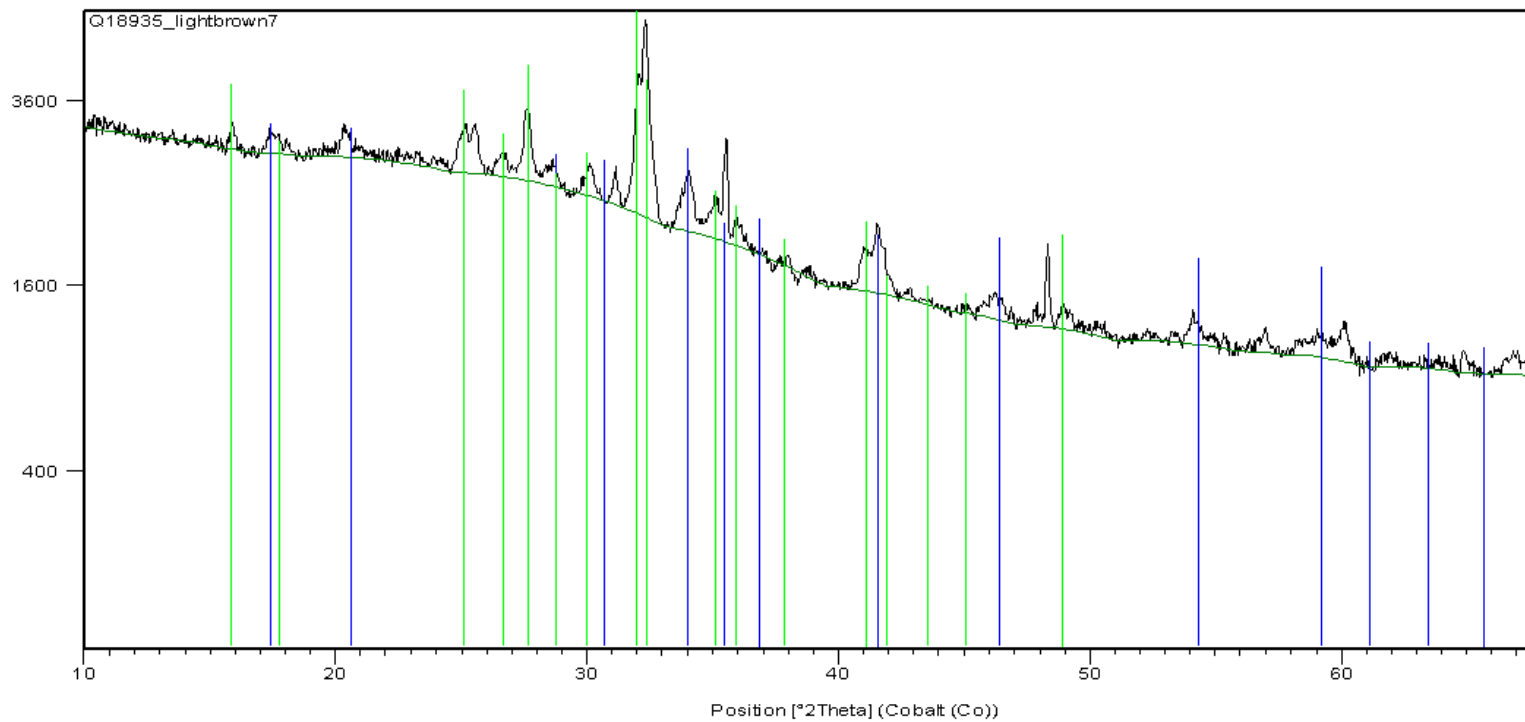
Peak List
00-010-0443; $K_2Fe_3(SO_4)_2(OH)_6$; Jarosite

Micro-XRD result of Sample F186.



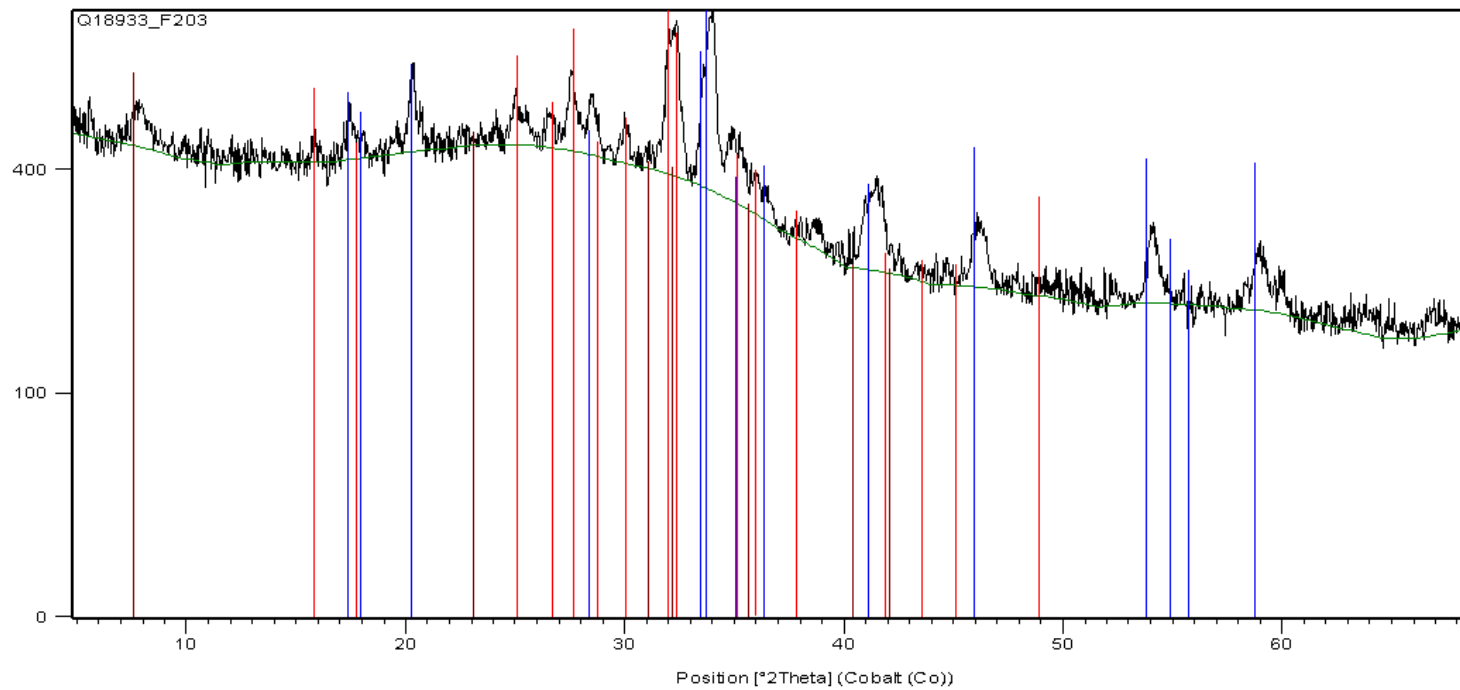
Peak List
01-088-0866; Fe ₃ O ₄ ; Magnetite
00-010-0443; K Fe ₃ (S O ₄) ₂ (OH) ₆ ; Jarosite
00-042-1352; Al ₄ (P O ₄) ₃ (OH) ₃ ; Trolleite
00-010-0361; Na _{0.71} K _{0.29} Al ₃ Si ₃ O ₈ ; Anorthoclase, syn

Micro-XRD result of Sample F186-b.



Peak List
00-002-0602; K ₂ O · 3Fe ₂ O ₃ · 4S O ₃ · 6H ₂ O; Jarosite
00-010-0357; (Na, K)(Si ₃ Al)O ₈ ; Sanidine, potassium, disordered, syn

Micro-XRD result of Sample F186-c.



Peak List
00-010-0357; (Na, K) (Si3Al) O8; Sanidine, potassium, disordered, syn
00-010-0443; K Fe3 (S O4) 2 (OH) 6; Jarosite
00-013-0259; Na0.3 (Al, Mg) 2 Si4 O10 (OH) 2 · x H2 O; Montmorillonite-14A

Micro-XRD result of Sample F203.